4´-Alkoxy Oligodeoxynucleotides: A Novel Class of RNA Mimics.

Radek Liboska, Jan Snášel, Ivan Barvík, Jr.[1], Miloš Buděšínský, Radek Pohl, Zdeněk Točík, Ondřej Páv, Dominik Rejman, Pavel Novák, and Ivan Rosenberg*

Institute of Organic Chemistry and Biochemistry, Academy of Sciences of the Czech Republic, v. v. i., Flemingovo 2, 166 10 Prague 6, Czech Republic

[1]Division of Biomolecular Physics, Institute of Physics, Charles University, Ke Karlovu 5, 12116 Prague 2, Czech Republic

Supplementary Material

1. Experimental

General.
Unless stated otherwise, the solvents were evaporated at 40 °C and 13 kPa using rotary evaporator. The products were dried over phosphorus pentoxide at 40–50 °C and 13 Pa. The course of the reactions was followed by TLC on Merck Silica gel 60 F_{254} aluminum sheets and the products were visualized by UV monitoring. Preparative column chromatography was performed on silica gel (40–60 μm, Fluka) whereby the amount of adsorbent used was 20–40 times the weight of the mixture separated. Elution was performed at the flow rate of 40 mL min^{-1}. In case of purification of dimethoxytrityl derivatives and phosphoramidites, the slurry of silica gel was prepared in the appropriate solvent containing triethylamine (2 ml per 100 ml of a silica gel bed).

Materials and methods.
The synthesis of oligonucleotides was performed in 0.5 micromolar scale on a GeneSyn synthesizer using solid support (CPG-dT) and standard phosphoramidite approach.
Final oligonucleotides were purified by semipreparative HPLC on reverse phase column (Luna C18-5μ, 10x250 mm, Phenomenex) using a linear gradient of acetonitrile in 0.1M-TEAA pH 7.5. Thermal characteristics of oligonucleotide complexes were recorded on Cary 100 Bio spectrophotometer (THERMAL program).
MALDI-TOF mass spectra were recorded on a Bruker Reflex4 spectrometer; N_2 laser 337 nm U.; 3-Hydroxypicolinic and picolinic acid (9:1) in acetonitrile and mQ-water (1:1, v/v) were used as matrices. Values of molecular mass of prepared oligonucleotides as determined by these measurements were all in accordance with the calculated ones, as follows:

Table S1 Molecular mass of oligomers obtained from MALDI TOF

Entry	T_{15}-strand	Molecular weight	
		calculated	found
1	dT_{15}	4499.93	4498.77
2	$(_{4'\text{-Me}}T)_{14}T$	4696.30	4696.12
3	$(T_{2'\text{-OMe}})_{14}T$	4920.29	4919.49
4	$(_{4'\text{-MeOEtO}}T)_{14}T$	5537.03	5535.15
5	$(_{4'\text{-MeO}}T)_{14}T$	4920.29	4922.02
6	$(^{4'\text{-MeO}}T)_{14}T$	4920.29	4919.36
7	$(T\text{-}T_{2'\text{-OMe}})_7T$	4710.11	4710.06
8	$(T\text{-}_{4'\text{-MeO}}T)_7T$	4710.11	4709.06
9	$(_{4'\text{-MeOEtO}}T\text{-}_{4'\text{-MeO}}T)_7T$	5228.66	5227.81
10	$(_{4'\text{-MeOEtO}}T\text{-}T_{2'\text{-OMe}})_7T$	5228.66	5229.05
11	$(_{4'\text{-MeO}}T\text{-}T_{2'\text{-OMe}})_7T$	4920.29	4919.65

Mass spectra (*m/z*) were recorded on ZAB-EQ (VG Analytical) instrument, using FAB+ and/or FAB- technique (Xe, 8 kV) with glycerol–thioglycerol (3:1) and 2-hydroxyethyldisulfide as matrices. MS HR ESI spectra (m/z) were recorded on LTQ Orbitrap XL (Thermo Fischer Scientific) instrument. Elemental analyses were carried out on a PE 2400 Series II analyzer.

NMR spectra were measured on Varian UNITY 500 spectrometer (^{1}H at 500 MHz; ^{13}C at 125.7 and ^{31}P at 202.3 MHz) and Bruker AVANCE 600 spectrometer (^{1}H at 600 MHz; ^{13}C at 125.8 MHz) in DMSO, $CDCl_3$, D_2O or C_6D_6 at 27 °C. Homonuclear 2D-H,H-COSY spectra were used for the structural assignment of coupled protons and 2D-H,H-ROESY spectra for detection spatially closed protons (assignment of geminal H-2´ and H-2´´ and determination of configuration at C-4‘ carbon atom). The 1D-^{13}C-„attached proton test“ (APT) spectra and heteronuclear 2D-H,C-HSQC and 2D-H,C-HMBC spectra were used for the structural assignment of carbon signals.

5'-Deoxy-5'-iodothymidine (4)[1]

A mixture of thymidine (20 g, 82.6 mmol), triphenylphosphine (27 g, 103 mmol), iodine (26 g, 103 mmol), and pyridine (16 ml, 200 mmol) in dioxane (400 ml) was stirred for 7 h at room temperature, and then methanol (25 ml) was added. Solvents were removed *in vacuo*, the residue was dissolved in boiling ethanol (250 ml), and the solution was left to crystallize (4 °C, 12 h). First crop of the title compound (17.8 g) was recovered by filtration. Column chromatography of the evaporated mother liquors on silica gel in chloroform-ethanol (0-5 %) yielded a second crop (4.0 g) of the product (overall yield, 75 %); m. p. 170-173 °C corresponded to the literature data.

1-(2,5-Dideoxy-β-D-*glycero*-pent-4-enofuranosyl)thymine (5)[1]

The iodo derivative **4** (21.8 g; 61.9 mmol) in 0.5M solution of sodium methoxide in methanol (400 ml) was heated at reflux for 8 h. The light brown solution was cooled to r. t. and neutralized by the addition of glacial acetic acid (9.5 ml). The solvent was evaporated, and the residue was crystallized from ethanol to give 11.2 g (81 %) of **5** as colorless needles; m. p. 207-209 °C corresponds to the literature data.

1-[3-*O*-(*tert*-Butyldimethylsilyl)-2,5-dideoxy-β-D-*glycero*-pent-4-enofuranosyl]thymine (6)[2]

A solution of **5** (16.2 g, 72.2 mmol), *tert*-butyldimethylchlorosilane (14.5 g, 96 mmol), and imidazole (4.9 g, 72.2 mmol) in pyridine (360 ml) was stirred at room temperature for 8 h. The reaction was quenched with methanol (10 ml), and the solvents were evaporated. Traces of pyridine were removed by co-evaporation with toluene (2 x 400 ml). The residue was dissolved in chloroform (400 ml), and washed with 1M triethylammonium hydrogen carbonate (2 x 100 ml). The chloroform extract was dried with anhydrous $MgSO_4$, and concentrated *in vacuo* to afford the crude product (19.4 g). This product in toluene was filtered through a silica gel column (100 ml) in toluene to remove *tert*-butyldimethylsilyl methyl ether, and the product **6** was eluted with ethyl acetate to give 16.9 g (69 %) of **6** as a white foam. HR-ESI: for $C_{16}H_{26}O_4N_2NaSi$ calculated: 361.15540; found: 361.15527; -0.36082 ppm

^{1}H NMR spectrum ($CDCl_3$): 8.90 b, 1 H (NH); 6.99 q, 1 H, *J*(6,CH_3) = 1.2 (H-6); 6.49 t, 1 H, *J*(1',2') = 6.1, *J*(1',2'') = 6.1 (H-1'); 4.75 ddt, 1 H, *J*(3',2') = 6.3, *J*(3',2'') = 3.4, *J*(3',5'a) = 1.1, *J*(3',5'b) = 1.0 (H-3'); 4.51 dd, 1 H, *J*(5'a,5'b) = 2.2, *J*(5'a,3') = 1.1 (H-5'a); 4.21 dd, 1 H, *J*(5'b,5'a) = 2.2, *J*(5'b,3') = 1.0 (H-5'b); 2.39 ddd, 1 H, *J*(2'',1') = 6.1, *J*(2'',2') = 13.6, *J*(2'',3') = 3.4 (H-2''); 2.19 dt, 1 H, *J*(2',1') = 6.1, *J*(2',2'') = 13.6, *J*(2',3') = 6.3 (H-2'); 1.92 d, 3 H, *J*(CH_3,6) = 1.2 (5-CH_3); 0.89 s, 9 H (C(CH_3)$_3$); 0.11 s, 6 H (Si(CH_3)$_2$).

^{13}C NMR spectrum ($CDCl_3$): 164.03 (C-4); 162.62 (C-4'); 150.29 (C-2); 134.44 (C-6); 111.56 (C-5); 85.93 (C-1'); 84.82 (C-5'); 70.56 (C-3'); 40.51 (C-2'); 25.57 (3 x CH_3 (t-Bu)); 17.91 (>C< (t-Bu)); 12.52 (5-CH_3); -4.78 and -4.86 (Si(CH_3)$_2$).

3'-*O*-(*tert*-Butyldimethylsilyl)-4'-methoxythymidine (7a) and 1-[3-*O*-(*tert*-butyldimethylsilyl)-2-deoxy-4-methoxy-α-L-*threo*-pentofuranosyl]thymine (7b).

To a stirred solution of **6** (1.015 g, 3 mmol) in anhydrous methanol (30 ml), 70% *m*-chloroperbenzoic acid (1.5 g, 6 mmol) was added. After 5 h at r. t. the mixture was diluted with chloroform (80 ml) and washed with 2M triethylammonium hydrogen carbonate (2x50 ml, 4 °C). The aqueous layer was washed with chloroform (2x80 ml), and the organic extracts were combined, dried with $MgSO_4$, and concentrated *in vacuo*. The residue was purified by silica gel chromatography (stepwise gradient, chloroform-ethanol 0-5 %) yielded less polar epimer **7b** (358 mg, 31 %), eluted at 4% ethanol in chloroform and the desired epimer **7a** (520 mg, 45 %) at ~5% ethanol in chloroform; both as amorphous solids.

HR-ESI **7a**: for $C_{17}H_{30}O_6N_2NaSi$ calculated: 409.17653; found: 409.17649; -0.11435 ppm;

7b: for $C_{17}H_{30}O_6N_2NaSi$ calculated: 409.17653; found: 409.17645; -0.21245 ppm.

7a: ^{1}H NMR spectrum ($CDCl_3$): 8.61 bs, 1 H (NH); 7.32 q, 1 H, *J*(6,CH_3) = 1.3 (H-6); 6.22 dd, 1 H, *J*(1',2') = 3.8, *J*(1',2'') = 8.0 (H-1'); 4.68 t, 1 H, *J*(3',2') = 8.3, J(3',2'') = 8.1 (H-3'); 3.84 d, 1 H, *J*(5'a,5'b) = 11.5 (H-5'a); 3.68 d, 1 H, *J*(5'b,5'a) = 11.5 (H-5'b); 3.43 s, 3 H (4'-OCH_3); 2.50 dt, 1 H, *J*(2'',1') = 8.0, *J*(2'',2') = 13.7, *J*(2'',3') = 8.1 (H-2''); 2.31 ddd, 1 H, *J*(2',1') = 3.8, *J*(2',2'') = 13.7, *J*(2',3') = 8.3 (H-2'); 1.92 d, 3 H, *J*(CH_3,6) = 1.3 (5-CH_3); 0.91 s, 9 H (C(CH_3)$_3$); 0.12 s, 3 H and 0.13 s, 3 H (Si(CH_3)$_2$).

^{13}C NMR spectrum ($CDCl_3$): 163.68 (C-4); 150.20 (C-2); 136.33 (C-6); 111.28 (C-5); 106.76 (C-4'); 84.68 (C-1'); 71.33 (C-3'); 61.49 (C-5'); 50.48 (OCH_3); 38.92 (C-2'); 25.74 (3 x CH_3 (t-Bu)); 18.13 (>C< (t-Bu)); 12.59 (5-CH_3); -4.80 and -4.87 (Si(CH_3)$_2$).

7b: ^{1}H NMR spectrum ($CDCl_3$): 8.41 bs, 1 H (NH); 7.26 q, 1 H, *J*(6,CH_3) = 1.2 (H-6); 6.63 dd, 1 H, *J*(1',2') = 8.3, *J*(1',2'') = 6.4 (H-1'); 4.33 dd, 1 H, *J*(3',2') = 4.6, *J*(3',2'') = 1.4 (H-3'); 3.88 bd, 1 H, *J*(5'a,5'b) = 12.1 (H-5'a); 3.84 d, 1 H, *J*(5'b,5'a) = 12.1 (H-5'b); 3.40 s, 3 H (4'-OCH_3); 2.24 ddd, 1 H, *J*(2'',1') = 6.4, *J*(2'',2') = 13.7, *J*(2'',3') = 1.4 (H-2''); 2.33 ddd, 1 H,

J(2',1') = 8.3, *J*(2',2'') = 13.7, *J*(2',3') = 4.6 (H-2'); 1.95 d, 3 H, *J*(CH_3,6) = 1.3 (5-CH_3); 1.78 bs (5'-OH); 0.92 s, 9 H ($C(CH_3)_3$); 0.13 s, 3 H and 0.14 s, 3 H ($Si(CH_3)_2$).
^{13}C NMR spectrum ($CDCl_3$): 163.21 (C-4); 150.46 (C-2); 135.54 (C-6); 111.72 (C-5); 110.73 (C-4'); 85.50 (C-1'); 76.31 (C-3'); 57.85 (C-5'); 49.47 (4'-OCH_3); 38.79 (C-2'); 25.64 (3 x CH_3 (t-Bu)); 17.91 (>C< (t-Bu)); 12.73 (5-CH_3); -4.73 and -5.20 ($Si(CH_3)_2$).

5'-*O*-(4,4'-Dimethoxytrityl)-4'-methoxythymidine (8a).
(a) Dimethoxytritylation of 7a. To a stirred solution of **7a** (0.52 g, 1.3 mmol) in anhydrous pyridine (13 ml), 4,4'-dimethoxytrityl chloride was added in three portions (3 x 0.18 g, 1.6 mmol). The solution was left to stand overnight, then triethylamine (0.3 ml, 2.1 mmol) and methanol (0.2 ml) were added, and the suspension was concentrated *in vacuo*. The residue was taken up with chloroform (60 ml), washed with 1M triethylammonium hydrogen carbonate (2 x 20 ml), and the aqueous layers were washed with chloroform (3 x 80 ml). The combined organic extracts were dried over anhydrous Na_2SO_4, and the solvent was evaporated to dryness. The obtained crude 3'-*O*-(*tert*-butyldimethylsilyl)-5'-*O*-(4,4'-dimethoxytrityl)-4'-methoxythymidine was subjected to the desilylation reaction.
(b) Desilylation. The product from the previous step was dissolved in 0.5M tetra-*n*-butylammonium fluoride in THF (10 ml), and the solution was left to stand overnight at room temperature. Then the suspension of Dowex 50Wx8 (Et_3NH^+ form, 20 ml) in aqueous 70% methanol (20 ml) was added, the mixture was stirred for 5 minutes, and the resin was filtered off. Sodium hydrogen carbonate (2 g) was added and the mixture was evaporated to dryness. The solid residue was extracted with chloroform (70 ml), and the chloroform extract was dried over anhydrous Na_2SO_4. Chromatography on a silica gel column using a stepwise gradient of ethanol in chloroform (0-4%) gave 0.72 g (96 %, based on **7a**) of **8a** as a white foam.
HR-ESI: for $C_{32}H_{34}O_8N_2Na$ calculated: 597.22074; found: 597.22060; -0.22598 ppm
^{1}H NMR spectrum (d_6-DMSO): 11.36 bs, 1 H (NH); 7.54 q, 1 H, J(6,CH_3) = 1.2 (H-6); 7.40 m, 2 H, 7.31 m, 2 H, and 7.25 m, 1 H (C_6H_5); 7.27 m, 2 H, 7.26 m, 2 H and 6.89 m, 4 H (2x C_6H_4); 6.13 dd, 1 H, *J*(1',2'a) = 3.6, *J*(1',2'b) = 7.7 (H-1'); 5.02 d, 1 H, *J*(3'-OH,3') = 8.1 (3'-OH); 4.70 bq, 1 H, *J*(3',2'a) = 8.6, *J*(3',2'b) = 9.1, *J*(3',OH) = 8.1 (H-3'); 3.74 s, 6 H (2x $PhOCH_3$); 3.16 s, 3 H (4'-OCH_3); 3.29 d, 1 H, and 3.08 d, 1 H, *J*(gem) = 9.8 (H-5'a + H-5'b); 2.34 ddd, 1 H, *J*(2'a,1') = 3.6, *J*(2'a,2'b) = 13.5, *J*(2'a,3') = 8.6 (H-2'a); 2.30 ddd, 1 H, *J*(2'a,1') = 7.7, *J*(2'a,2'b) = 13.5, *J*(2'a,3') = 9.1 (H-2'a); 1.50 d, 3 H, *J*(CH_3,6) = 1.2 (CH_3).
^{13}C NMR spectrum (d_6-DMSO): 163.87 (C-4);158.36, 158.35, 135.36, 135.34, 130.00 (2), 26.96 (2), 113.40 (2) and 113.39 (2) (2xC_6H_4); 150.50 (C-2); 144.82, 128.06(2), 127.89(2) and 126.98 (C_6H_5); 136.08 (C-6); 109.90 (C-5); 105.42 (C-4'); 82.38 (C-1'); 80.13 (>C< (DMTr)); 70.48 (C-3'); 61.85 (C-5'); 55.21(2xOCH_3 (DMTr)); 49.50 (4'-OCH_3); 36.86 (C-2'); 11.98 (CH_3).

1-[2'-Deoxy-5'-*O*-(4,4'-dimethoxytrityl)-4'-methoxy-α-L-*threo*-pentofuranosyl]thymine (8b)
The title compound was prepared according to the procedure described for **8a** starting from **7b** (0.4 g, 1 mmol). Yield of **8b** 0.53 g (92%, white foam).
^{1}H NMR spectrum (d_6-DMSO): 11.30 bs, 1 H (NH); 7.26 q, 1 H, *J*(6,CH_3) = 1.2 (H-6); 7.33 m, 2 H, 7.30 m, 2 H and 6.88 m, 4 H (2xC_6H_4); 7.46 m, 2 H, 7.30 m, 2 H and 7.23 m, 1 H (C_6H_5); 6.44 dd, 1 H, *J*(1',2'a) = 8.5, *J*(1',2'b) = 6.5 (H-1'); 5.62 d, 1 H, *J*(OH,3') = 5.5 (3'-OH); 4.34 bt, 1 H, *J*(3',2'a) = 4.6, *J*(3',OH) = 5.5, *J*(3',2'b) < 1 (H-3'); 3.737 s, 3 H and 3.734 s, 3 H (2x $PhOCH_3$); 2.82 s, 3 H (4'-OCH_3); 3.42 d, 1 H, and 2.93 d, 1 H, *J*(gem) = 9.7 (H-5'a + H-5'b); 2.42 m, 1 H, *J*(2'a,1') = 8.5, *J*(2'a,2'b) = 13.6, *J*(2'a,3') = 4.6 (H-2'a); 2.17 m, 1 H, *J*(2'b,1') = 6.5, *J*(2'b,2'a) = 13.6, *J*(2'b,3') < 1 (H-2'b); 1.76 d, 3 H, *J*(CH_3,6) = 1.2 (5-CH_3).

^{13}C NMR spectrum (d_6-DMSO): 163.63 (C-4); 158.29(2), 135.68, 135.18, 130.12(2), 130.00(2), 113.21(2) and 113.12(2) (2xC_6H_4); 150.98 (C-2); 144.85, 127.98(2), 127.86(2) and 126.85 (C_6H_5); 135.82 (C-6); 110.44 (C-5); 110.37 (C-4'); 85.50 (>C< (DMTr)); 84.16 (C-1'); 74.18 (C-3'); 57.18 (C-5'); 55.19 (2xOCH_3 (DMTr)); 37.78 (C-2'); 12.45 (5-CH_3).

5'-*O*-(4,4'-Dimethoxytrityl)-4'-methoxythymidine-3'-*O*-(2-cyanoethyl-*N*,*N*-diiso-propyl)phosphoramidite (9a)

Compound **8a** (0.36 g, 0.62 mmol) was dried by co-distillation with anhydrous toluene (2 x 8 ml), dissolved in THF (3.2 ml), and *N*,*N*-diisopropylethylamine (0.43 ml, 2.47 mmol) followed by 2-cyanoethyl *N*,*N*-diisopropylphosphoramidochloridite (0.25 ml, 1.12 mmol) were added under argon. The solution was stirred at room temperature for 40 minutes (reaction complete, monitored by TLC), and then the mixture was partitioned between ethyl acetate (60 ml) and an ice-cold saturated sodium hydrogen carbonate solution (50 ml). The organic layer was washed with the same solution (3 x 50 ml), and the aqueous washings were re-extracted with ethyl acetate (30 ml). Combined ethyl acetate layers were shortly dried with anhydrous Na_2SO_4 and evaporated with addition of anhydrous toluene. The residue was then purified on a silica gel column (pre-treated with 2% of triethylamine) using a toluene-ethyl acetate (0-8 %) gradient, to give, after lyophylisation from benzene, 0.42 g (86 %) of **9a** as a pale yellow foam.

^{1}H NMR spectrum (C_6D_6): 9.37 b + 9.28 b, 1H, NH); ~7.74 m, 2H, Ar-H (DMTr); 7.67 q + 7.72 q, 1H, *J*(6,CH_3)=1.2 (H-6); ~7.58 m, 4H, Ar-H(DMTr); ~7.31 m, 2H, Ar-H (DMTr); 7.17 m, 1H, Ar-H (DMTr); ~6.90 m, 4H, Ar-H (DMTr); 6.51 dd + 6.58 dd, 1H, *J*(1',2')=3.0, *J*(1',2")=8.0, (H-1'); 5.34 m, 1H (H-3'); 3.96 d, 1H, *J*(5'a,5'b)=9.6 (H-5'a); 3.61 dh + 3.58 dh, 2H, *J*(CH,P)=10.2, *J*(CH,CH_3)=6.8 (6x) (>N-CH (N-iPr_2)); 3.54 m + 3.43 m and 3.54 m + 3.22 m, 2H (P-OCH_2); 3.54 d + 3.60 d, 1H, *J*(5'b,5'a)=9.6 (H-5'b); 3.43 s +3.41 s and 3.42 s + 3.40 s, 6H (2xOMe (DMTr)); 3.14 s + 3.17 s, 3H (4'-OMe); 2.69 ddd + 2.75 ddd, 1H, *J*(2",1')=8.0, *J*(2",2')=13.6, *J*(2",3')=8.5 (H-2"); 2.45 ddd + 2.63 ddd, 1H, *J*(2',1')=3.0, *J*(2',2")=13.6, *J*(2',3')=8.5 (H-2'); 1.89 m + 1.82 m, 2H (CH_2CN); 1.68 d + 1.74 d, 3H, *J*(CH_3,6)=1.2 (5-CH_3); 1.25 d + 1.16 d and 1.20 d + 1.16 d, 12H, *J*(CH_3,CH)=6.8, 4xCH_3 (N-iPr_2)).

^{13}C NMR spectrum (C_6D_6): 163.16 (C-4); 159.04 +158.97 and 159.01 + 158.94 (2x Ar-C (DMTr)); 150.11 + 150.26 (C-2); 144.64 + 144.75 (Ar-C (DMTr)); 135.21 + 135.45 and 135.05 + 135.32 (2x Ar-C (DMTr)); 134.65 + 135.02 (C-6); 130.46 + 130.40 and 130.43 + 130.37 (4x Ar-CH (DMTr)); 128.42 + 128.40 (2x Ar-CH (DMTr)); 127.67 (2x Ar-CH (DMTr)); 127.06 + 126.96 (Ar-CH (DMTr); 117.22 + 117.31 (CN); 113.25 + 113.27 and 113.19 + 113.22 (4x Ar-CH (DMTr)); 111.10 + 111.12 (C-5); 106.39 d, *J*(C,P)=5.4 + 106.40 d, *J*(C,P)=7.0 (C-4'); 83.31 + 83.41 (C-1'); 70.50 d, *J*(C,P)=19.0 + 71.97 d, *J*(C,P)=17.4 (C-3'); 61.40 + 61.87 (C-5'); 58.60 d, *J*(C,P)=16.7 + 57.57 d, *J*(C,P)=19.3 (P-OCH_2); 54.42 + 54.36 and 54.11 + 54.36 (2xOMe (DMTr)); 49.37 + 49.49 (4'-OMe); 43.04 d, *J*(C,P)=12.6 + 43.11 d, *J*(C,P)=12.7 (2x N-CH (N-iPr_2)); 37.10 + 37.71 (C-2'); 24.29 + 24.25 and 24.20 + 24.15 (4x Me (N-iPr_2)); 19.35 d, *J*(C,P)=5.5 + 19.62 d, *J*(C,P)=6.8 ($\underline{CH_2}$-CN); 11.76 + 11.78 (5-Me).

^{31}P NMR spectrum (C_6D_6): 151.65, 150.71.

1-[2'-Deoxy-5'-*O*-(4,4'-dimethoxytrityl)-4'-methoxy-α-L-*threo*-pentofuranosyl]thymine 3'-*O*-(2-cyanoethyl-*N*,*N*-diisopropyl)phosphoramidite (9b)

The title compound was prepared according to the procedures described for **8a** and **9**. Starting from **7b** (358 mg, 0.9 mmol), we obtained, in three steps, after freeze drying from benzene, 315 mg (46 %, 0.41 mmol) of the title phosphoramidite **9b**. For $C_{41}H_{51}N_4O_9P$ (774.85)

calculated: 63.55 %C, 6.63 %H, 7.23 %N, 4 %P; found: 63.49 %C, 6.82 %H, 7.09 %N. FAB: for $C_{41}H_{51}N_4O_9PK$ calculated, 813.95; found, 813.50 ($M+K^+$).
^{1}H NMR spectrum (C_6D_6): 9.12 b, 1H, NH); 7.84 m + 7.86 m, 2H, Ar-H (DMTr);
7.70 m + 7.69 m + 7.66 m, 4H, Ar-H(DMTr); ~7.35 m, 2H, Ar-H (DMTr); 7.21 m, 1H, Ar-H (DMTr); 7.00 dd + 7.07 dd, 1H, *J*(1',2')=8.8, *J*(1',2")=6.1 (H-1'); 6.99 q + 7.07 q, 1H, *J*(6,CH_3)=1.2 (H-6); 6.955 m + 6.92 m and 6.945 m + 6.925 m, 4H (Ar-H(DMTr); 4.90 bddd + 4.675 bddd, 1H, *J*(3',2')=4.2, *J*(3',2")<1, *J*(3',P)=8.7 + 7.3 (H-3'); 4.00 d + 3.88 d, 1H, *J*(5'a,5'b)=10.3 (H-5'a); 3.72 d + 3.85 d, 1H, *J*(5'b,5'a)=10.3 (H-5'b); 3.64 dh + 3.58 dh, 2H, *J*(CH,P)=10.6, *J*(CH,CH_3)=6.8 (6x) (>N-CH (N-iPr_2)); 3.485 s +3.46 s and 3.45 s + 3.44 s, 6H (2xOMe (DMTr)); 3.465 m + 3.33 m and 3.325 m + 3.22 m, 2H (P-OCH_2); 2.94 s + 3.07 s, 3H (4'-OMe); 2.66 ddd + 2.83 ddd, 1H, *J*(2",1')=6.1, *J*(2",2')=13.8, *J*(2",3')<1 (H-2");
2.23 ddd + 2.31 ddd, 1H, *J*(2',1')=8.8, *J*(2',2")=13.8, *J*(2',3')=4.2 (H-2'); 1.795 d + 1.81 d, 3H, *J*(CH_3,6)=1.2 (5-CH_3); 1.73 m + 1.80 m, 2H (CH_2CN); 1.25 d + 1.15 d and 1.24 d + 1.18 d, 12H, *J*(CH_3,CH)=6.8, 4x CH_3 (N-iPr_2));
^{13}C NMR spectrum (C_6D_6): 162.80 +162.77 (C-4); 158.90 +158.87 and 158.87 + 158.84 (2x Ar-C (DMTr)); 150.45 + 150.64 (C-2); 145.16 + 145.18 (Ar-C (DMTr)); 135.57 + 135.80 and 135.55 + 135.62 (2x Ar-C (DMTr)); 134.69 + 134.76 (C-6); 130.69 + 130.58 and 130.58 + 130.50 (4x Ar-CH (DMTr)); 128.57 + 128.47 (2x Ar-CH (DMTr)); 127.60 (2x Ar-CH (DMTr)); 126.75 + 126.73 (Ar-CH (DMTr); 117.10 + 117.20 (CN); 113.09 + 113.11 and 113.02 + 113.08 (4x Ar-CH (DMTr)); 111.13 + 111.24 (C-5); 110.30 d, *J*(C,P)=7.2 + 110.02 d, *J*(C,P)=6.9 (C-4'); 84.42 + 84.50 (C-1'); 77.92 d, *J*(C,P)=9.0 + 77.04 d, *J*(C,P)=8.4 (C-3');
58.48 d, *J*(C,P)=18.6 + 58.28 d, *J*(C,P)=20.7 (P-OCH_2); 58.40 + 59.88 (C-5'); 54.42 + 54.41 and 54.40 + 54.38 (2xOMe (DMTr)); 48.78 + 49.47 (4'-OMe); 43.38 d, *J*(C,P)= 2.6 + 43.12 d, *J*(C,P)=2.8 (2x N-CH (N-iPr_2)); 37.08 d, *J*(C,P)= 7.9 + 36.58 d, *J*(C,P)= 6.6 (C-2'); 24.33 + 24.23 and 23.97 + 24.23 (4x Me (N-iPr_2)); 19.50 d, *J*(C,P)=7.7 + 19.64 d, *J*(C,P)=7.3 ($\underline{CH_2}$-CN); 12.36 + 12.37 (5-Me).
^{31}P NMR spectrum (C_6D_6): 149.7, 149.82.

4'-(2-Methoxyethoxy)thymidine (10a) and 1-[4-methoxy-α-L-*threo*-pentofuranosyl]-5-methyluracil (10b).
Compound **5** (2.24 g, 10 mmol) was dissolved in anhydrous 2-methoxyethanol (100 ml) and then 70% *m*-chloroperbenzoic acid (5 g, 20 mmol) was added under stirring. After 4 h of stirring at r. t., the solution was concentrated, and the solid residue was treated with boiling diethyl ether (2 x 100 ml). Subsequent chromatography on a reversed phase column using a linear gradient of methanol in water (0-25 %) yielded 0.65 g (21 %) of the compound **10a**, along with 0.32 g (10 %) of **10b** which was not further exploited**.** For **10a**, $C_{13}H_{20}O_7N_2Na$ calculated: 339.11627; found: 339.11620; -0.22302 ppm.
^{1}H NMR spectrum of **10a** (d_6-DMSO): 11.29 bs, 1 H (NH); 7.66 q, 1 H, *J*(6,CH_3) = 1.2 (H-6); 6.12 dd, 1 H, *J*(1',2') = 3.2, *J*(1',2") = 7.7 (H-1'); 5.23 b, 1 H and 4.98 b, 1 H (3'-OH and 5'-OH); 4.42 bt, 1 H, *J*(3',2') = 8.2, *J*(3',2") = 9.1 (H-3'); 3.76 m, 1 H, 3.59 m, 1 H, 3.46 m, 1 H and 3.42 m, 1 H (O-CH_2-CH_2-O); 3.63 d, 1 H, *J*(5'a,5'b) = 11.8 (H-5'a); 3.48 d, 1 H, *J*(5'b,5'a) = 11.8 (H-5'b); 3.26 s, 3 H (OCH_3); 2.26 ddd, 1 H, *J*(2',1') = 7.7, *J*(2",2') = 13.2, *J*(2",3') = 9.1 (H-2'); 2.16 ddd, 1 H, *J*(2',1') = 3.2, *J*(2',2") = 13.2, *J*(2',3') = 8.2 (H-2'); 1.75 d, 3 H, *J*(CH_3,6) = 1.2 (5-CH_3). ^{13}C NMR spectrum of **10a** (d_6-DMSO): 163.92 (C-4); 150.51 (C-2); 136.30 (C-6); 109.42 (C-5); 106.59 (C-4'); 82.27 (C-1'); 71.70 and 61.14 (O-CH_2-CH_2-O); 69.14 (C-3'); 59.84 (C-5'); 58.25 (OCH_3); 37.60 (C-2'); 12.47 (5-CH_3).

2'-Deoxy-5'-*O*-(4,4'-dimethoxytrityl)-4'-(2-methoxyethoxy)thymidine-3'-*O*-(2-cyanoethyl-*N*,*N*-diisopropyl)phosphoramidite (12).

(a) Dimethoxytritylation of 10a. To a stirred solution of **10a** (0.63 g, 2 mmol) in anhydrous pyridine (40 ml), 4,4'-dimethoxytrityl chloride was added in four portions (4 x 0.24 g, 2.8 mmol) during 24 h. The solution was left to stand at room temperature for additional 24 h, then triethylamine (1 ml, 7 mmol) was added, and the solvents were evaporated. The residue was purified on a silica gel column using a linear gradient of ethanol in chloroform (0-4 %) to give 1.16 g (94 %) of **11**, which on checking by TLC was considered of satisfactory purity for the subsequent reaction.

(b) Phosphitylation of 11. Compound **11** (619 mg, 1 mmol) was dried by co-distillation with anhydrous toluene (2 x 15 ml), then it was dissolved in THF (5 ml), and *N*,*N*-diisopropylethylamine (0.68 ml, 3.93 mmol) and 2-cyanoethyl *N*,*N*-diisopropylphosphoramidochloridite (0.40 ml, 1.77 mmol) were subsequently added under argon. The solution was stirred at room temperature for 90 minutes, the mixture then partitioned between ethyl acetate (80 ml) and saturated ice-cold sodium hydrogen carbonate solution (80 ml), and the organic layer was washed with the same solution (3 x 80 ml). Ethyl acetate layer was dried over Na_2SO_4 and the solvent was evaporated with adding toluene. The residue was co-evaporated with anhydrous toluene and purified by flash chromatography on a silica gel column using a linear gradient of ethyl acetate in toluene (0-10 %) to give 566 mg (69 %, 0.41 mmol) of **12** after lyophilisation from benzene. HR-FAB: For $C_{43}H_{55}N_4O_{10}PK$ calculated, 857.3772; found, 857.5016 ($M+K^+$).

^{1}H NMR spectrum (C_6D_6) – two diastereoisomers ~1:1; the most of signals are doubled: 9.66 bs, 1 H (NH); 7.71 q and 7.69 q, 1 H, *J*(6,CH_3) = 1.2 (H-6); 7.62-7.58 m, 4 H and 7.18 m, 1 H (C_6H_5); 7.75 m, 2 H, 7.34-7.31 m, 2 H and 6.92 m, 4 H (2x C_6H_4); 6.68 dd, *J*(1',2') = 3.0, *J* (1',2'') = 8.1 and 6.64 dd, *J*(1',2') = 2.7, *J*(1',2'') = 8.0 (H-1'); 5.36 dt, *J*(3',2') = 8.7, *J*(3',2'') = 9.5, *J*(3',P) = 10.9 and 5.32 q, *J*(3',2') = 8.6, *J*(3',2'') = 9.2, *J*(3',P) = 9.1 (H-3'); 3.987 d, *J*(5'a,5'b) = 9.9 and 3.984 d, *J*(5'a,5'b) = 9.9 (H-5'a); 3.85 m + 3.51 m and 3.77 m + 3.46 m, 2 H (4'-O-CH_2-); 3.64 d, *J*(5'b,5'a') = 9.9 and 3.57 d, *J*(5'b,5'a') = 9.9 (H-5'b); 3.62 m, 2 H (2x N-CH<); 3.50 m, 3.46 m and 3.31 m, 2 H (P-O-CH_2-); 3.45 s, 3.443 s, 3.434 s and 3.428 s (2x OCH_3 (DMTr)); 3.35 m + 3.27 m and 3.27 m + 3.23 m, 2 H (-$\underline{CH_2}$-OMe); 3.23 s and 3.19 s (OCH_3); 2.86 ddd, *J*(2'',1') = 8.1, *J*(2'',2') = 13.6, *J*(2'',3') = 9.2 and 2.81 ddd, *J*(2'',1') = 8.0, *J*(2'',2') = 13.4, *J*(2'',3') = 9.5 (H-2''); 2.64 ddd, *J*(2',1') = 3.0, *J*(2',2'') = 13.6, *J*(2',3') = 8.6 and 2.45 ddd, *J*(2',1') = 2.7, *J*(2',2'') = 13.4, *J*(2',3') = 8.7 (H-2'); 2.11 m + 2.04 m and 1.92 m, 2 H (-CH_2-CN); 1.747 d and 1.689 d, *J*(CH_3,6) = 1.2, 3 H (5-CH_3); 1.26 d, 1.21 d, 1.19 d and 1.18 d, *J* = 6.8 (2x CH($\underline{CH_3}$)$_2$).

^{13}C NMR spectrum (C_6D_6) – two diastereoisomers ~1:1; the most of signals are doubled: 163.36 and 163.30 (C-4); 159.02, 158.99, 158.94, 158.92, 135.47, 135.36, 135.21, 135.09, 128.44, 128.42, 127.86, 127.82, 113.24, 113.22, 113.19 and 113.15 (2x C_6H_4); 150.33 and 150.20 (C-2); 144.75, 144.60, 130.46, 130.41, 130.38, 130.34, 127.02 and 126.93 (C_6H_5); 135.14 and 134.73 (C-6); 117.33 and 117.32 (CN); 111.08 and 111.06 (C-5); 106.19 d, *J*(C,P) = 7.3 and 106.18 d, *J*(C,P) = 5.3 (C-4'); 87.09 and 87.05 (>C< (DMTr)); 83.45 and 83.25 (C-1'); 71.83 d, *J*(C,P) = 14.5 and 70.34 d, *J*(C,P) = 19.9 (C-3'); 71.63, 71.55, 61.62 and 61.52 (O-CH_2-CH_2-O); 62.04 and 61.68 (C-5'); 58.79 d, *J*(C,P) = 15.9 and 57.74 d, *J*(C,P) = 19.2 (P-O-CH_2-); 58.22 and 58.15 (OCH_3); 54.41, 54.40 and 54.34 (2 x OCH_3 (DMTr)); 43.13 d, *J*(C,P) = 12.8 and 43.03 d, *J*(C,P) = 12.7 (2x N-CH<); 37.41 d, *J*(C,P) = 2.7 and 36.94 d, *J*(C,P) = 2.5 (C-2'); 24.26 d, *J*(C,P) = 7.8, 24.24 d, *J*(C,P) = 6.8, 24.16 d, *J*(C,P) = 6.7 and 24.14 d, *J*(C,P) = 8.1 (2x CH($\underline{CH_3}$)$_2$); 19.61 d, *J*(C,P) = 6.5 and 19.44 d, *J*(C,P) = 5.1 (-$\underline{CH_2}$-CN); 11.75 and 11.72 (5-CH_3).

^{31}P NMR spectrum (C_6D_6): 151.72, 150.55.

2. NMR data, and conformation analysis of compounds 3a and 3b

The configuration at carbon C(4') and the preferred orientation of thymine in compounds **3a** and **3b** were determined from the observed NOE contacts in 2D-H,H-ROESY spectra in DMSO (see Figure S1). The absence of hydrogen at position 4' reduces the number of proton vicinal couplings and limits a common NMR conformation analysis using PSEUROT[3] program. Therefore, we used an approximate method described for the estimation of the population of "south"–type conformer (usually C(2')-*endo*) based on the relation [1], as described for deoxyribo-nucleosides by Rinkel and Altona.[4]

(%) south C(2')-*endo* conformer = [31.5 - *J*(1',2") – *J*(2',2") – *J*(2",3')] / 10.9] x 100 [1]

The observed *J*-values in **3a** (Figure S1) then lead to a high preference of the "north"- type C(3')-*endo* conformation (84 %). On the other hand, the observed *J*-values in **3b** indicate a high population of the "south"- type C(2')-*endo* conformer (83 %).

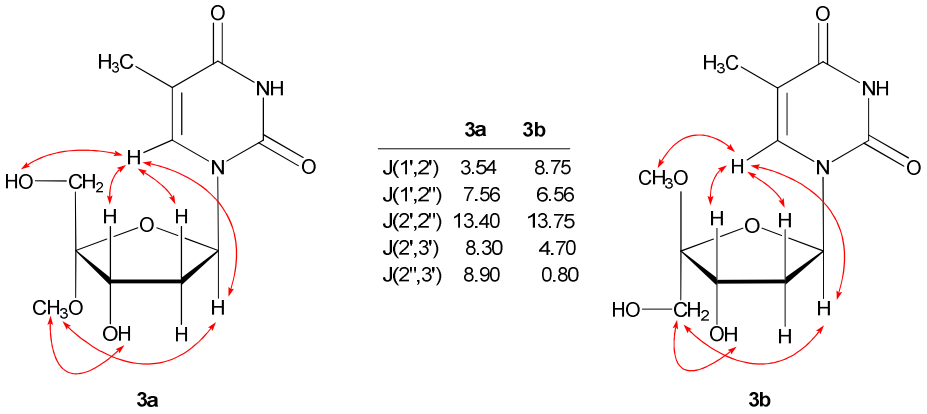

	3a	3b
J(1',2')	3.54	8.75
J(1',2")	7.56	6.56
J(2',2")	13.40	13.75
J(2',3')	8.30	4.70
J(2",3')	8.90	0.80

Figure S1. The selected nontrivial NOEs (shown with red arrows) and vicinal proton couplings in furanose ring observed in compounds **3a** and **3b** in DMSO.

4'-Methoxythymidine (3a)
^{1}H NMR spectrum (600 MHz; d_6-DMSO): 11.30 bs, 1H (NH); 7.66 q, 1H, *J*(6,CH_3) = 1.3 (H-6); 6.12 dd, 1H, *J*(1',2') = 3.5, *J*(1', 2") = 7.5 (H-1'); 5.21 dd, 1H, *J*(OH,5'a) = 5.5, *J*(OH,5'b) = 5.8 (5'-OH); 4.91 d, 1H, *J*(OH,3') = 7.0 (3'-OH); 4.42 ddd, 1H, *J*(3',OH) = 7.0, *J*(3',2') = 8.3, *J*(3',2") = 8.9 (H-3'); 3.65 dd, 1H, *J*(5'a,OH) = 5.5, *J*(5'a,5'b) = 11.7 (H-5'a); 3.47 dd, 1H, *J*(5'b,OH) = 5.8, *J*(5'b,5'a) = 11.7 (H-5'b); 3.28 s, 3H (OCH_3); 2.24 ddd, 1H, *J*(2",1') = 7.5, *J*(2",2') = 13.4, *J*(2",3') = 8.9 (H-2"); 2.18 ddd, 1H, *J*(2',1') = 3.5, *J*(2',2") = 13.4, *J*(2',3') = 8.3 (H-2'); 1.76 d, 3H, *J*(CH_3,6) = 1.3 (5-CH_3). ^{13}C NMR spectrum (150.9 MHz; d_6-DMSO): 163.98 (C-4); 150.58 (C-2); 138.36 (C-6); 109.49 (C-5); 106.58 (C-4'); 82.30 (C-1'); 69.22 (C-3'); 59.40 (C-5'); 49.63 (4'-OCH_3); 37.70 (C-2'); 12.52 (5-CH_3).

1-[2-Deoxy-4-methoxy-α-L-*threo*-pentofuranosyl]thymine (3b)
^{1}H NMR spectrum (600 MHz; d_6-DMSO): 11.35 bs, 1H (NH); 7.30 q, 1H, *J*(6,CH_3) = 1.3 (H-6); 6.44 dd, 1H, *J*(1',2') = 8.7, *J*(1', 2") = 6.5 (H-1'); 5.38 d, 1H, *J*(OH,3') = 5.0 (3'-OH); 4.65 dd, 1H, *J*(OH,5'a) = 5.8, *J*(OH,5'b) = 6.0 (5'-OH); 4.08 bt, 1H, *J*(3',OH) = 5.0, *J*(3',2') = 4.7, *J*(3',2") < 1 (H-3'); 3.62 dd, 1H, *J*(5'a,OH) = 5.8, *J*(5'a,5'b) = 12.1 (H-5'a); 3.57 dd, 1H, *J*(5'b,OH) = 6.0, *J*(5'b,5'a) = 12.1 (H-5'b); 3.24 s, 3H (OCH_3); 2.33 ddd, 1H, *J*(2',1') = 8.7, *J*(2',2") = 13.7, *J*(2',3') = 4.7 (H-2'); 2.10 bdd, 1H, *J*(2",1') = 6.5, *J*(2",2') = 13.7, *J*(2",3') < 1 (H-2"); 1.80 d, 3H, *J*(CH_3,6) = 1.3 (5-CH_3). ^{13}C NMR spectrum (150.9 MHz; d_6-DMSO):

163.74 (C-4); 151.02 (C-2); 135.96 (C-6); 111.12 (C-4'); 110.46 (C-5); 84.32 (C-1'); 73.69 (C-3'); 55.62 (C-5'); 48.54 (4'-OCH_3); 37.62 (C-2'); 12.58 (5-CH_3).

We also performed the ^{1}H NMR measurements of **3a** and **3b** in different solvents ($CDCl_3$, DMSO-d_6 and D_2O) and different temperatures (D_2O solutions at +7 °C, +27 °C, and +47 °C; see Tables S2 and S3). The change of solvent, as well as temperature, did not significantly change the conformer ratio, calculated using the relation [1].

Although the missing coupling constant J(3',4') limits fitting of the experimental data by PSEUROT, we tried an alternative approach consisting in systematical stepwise changing of the north/south conformer ratio from 0:100 to 100:0 by 10 % per step and optimising all remaining parameters – phase angle P and pucker amplitude ϕ_{max}. Using this approach, we calculated the pseudorotation parameters of **3a** and **3b** in different solvents (Table S4). The sets of coupling constants obtained in D_2O at +7 °C, +27 °C and +47 °C enabled us to perform the PSEUROT conformation analysis and fit all the pseudorotation parameters, supposing that only the population of conformers changes with temperature (Table S5). The results show that the effect of solvent as well as temperature on the conformation is very small for both nucleosides **3a** and **3b**.

In order to support the results obtained from the ^{1}H NMR conformation analysis using vicinal proton coupling constant, we decided to explore the conformation behaviour of compounds **3a** and **3b** by molecular modelling. We used the well-known concept of pseudorotation[5] for the sugar ring conformation of nucleosides. First, we performed "pucker-scan" that gave us information about optimal pucker amplitudes ϕ_{max} for the next step – the conformation analysis. For this purpose, we generated 13 conformers with phase angle P = 180° ($_3T^2$ conformation) and ϕ_{max} stepwise changing from 0° to 60° by 5° per step. Geometries with restrained endocyclic torsion angles ϕ_0 and ϕ_3 were taken for geometry optimisation (B3LYP/6-31G** *in vacuo*). Optimal pucker amplitudes ϕ_{max} = 30° for **3a** and ϕ_{max} = 35° for **3b** were found as the energy minima on a curve of the calculated energy versus ϕ_{max} (see Figure S2).

In the next step, for each nucleoside **3a** and **3b** (with its optimised ϕ_{max}) we generated a set of 20 conformers covering the whole pseudorotation pathway in 18 degree steps representing the envelope and twisted conformations with two restricted endocyclic dihedral angles ϕ_0 and ϕ_3. The geometry of the molecule was optimised for each conformer using DFT/B3LYP/6-31G** theory level. Predominant conformations can be found as the energy minima by plotting calculated energy against the phase angle P (Figure S3). The energy minima were

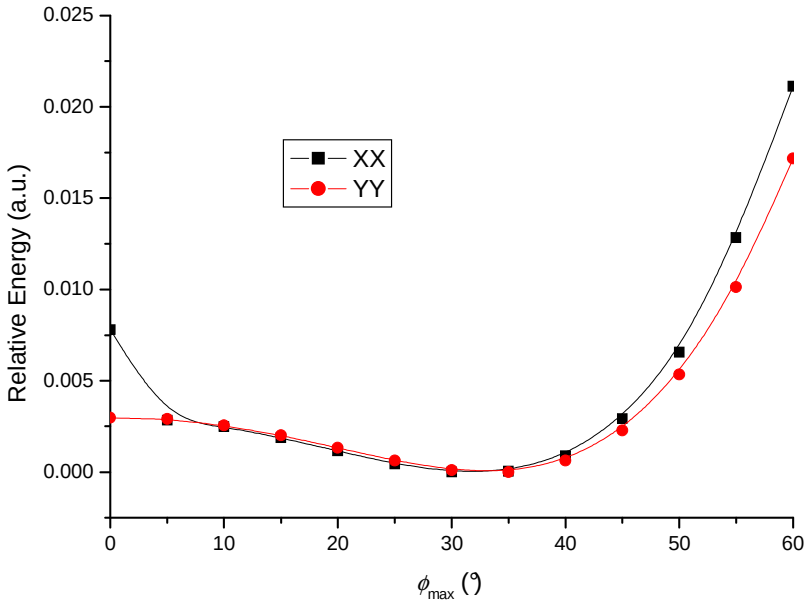

Figure S2. Pucker-scan for furanose ring in nucleoside **3a** and **3b**.

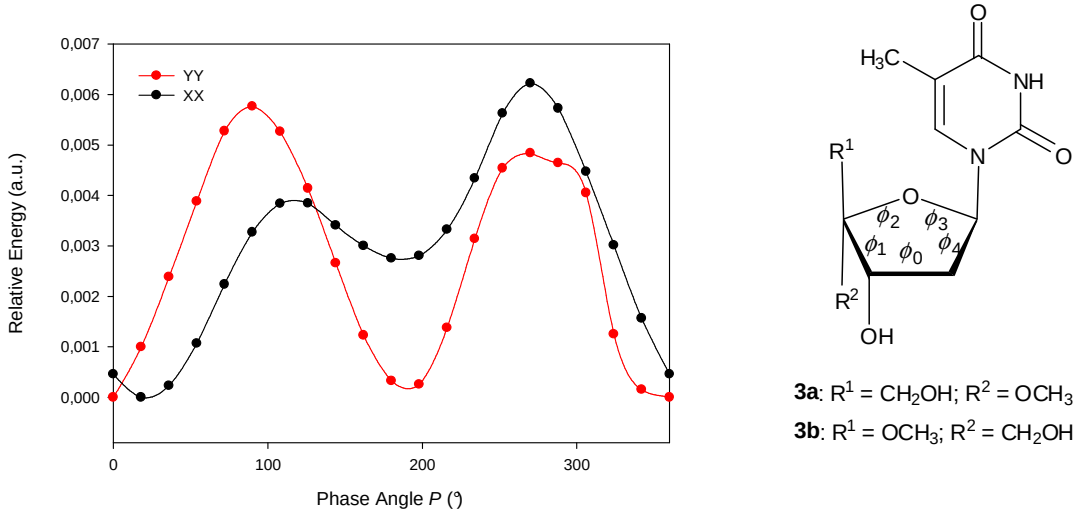

Figure S3. (a) Conformation analysis of furanose ring in **3a** and **3b** by DFT calculation; (b) definition of endocyclic torsion angles ϕ_0 to ϕ_4.

then fully optimised *in vacuo* (DFT/B3LYP/6-31G**) and in water (DFT/B3LYP/6-31G* with PCM model for solvation) and Gibbs free energy was calculated for such two predominant conformers. Equilibrium constants were then calculated providing population of "north" and "south" conformers for both **3a** and **3b** nucleosides. The results of conformation analysis are shown in Table S6. The populations obtained by this procedure were in very good agreement with the results obtained from the NMR data.

Table S2. Proton coupling constants of nucleosides **3a** and **3b** in $CDCl_3$, DMSO and D_2O at +27 °C and calculated ratio of "south" and "north" conformer using relation [1]

Compound	Solvent	*J*(1',2')	*J*(1',2")	*J*(2',2")	*J*(2',3')	*J*(2",3')	South / North (%)
3a	$CDCl_3$	5.28	6.54	13.86	7.95	7.74	31 : 69
	DMSO	3.54	7.56	13.40	8.30	8.90	15 : 85
	D_2O	4.56	6.80	14.02	8.70	8.90	16 : 84
3b	$CDCl_3$	8.13	6.80	14.18	4.68	1.60	82 : 18
	DMSO	8.75	6.56	13.75	4.70	0.80	95 : 5
	D_2O	8.34	6.84	14.70	5.04	0.87	83 : 17

Table S3. Proton coupling constants of nucleosides **3a** and **3b** in D_2O at +7 °C, +27 °C and +47 °C and calculated ratio of "south" and "north" conformer using relation [1]

Compound	Temp.	*J*(1',2')	*J*(1',2")	*J*(2',2")	*J*(2',3')	*J*(2",3')	South / North (%)
3a	7 °C	4.32	7.09	14.05	8.82	9.07	12 : 88
	27 °C	4.56	6.80	14.02	8.70	8.90	16 : 84
	47 °C	4.86	6.65	14.05	8.76	8.83	18 : 82
3b	7 °C	8.40	6.84	14.70	5.04	0.80	84 : 16
	27 °C	8.34	6.84	14.70	5.04	0.87	83 : 17
	47 °C	8.28	6.87	14.73	5.16	0.90	83 : 17

Table S4. Conformation analysis using PSEUROT and experimental ^3J(H,H) from Table S2.

Compound	Solvent	*P* (N) [deg]	ϕ_{max} (N) [deg]	*X* (N) [%]	*P* (S) [deg]	ϕ_{max} (S) [deg]	*X* (S) [%]	rms [Hz]
3a	$CDCl_3$	61	44	100	192	45	0	0.927
	DMSO	48	41	100	192	45	0	0.678
	D_2O	55	44	100	192	45	0	1.061
3b	$CDCl_3$	-10	35	8	196	38	92	0.246
	DMSO	-10	35	0	196	38	100	0.253
	D_2O	-10	35	0	196	38	100	0.290

Table S5. Conformation analysis using PSEUROT and three sets of ^3J(H,H) at +7 °C, +27 °C and +47 °C in D_2O from Table S3.

Compound	Temp.	*P* (N) [deg]	ϕ_{max} (N) [deg]	*X* (N) [%]	*P* (S) [deg]	ϕ_{max} (S) [deg]	*X* (S) [%]	rms [Hz]
3a	7 °C			91			9	1.513
	27 °C	32	41	90	186	40	10	1.581
	47 °C			90			10	1.711
3b	7 °C			1			99	0.176
	27 °C	-27	44	2	199	37	98	0.174
	47 °C			2			92	0.152

Table S6 Results of conformation analysis of furanose ring in compound **3a** and **3b** using molecular modeling in water and *in vacuo* (values in brackets).

Compound	Conformer	P [deg]	ϕ_{max} [deg]	rel ΔG [a] [kcal/mol]	X_{calc} [b] [%]	X_{NMR} [c] [%]
3a	north	53 (31)	40 (36)	0 (0)	98 (97)	84
	south	192 (186)	34 (33)	2.31 (2.10)	2 (3)	16
3b	north	345 (353)	30 (34)	0.99 (0.31)	16 (37)	17
	south	196 (193)	38 (33)	0 (0)	84 (63)	83

[a] rel ΔG – difference between Gibbs free energies of optimised conformers (for more stable conformer $G = 0$)
[b] X_{calc} – percentage of conformer calculated from rel ΔG (at 25 °C)
[c] X_{NMR} – percentage of conformer in D_2O at 27 °C calculated from ^3J(H,H) using relation [1]

3. Copies of 1H and 13C NMR spectra

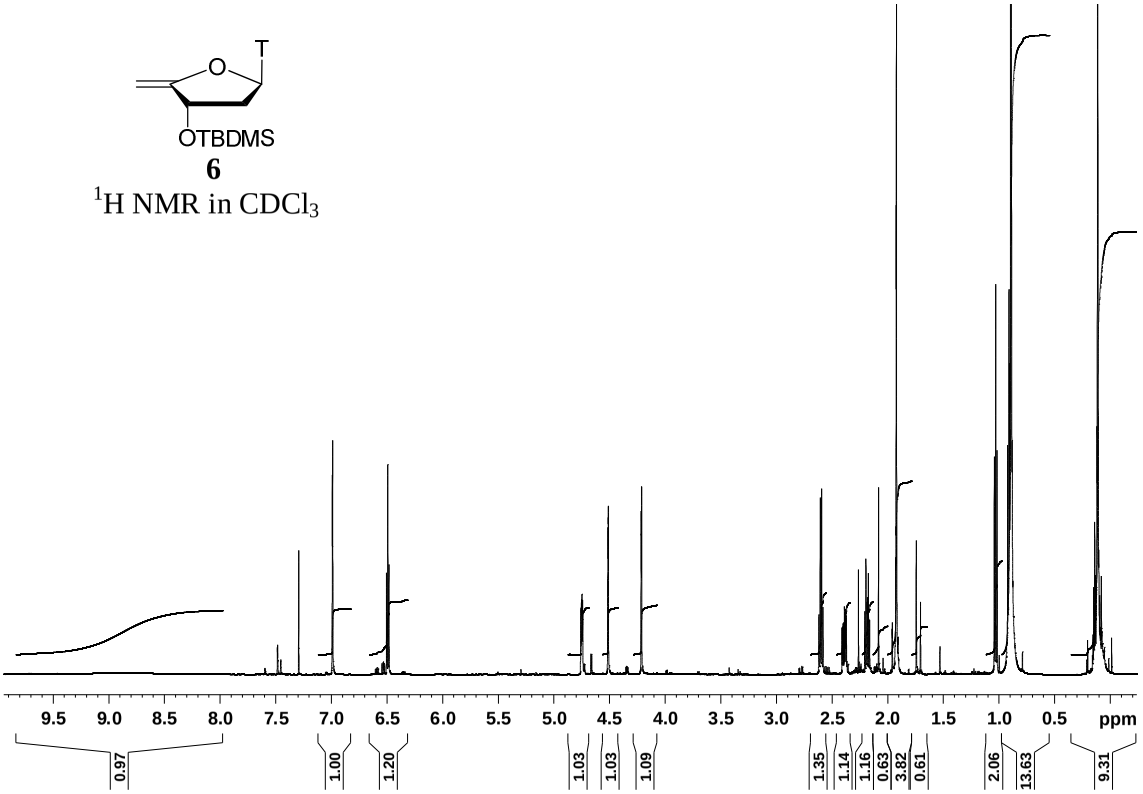

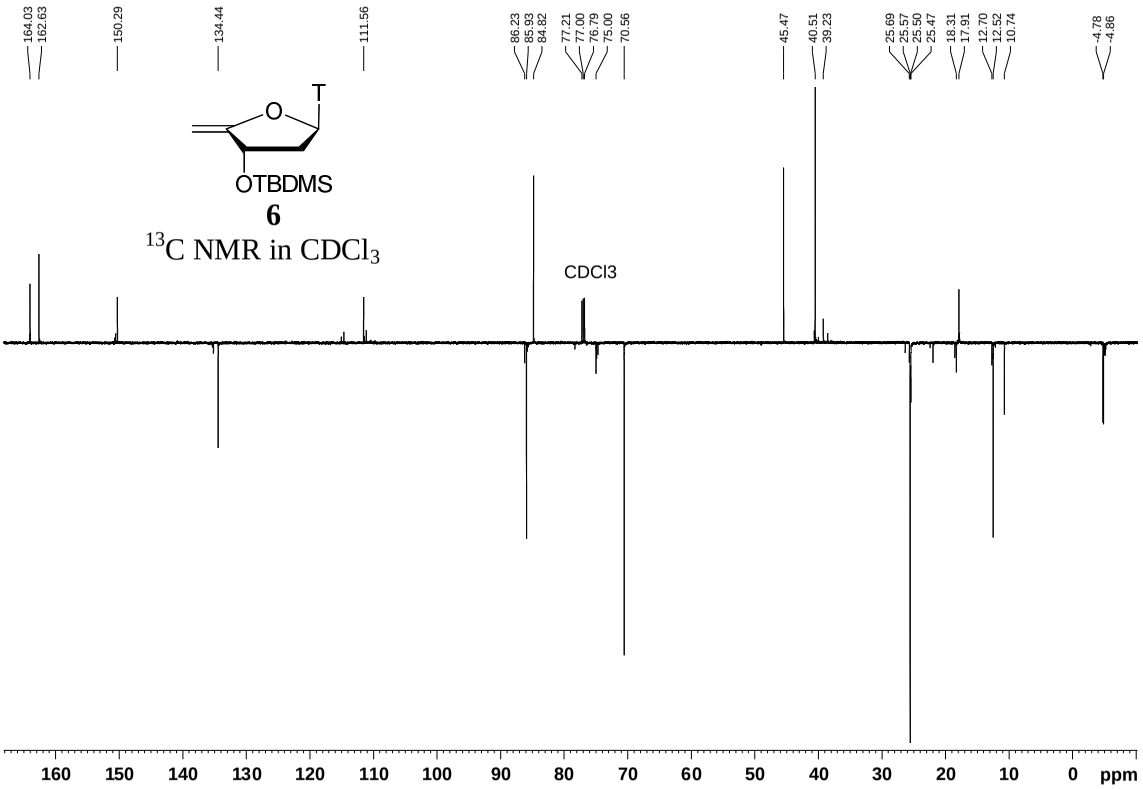

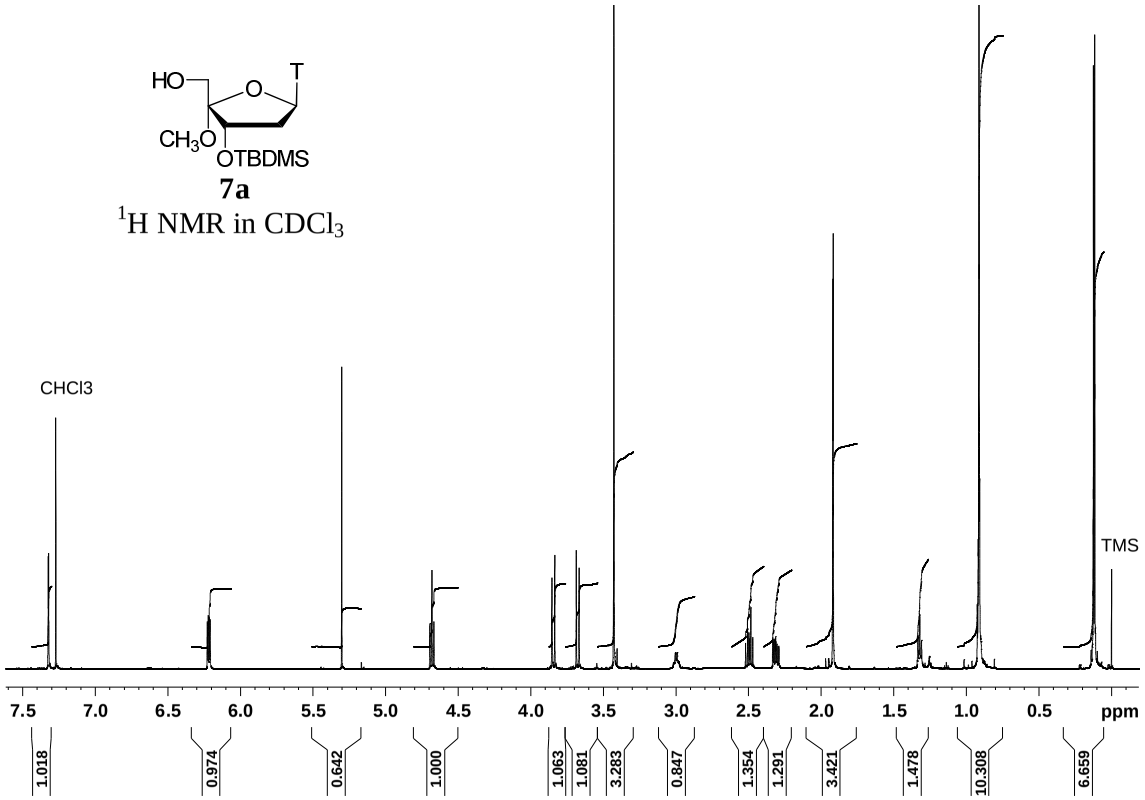

7a

^{1}H NMR in $CDCl_3$

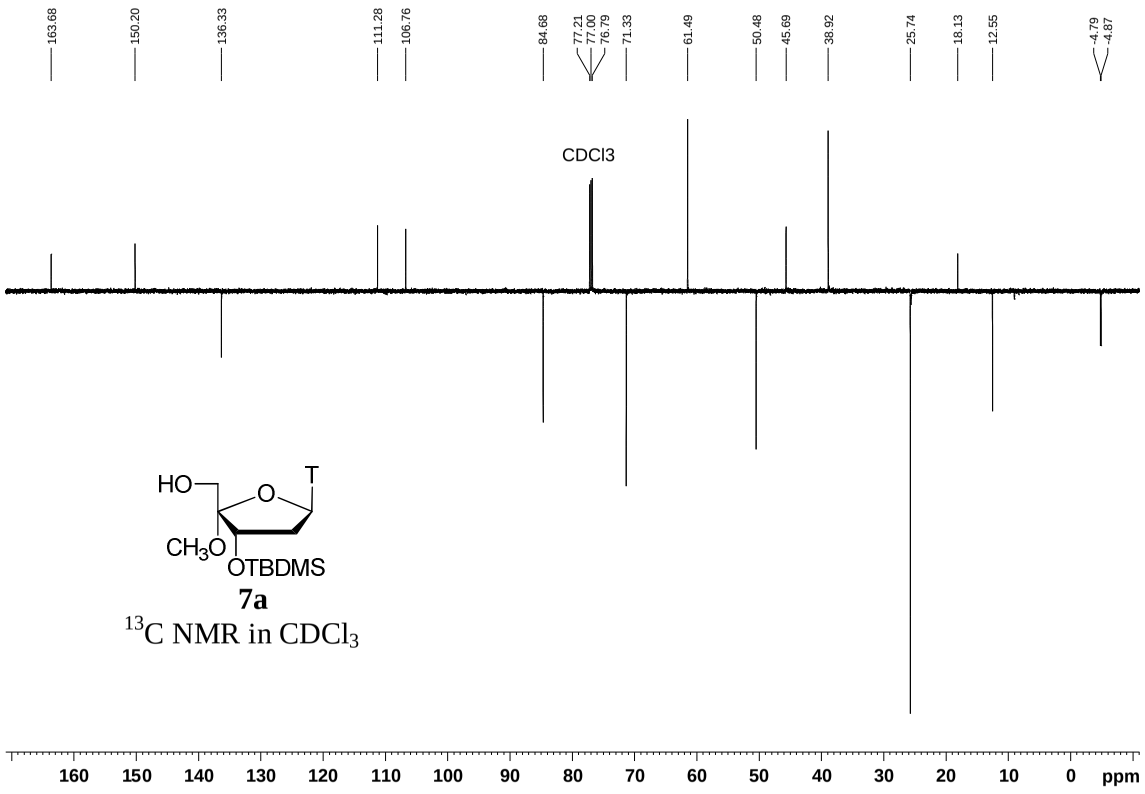

7a

^{13}C NMR in $CDCl_3$

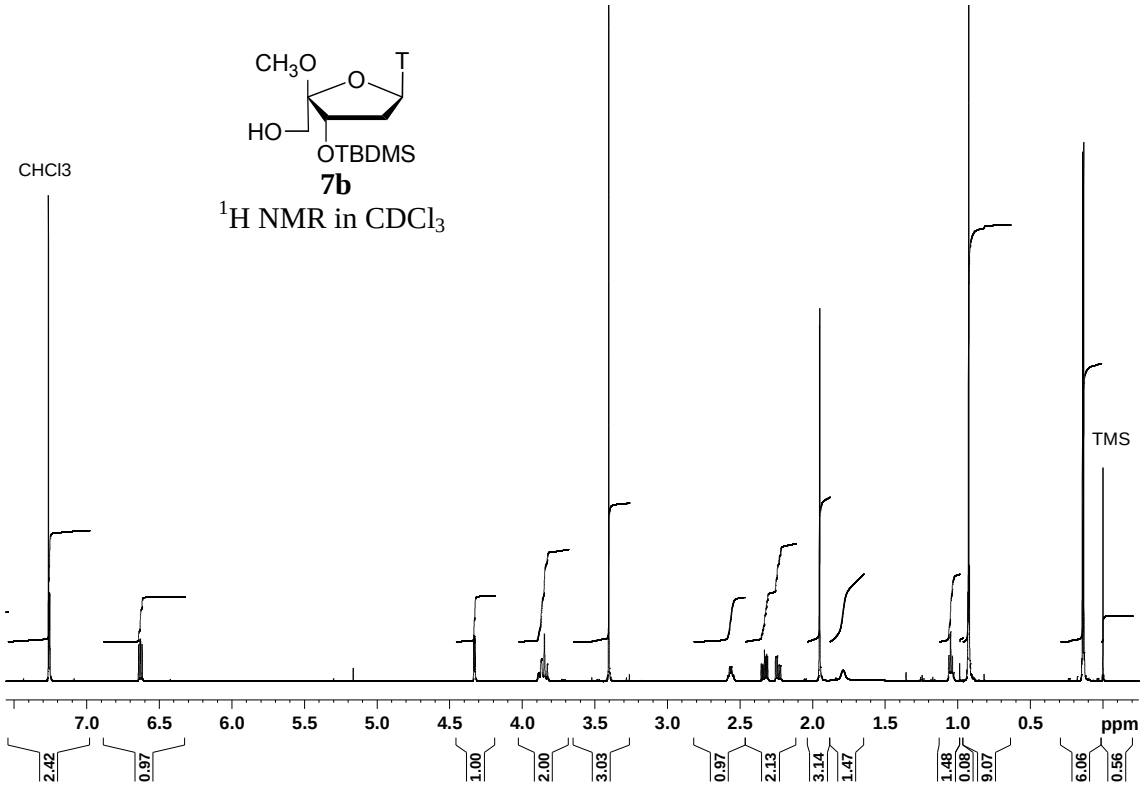

7b

^{1}H NMR in $CDCl_3$

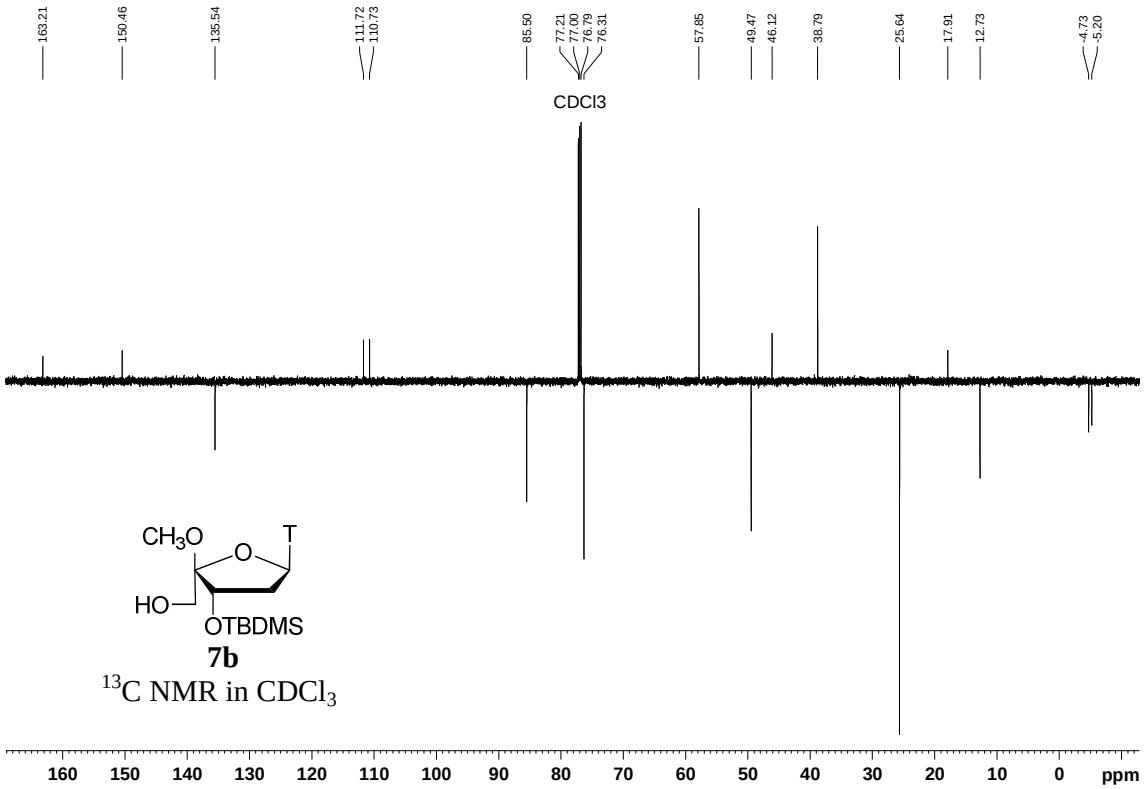

7b

^{13}C NMR in $CDCl_3$

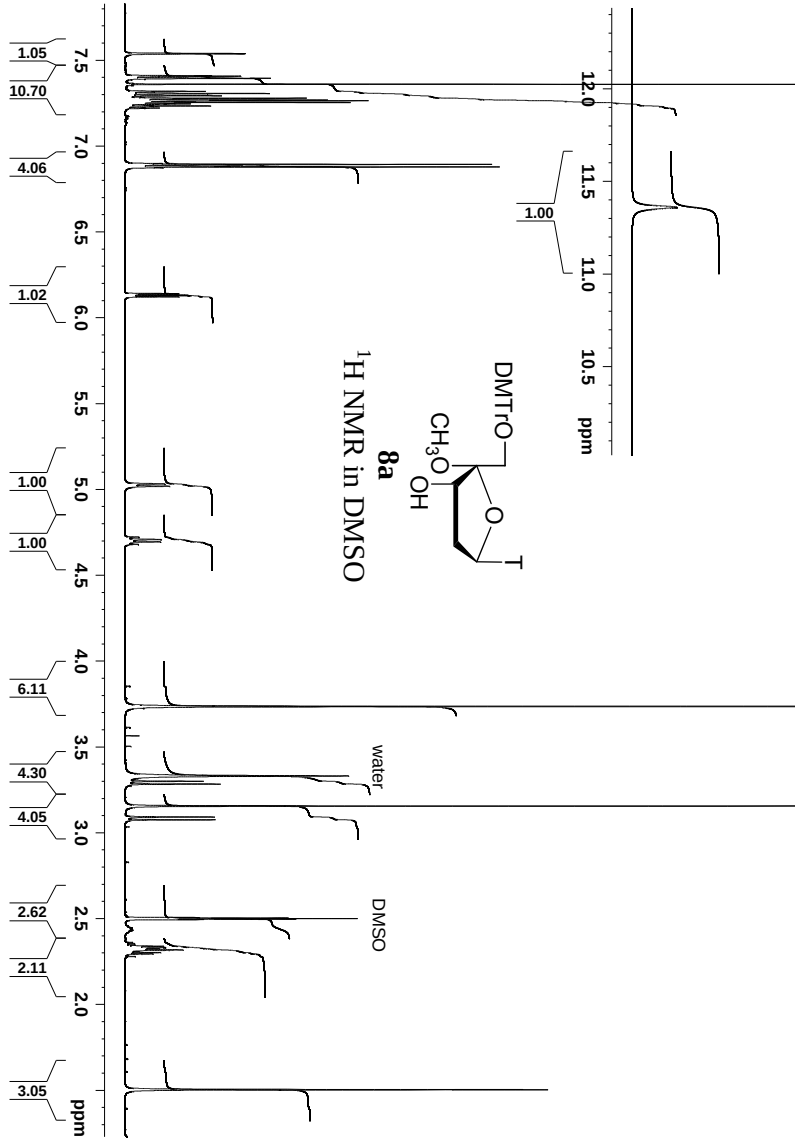

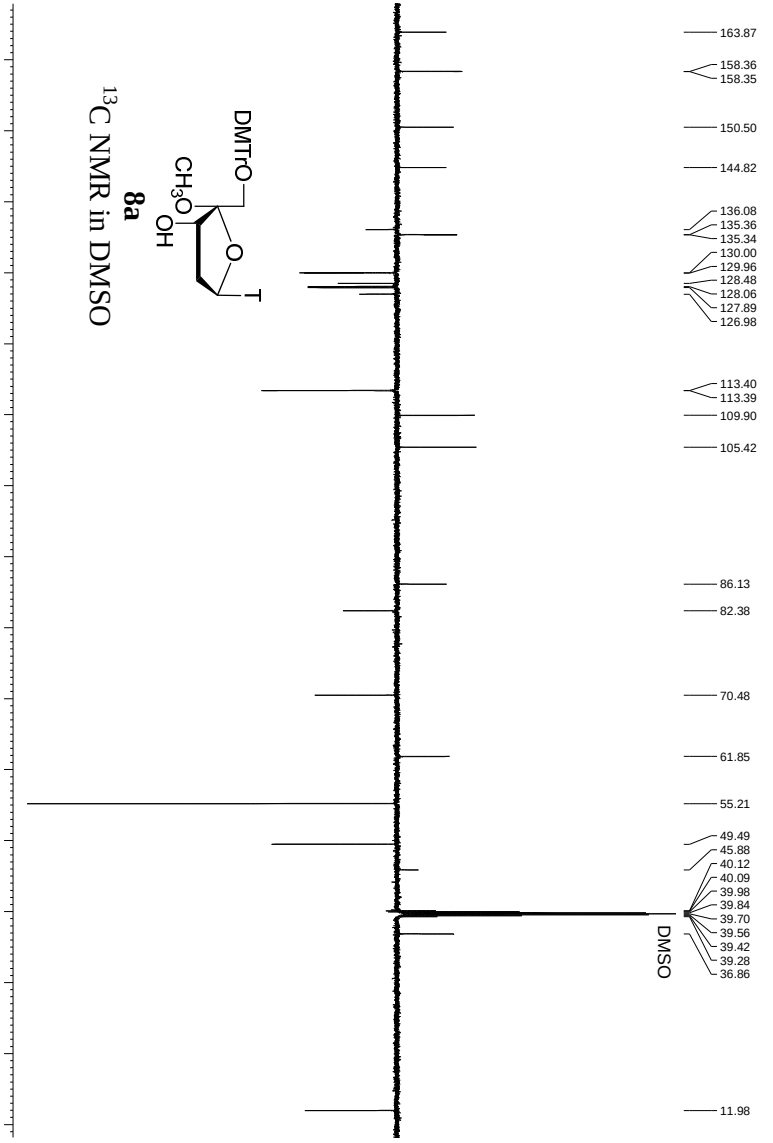

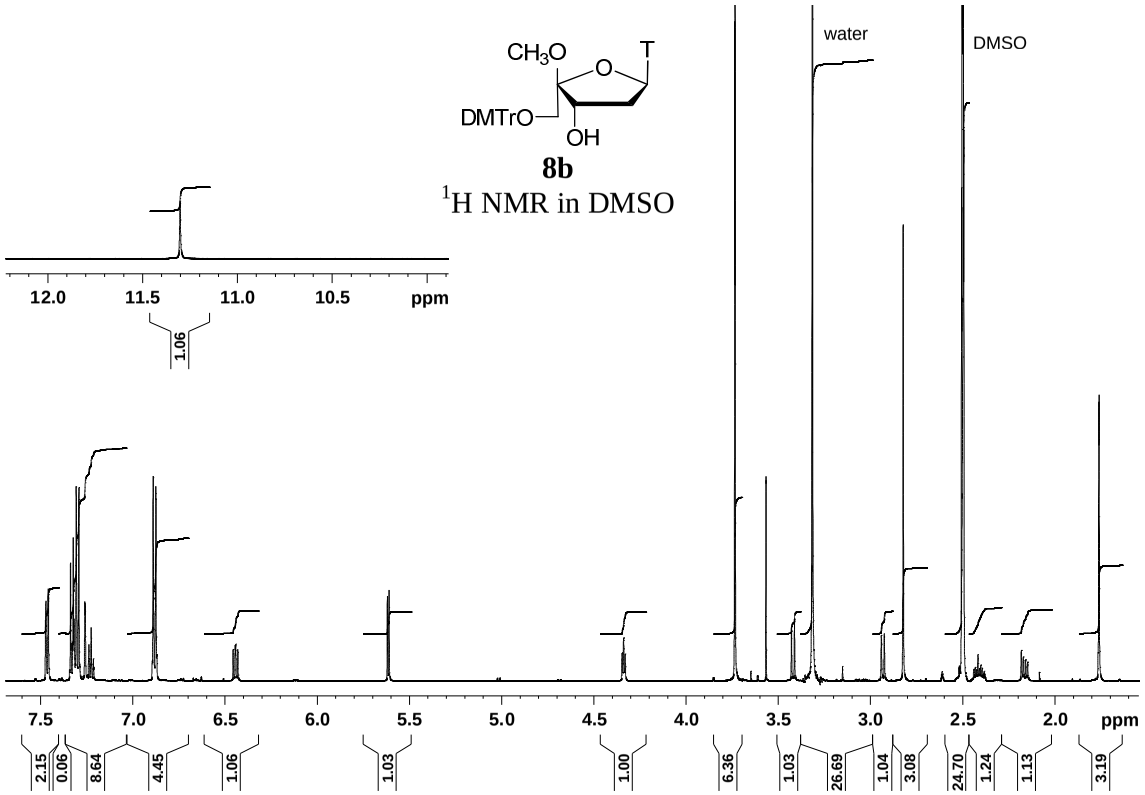

8b

^{1}H NMR in DMSO

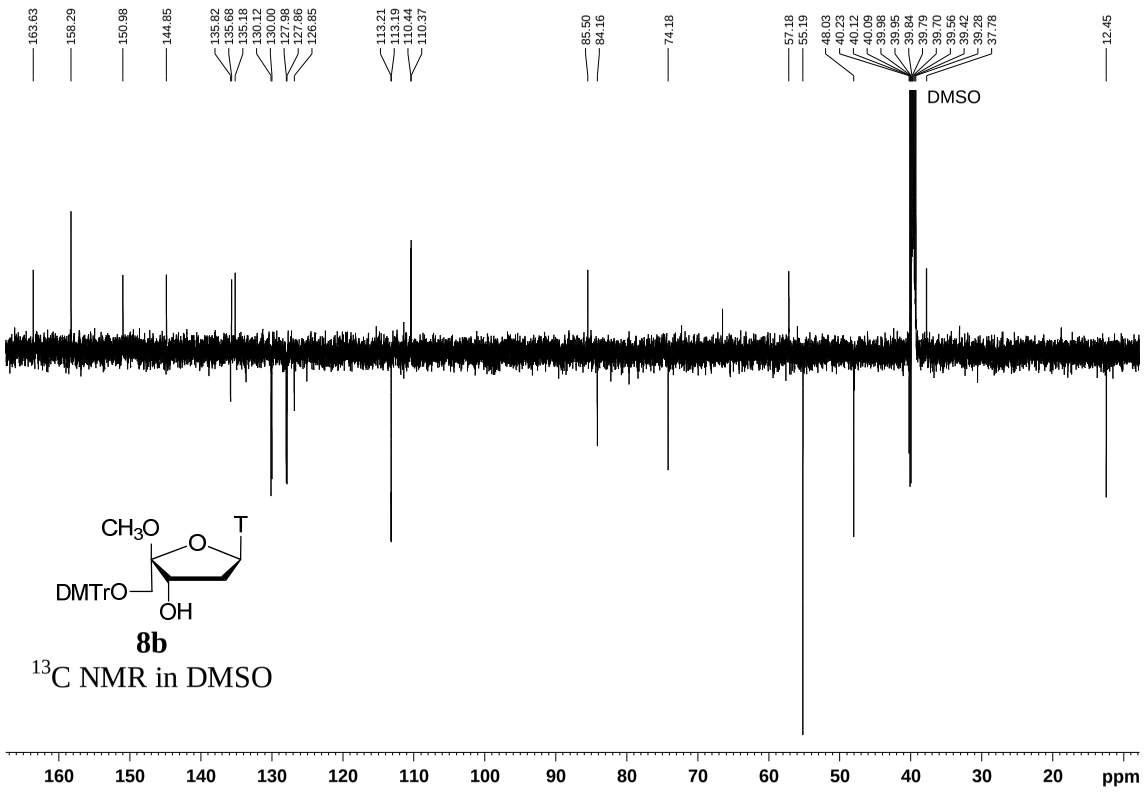

8b

^{13}C NMR in DMSO

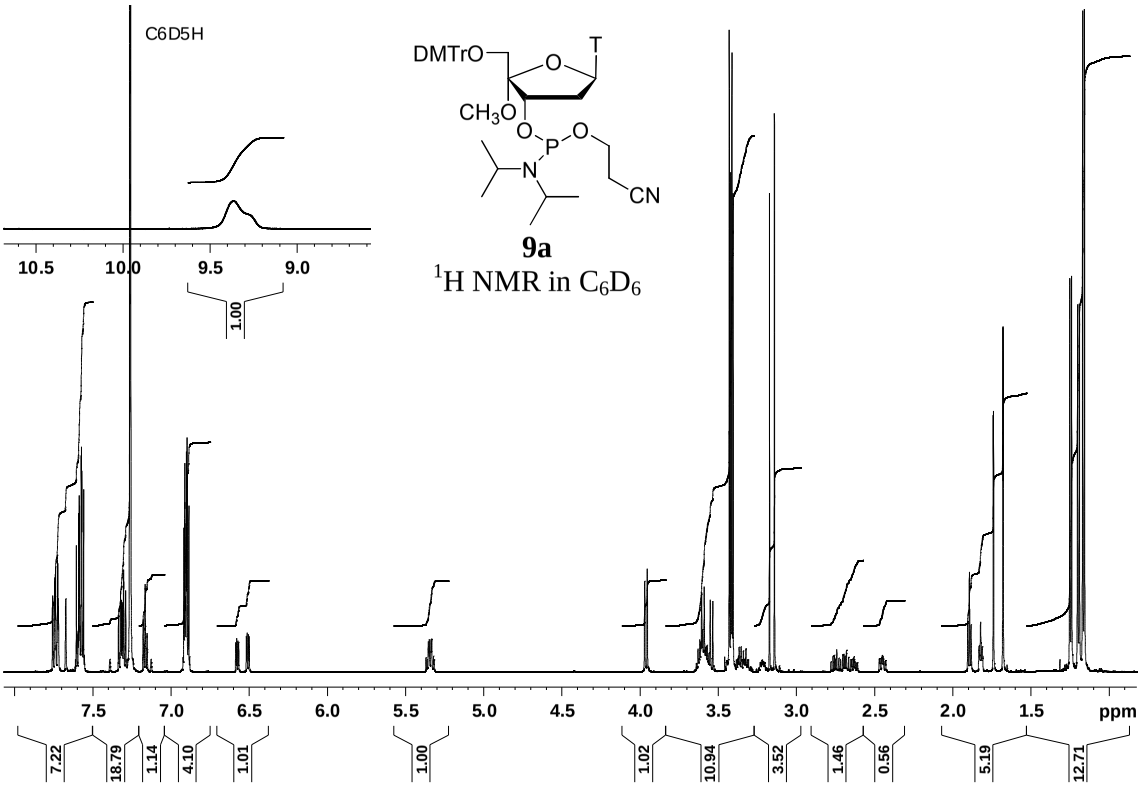

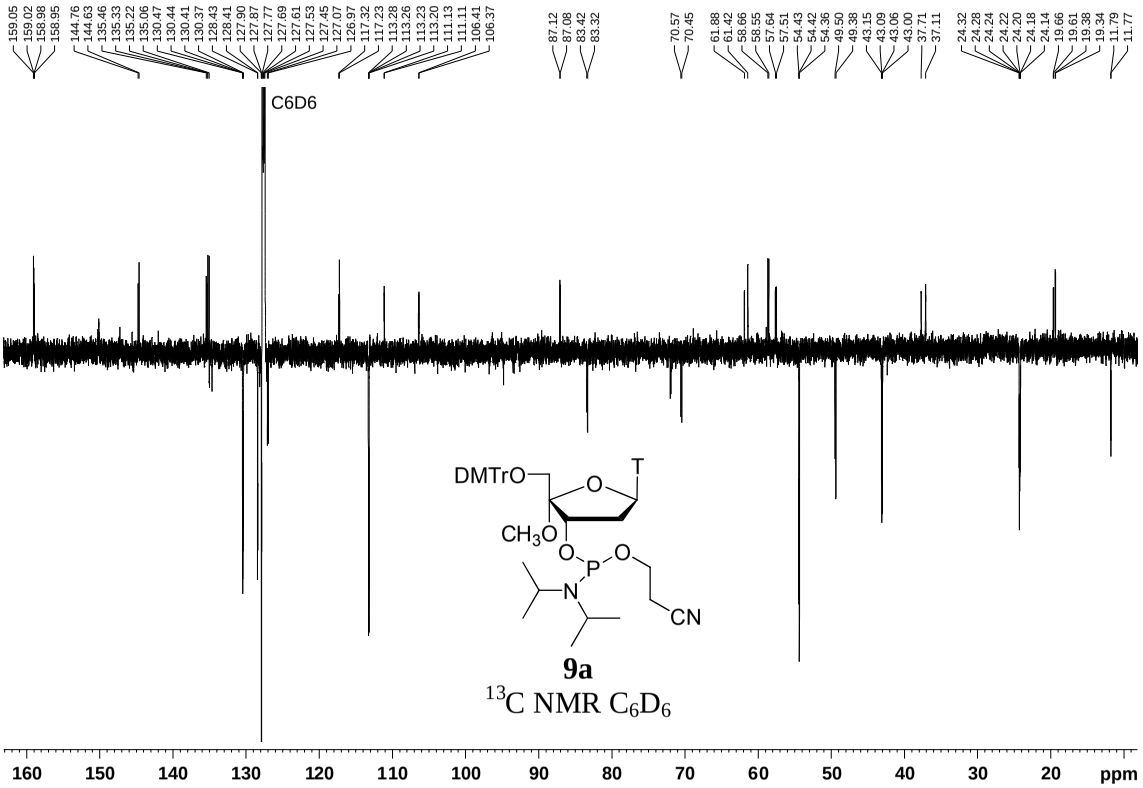

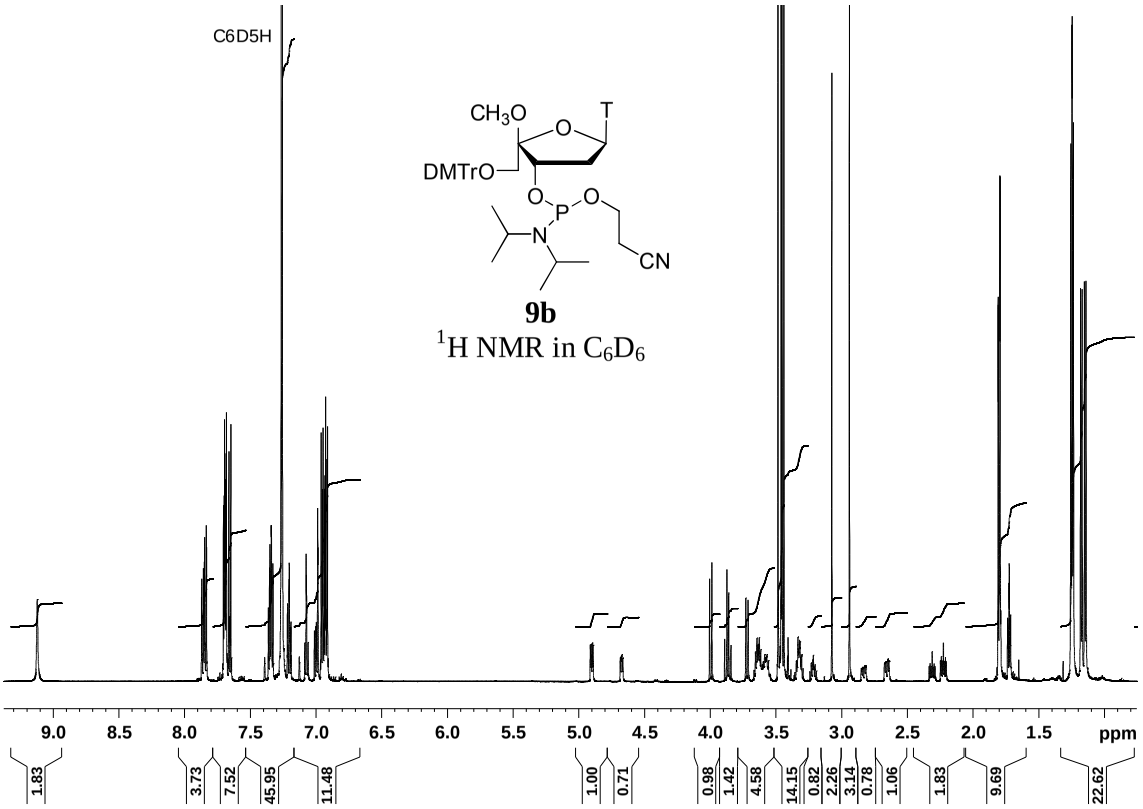

9b

^{1}H NMR in C_6D_6

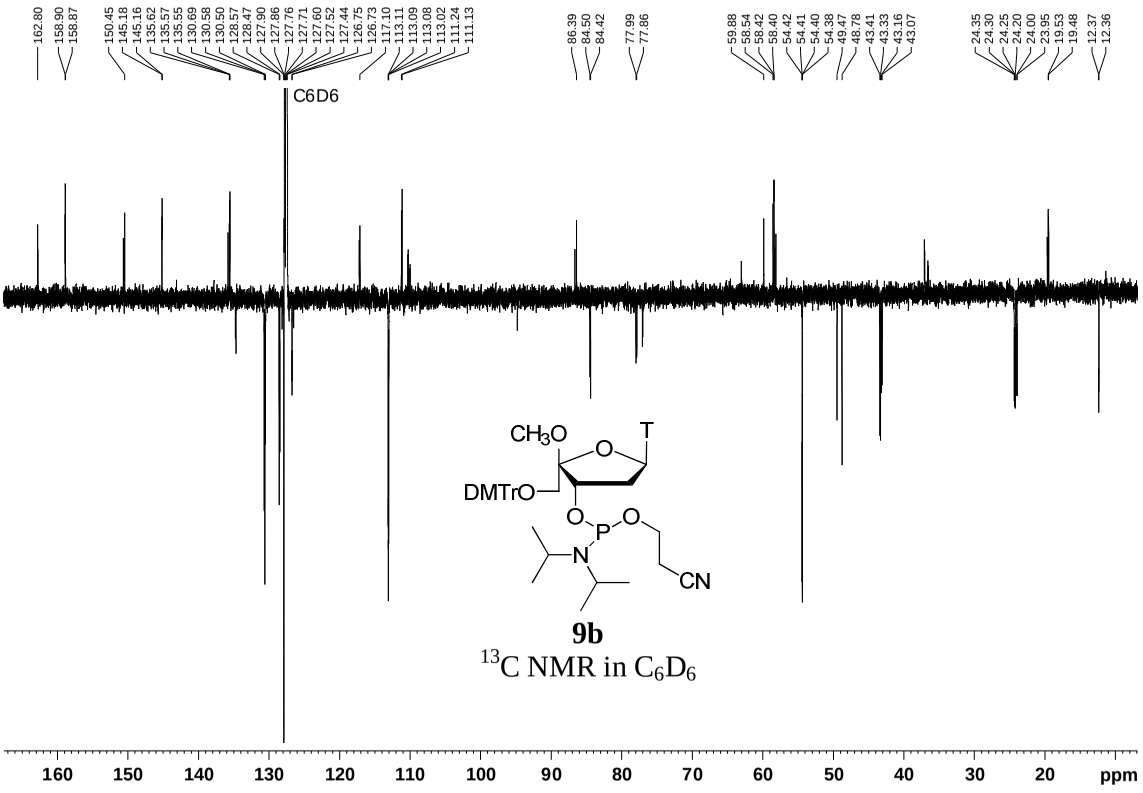

9b

^{13}C NMR in C_6D_6

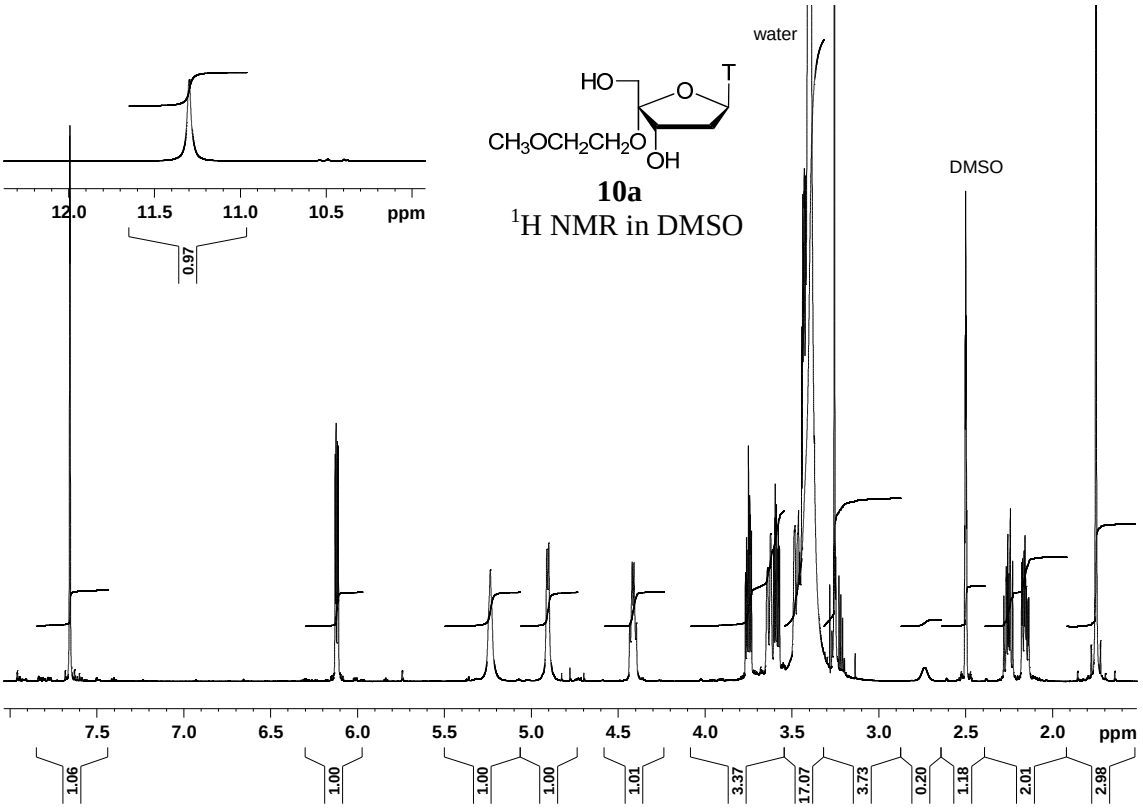

10a

^{1}H NMR in DMSO

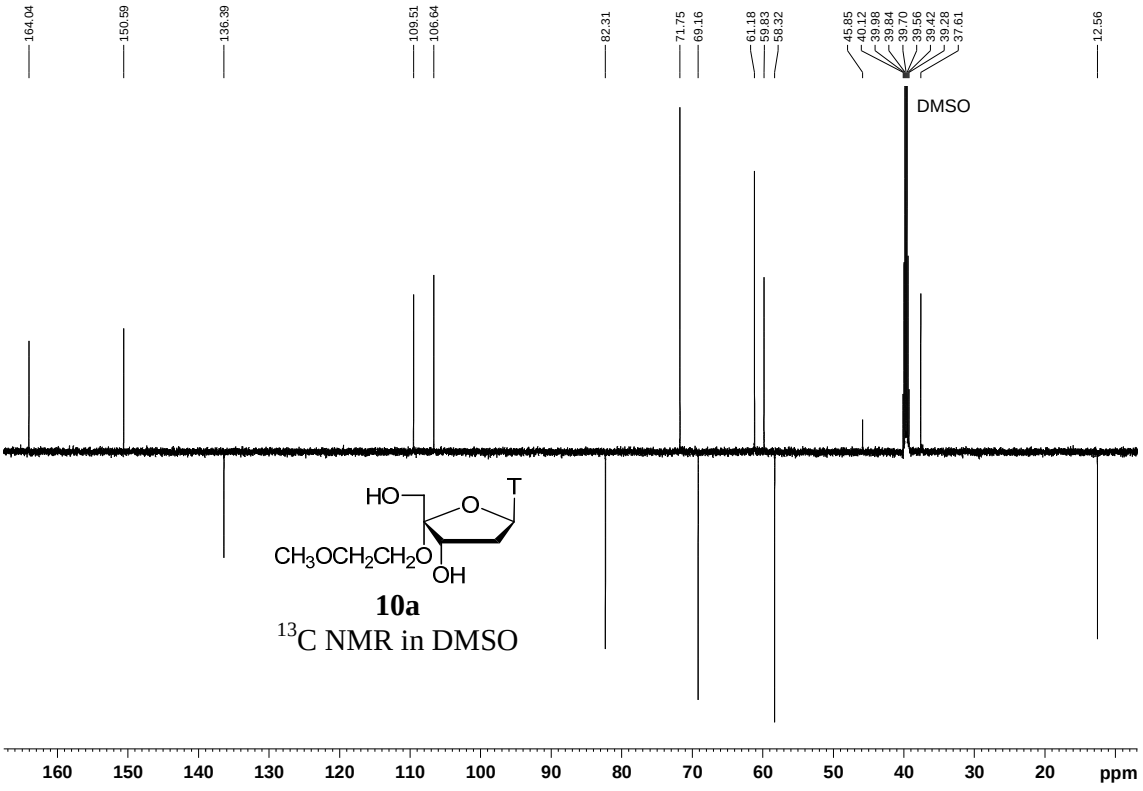

10a

^{13}C NMR in DMSO

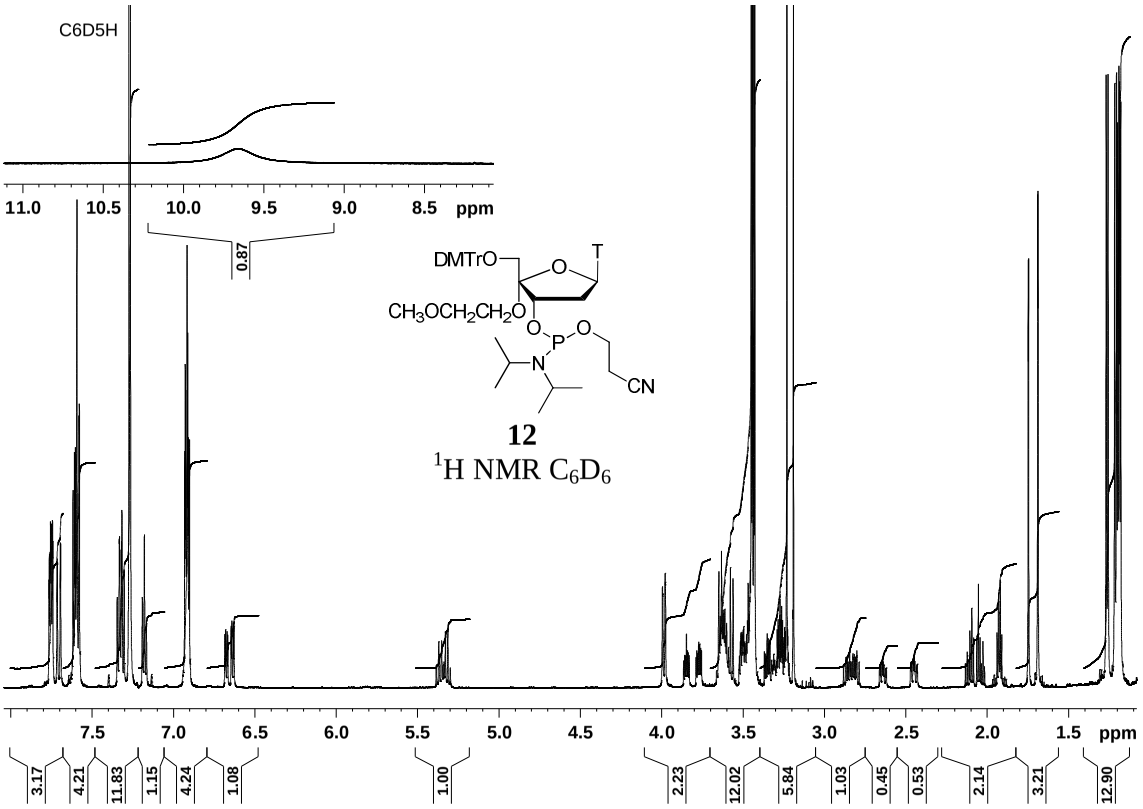

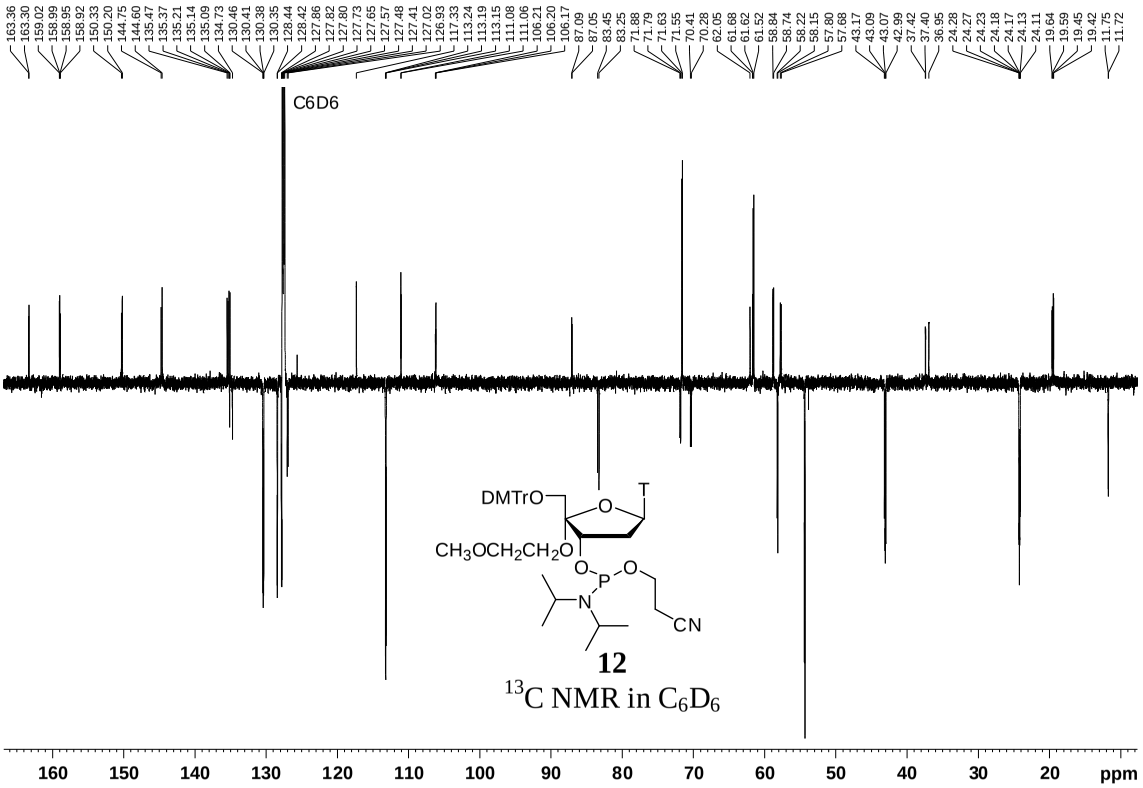

4. Hybridisation study - measurement of T_m values (Table 1)

Thermal experiments were performed at 260 and 295 nm on a CARY 100 Bio UV Spectrophotometer (Varian Inc.) equipped with a Peltier temperature controller and thermal analysis software. The samples were prepared by mixing of equal molar amounts of modified T_{15} and natural dA_{15} (or rA_{15}) strands to give a 4 μM final concentration in 50 mM TRIS-HCl pH 7.2, 1 mM EDTA either with 100 mM Na^+ or 10 mM Mg^{2+} ions. A heating-cooling cycle in the range 18–70 °C with a gradient of 0.2 °C/min was applied. T_m values were determined from the maxima of the first derivative plots of absorbance versus temperature (T_m ± 0.5 °C). In all cases, we observed single transition profiles. Characterization of the type of the complexes (see Table 1) was performed by a native PAGE at 15 °C. (for details and patterns, see SM bellow).

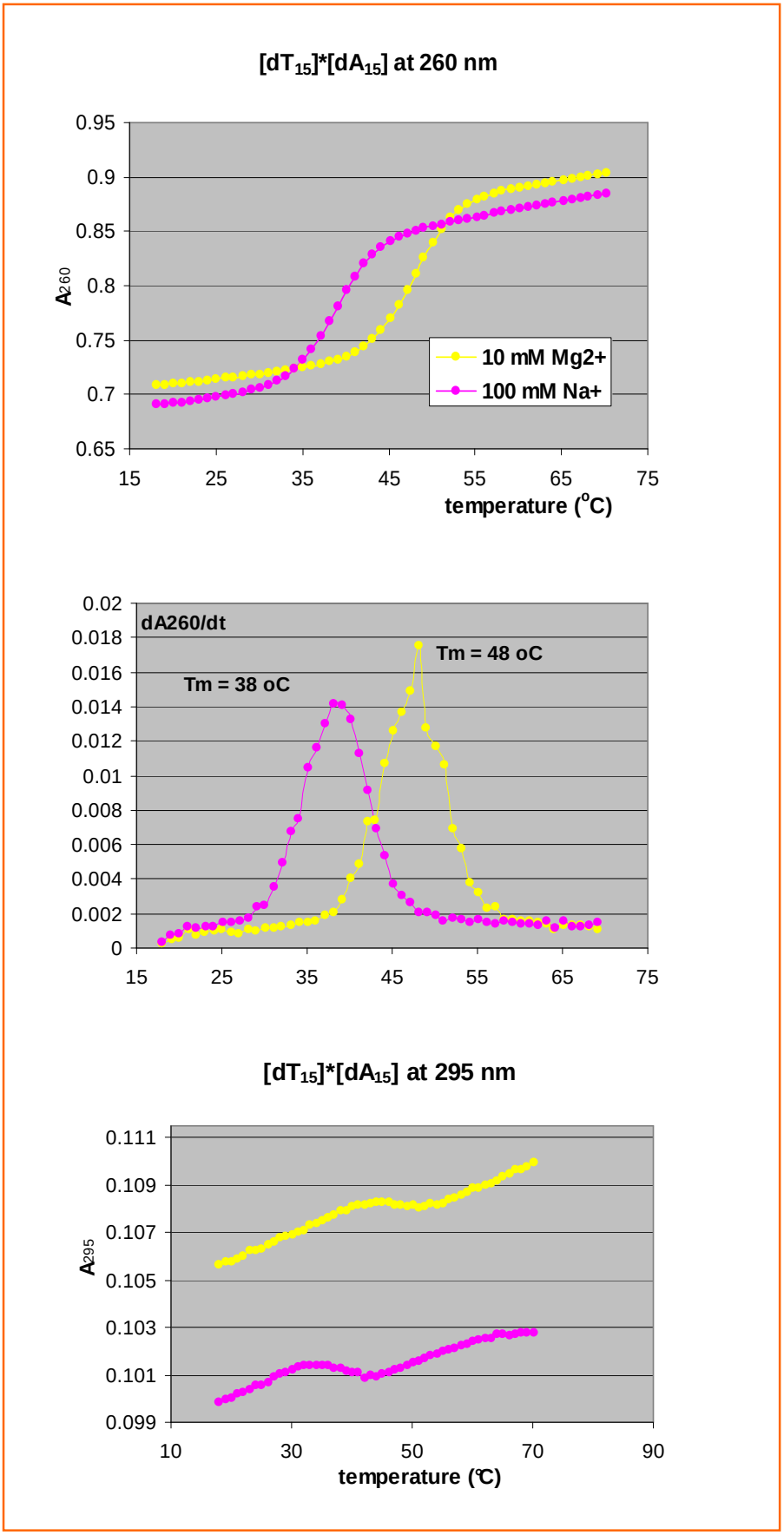

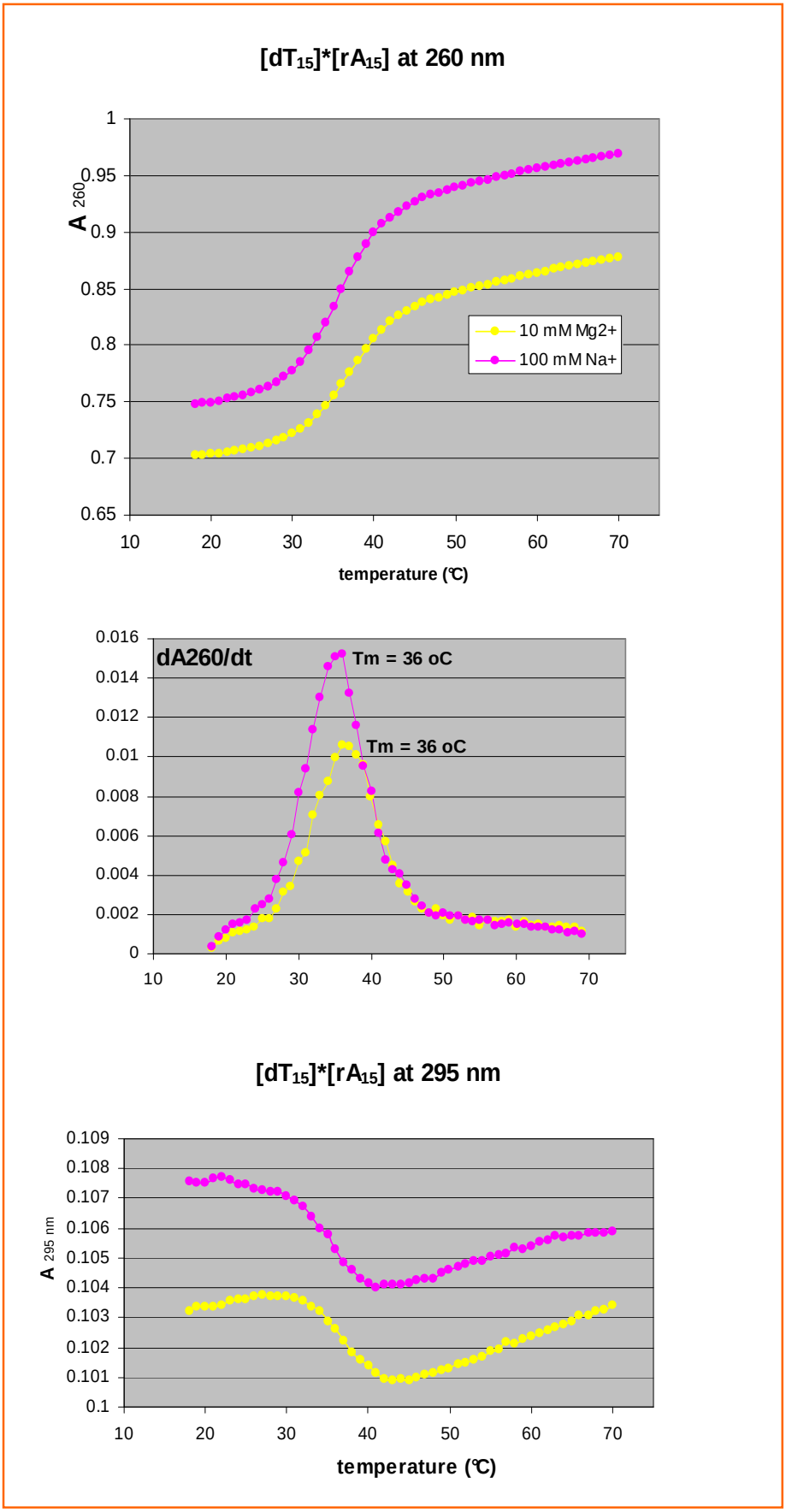

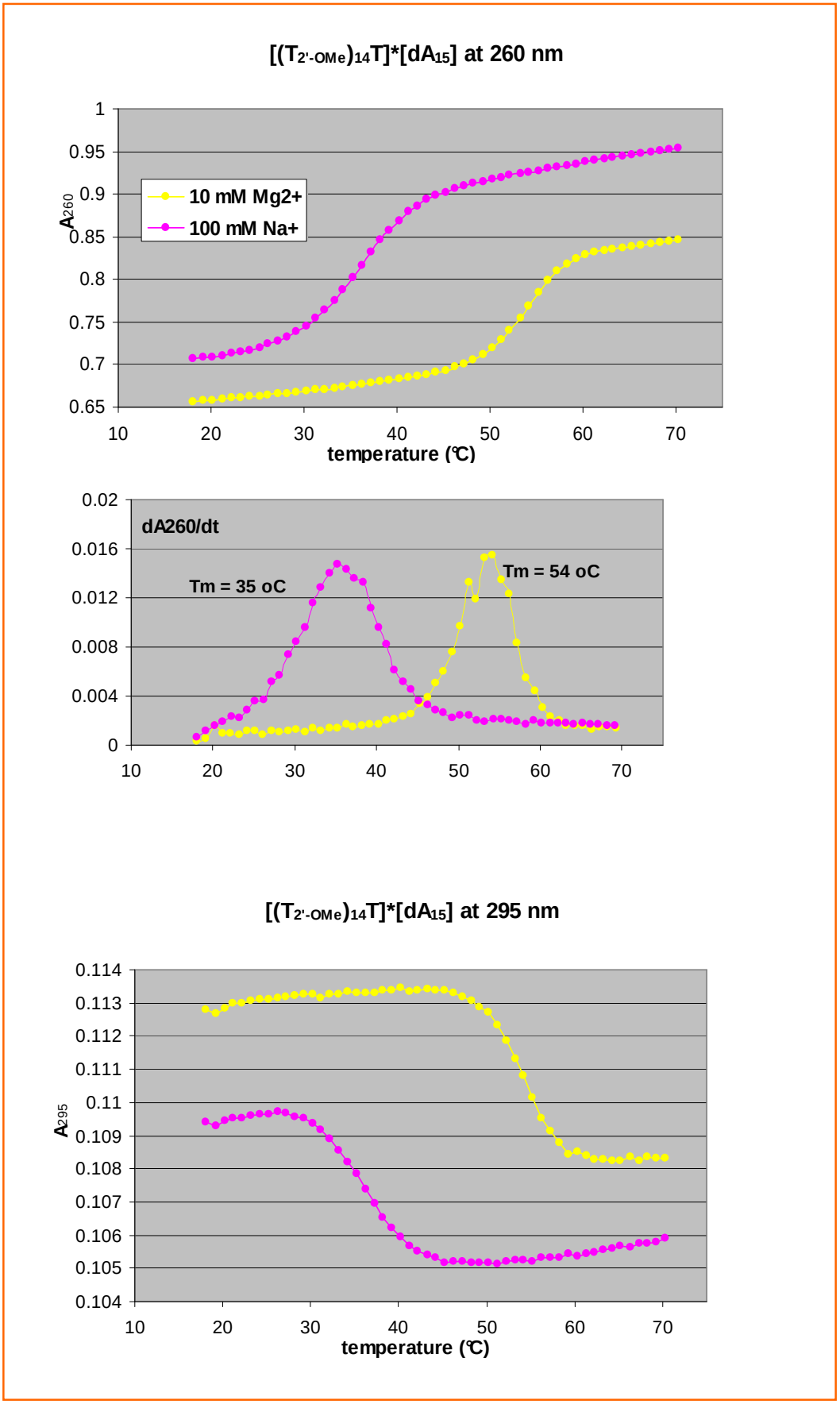

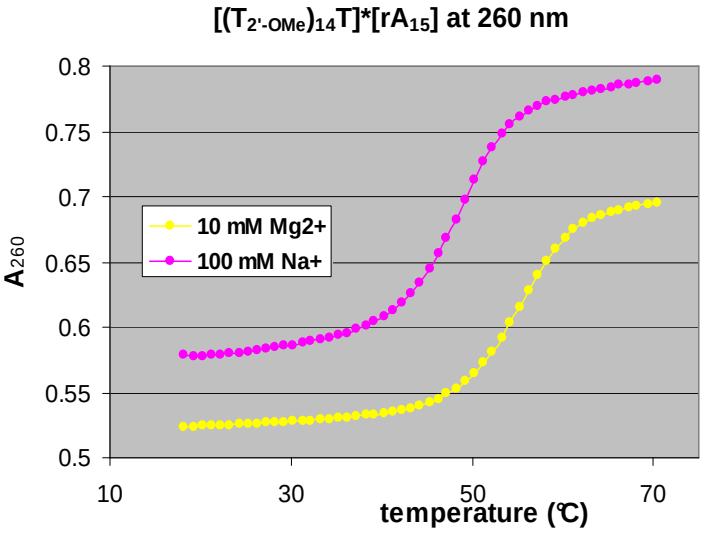

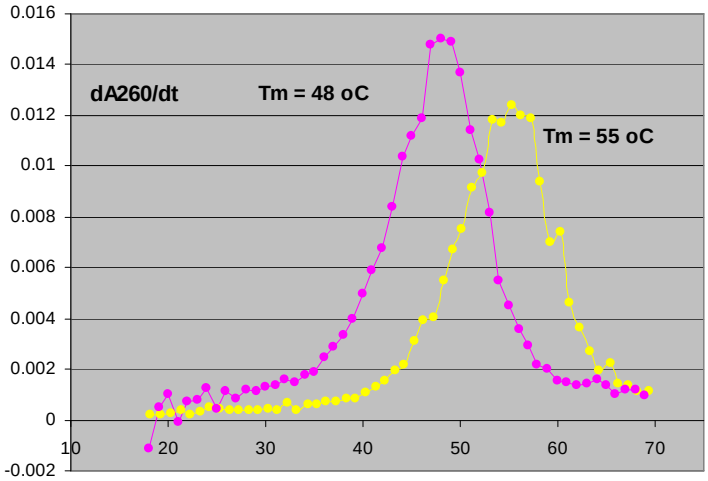

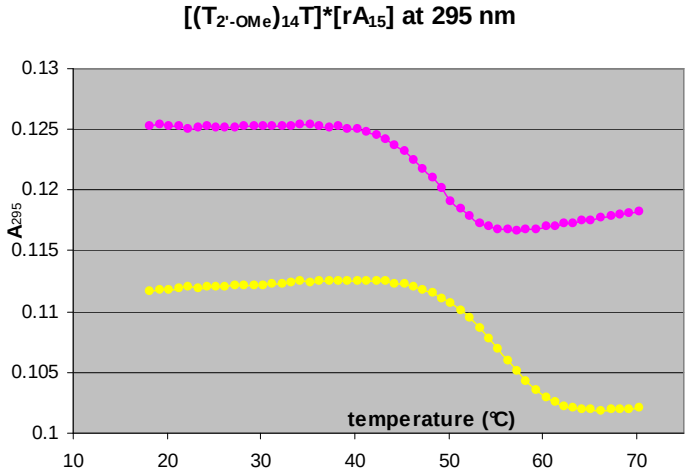

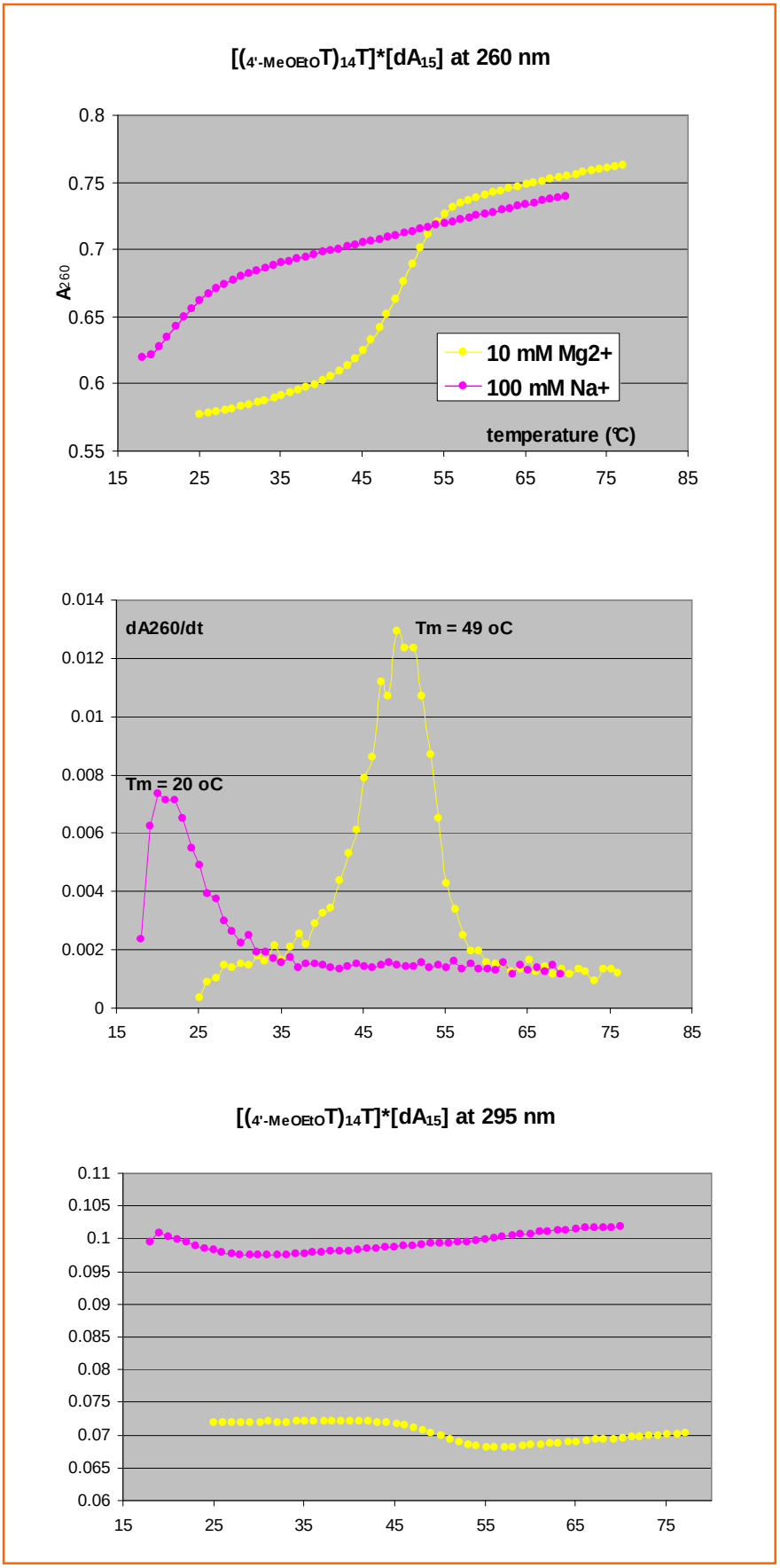

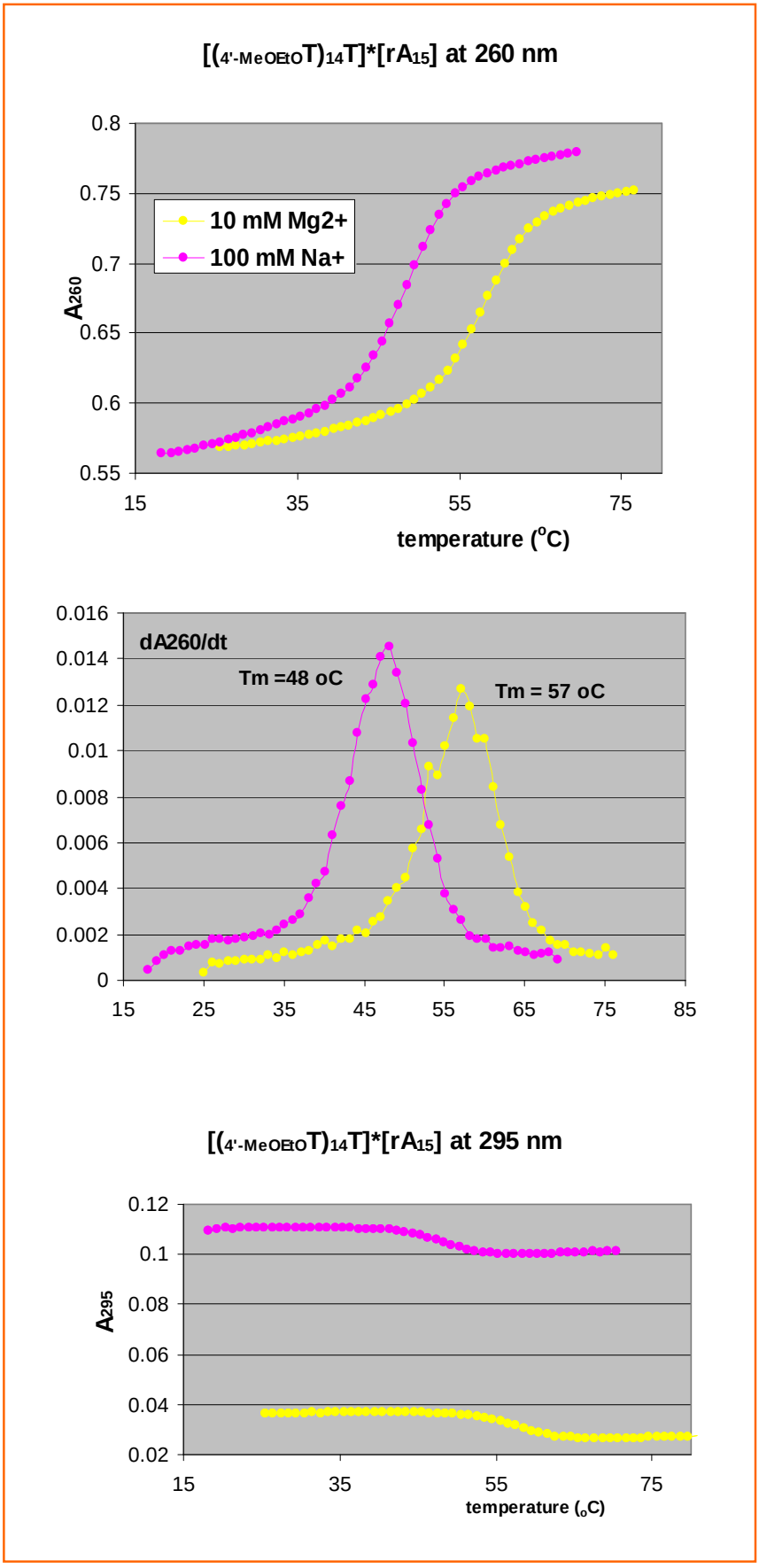

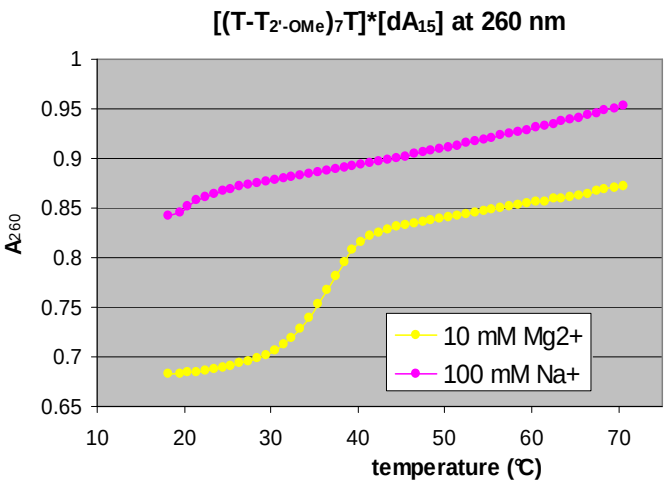

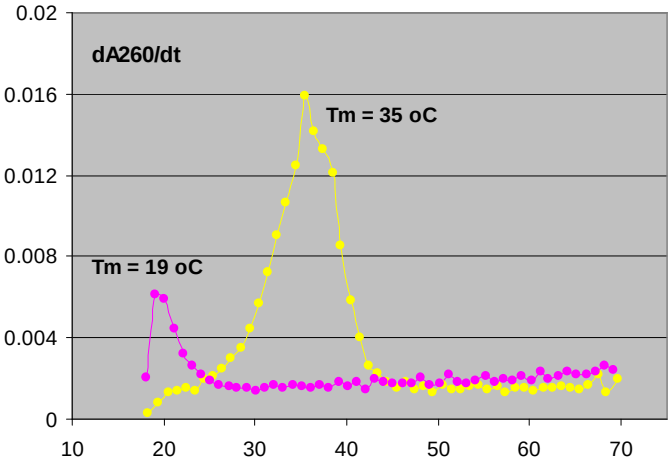

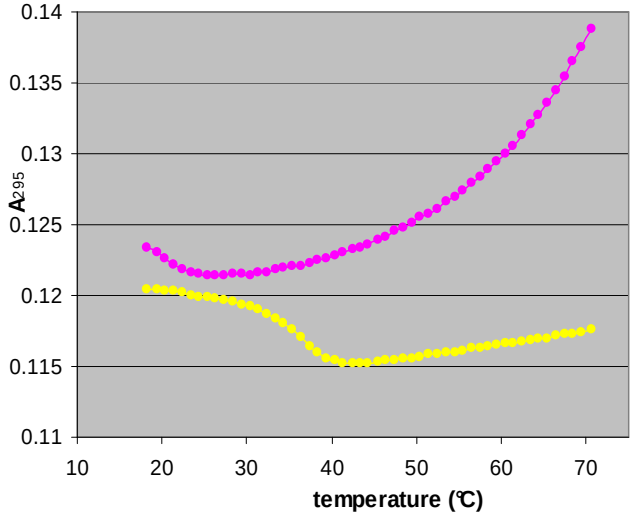

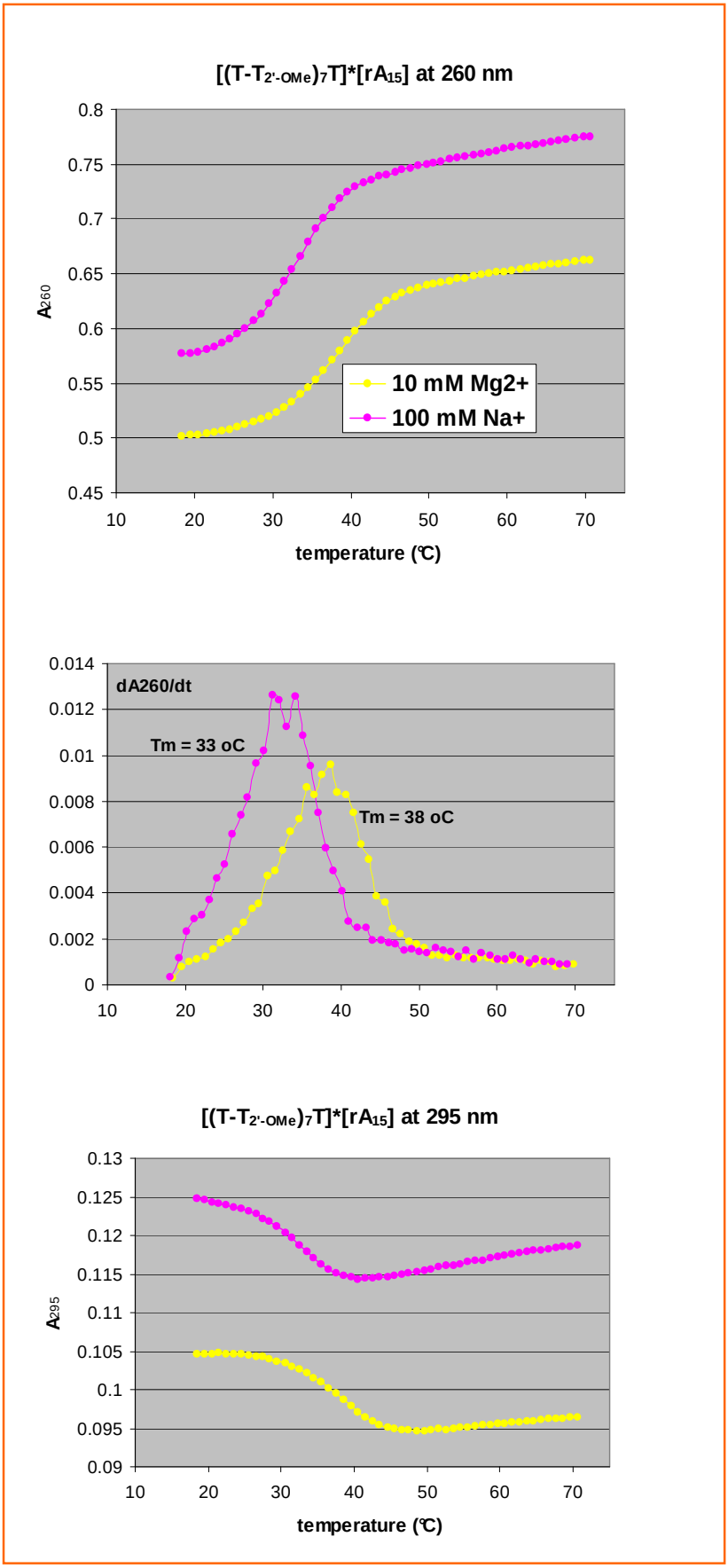

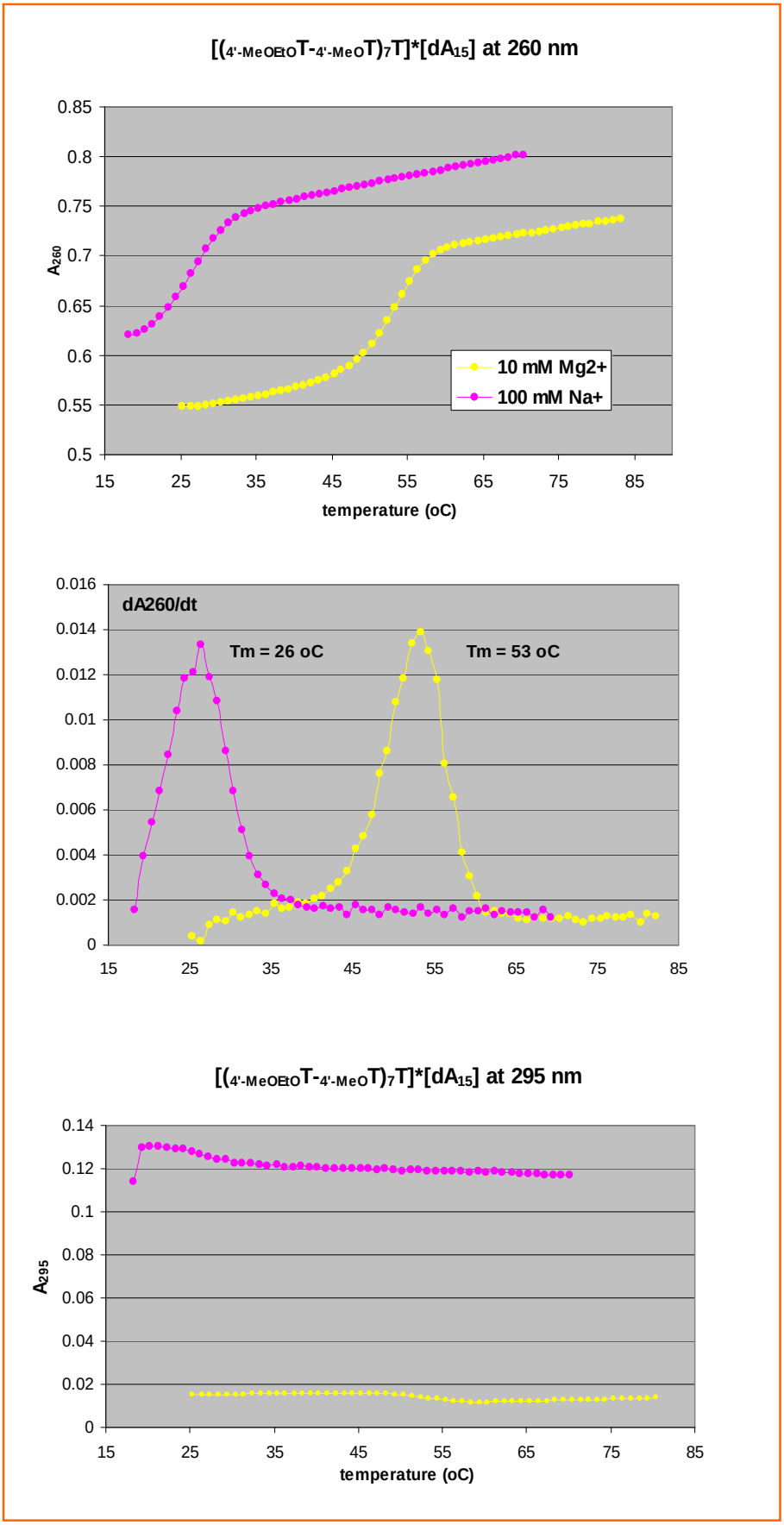

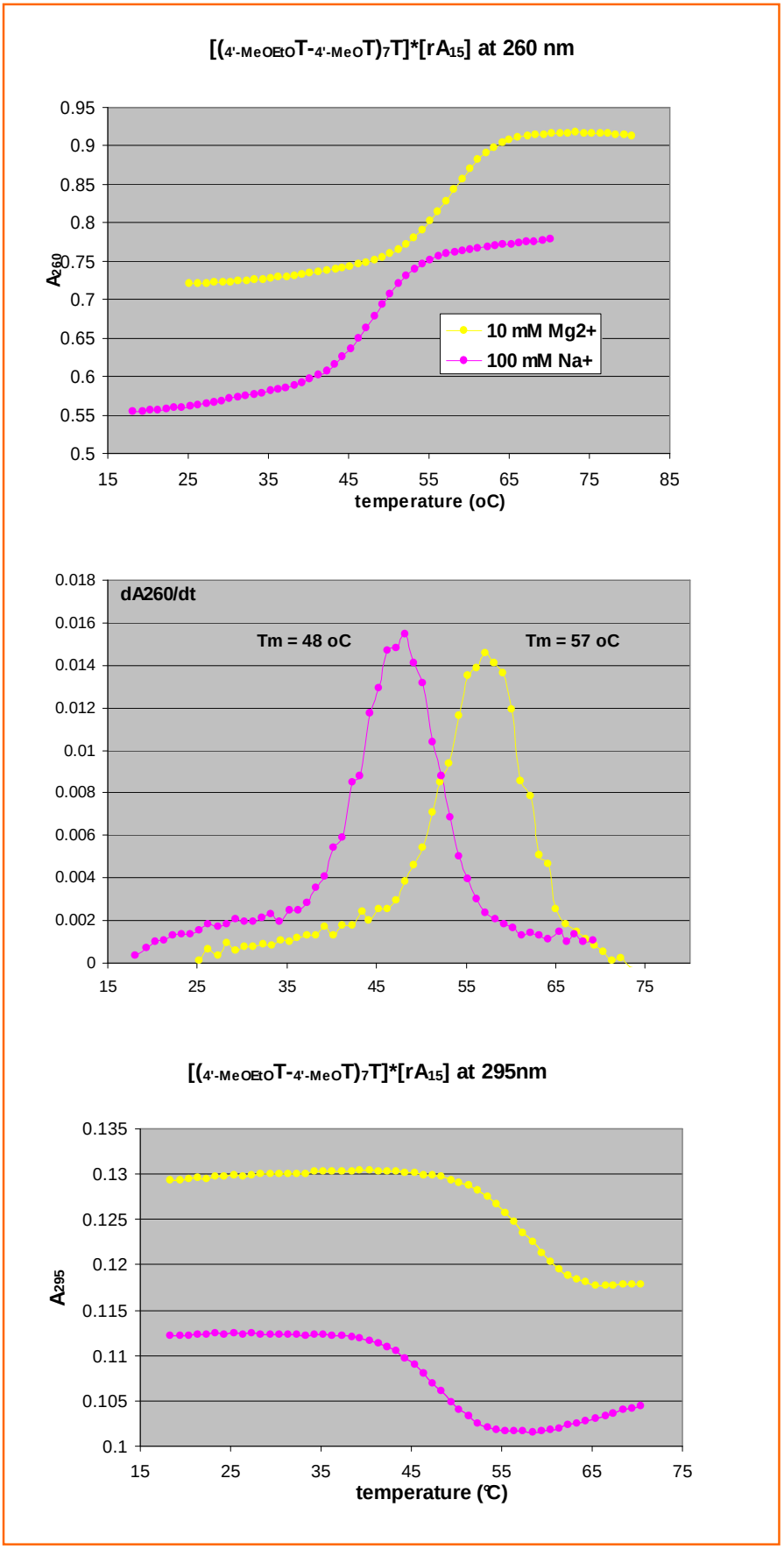

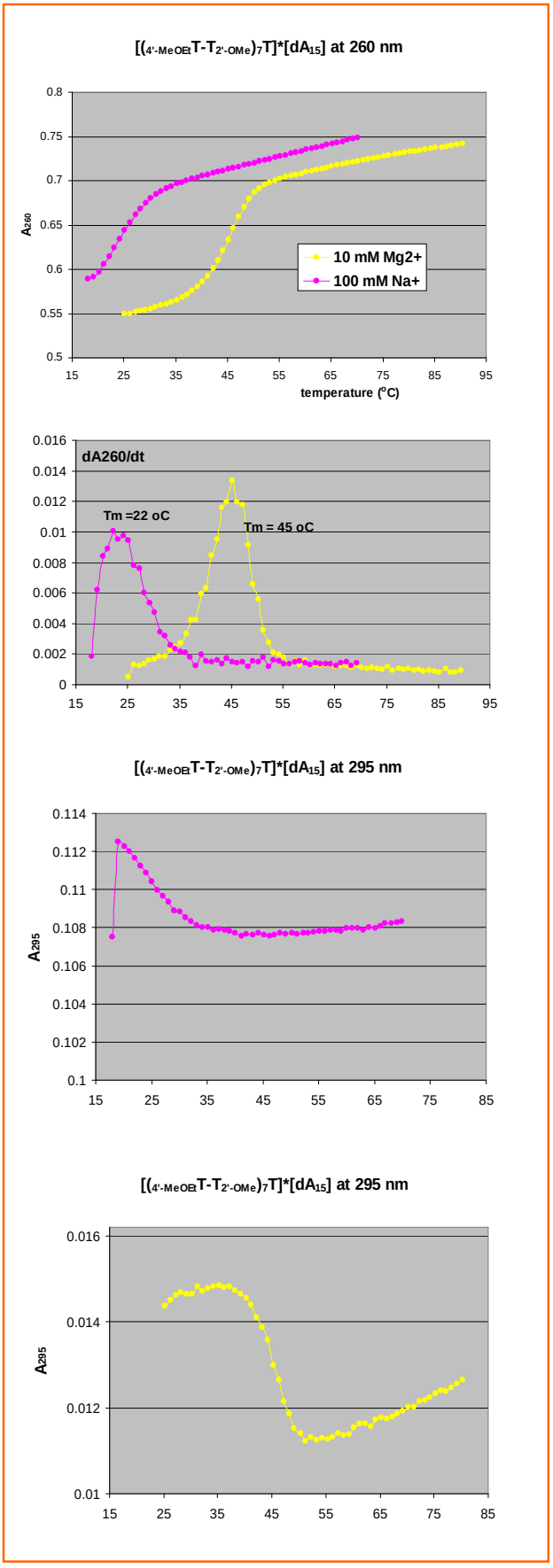

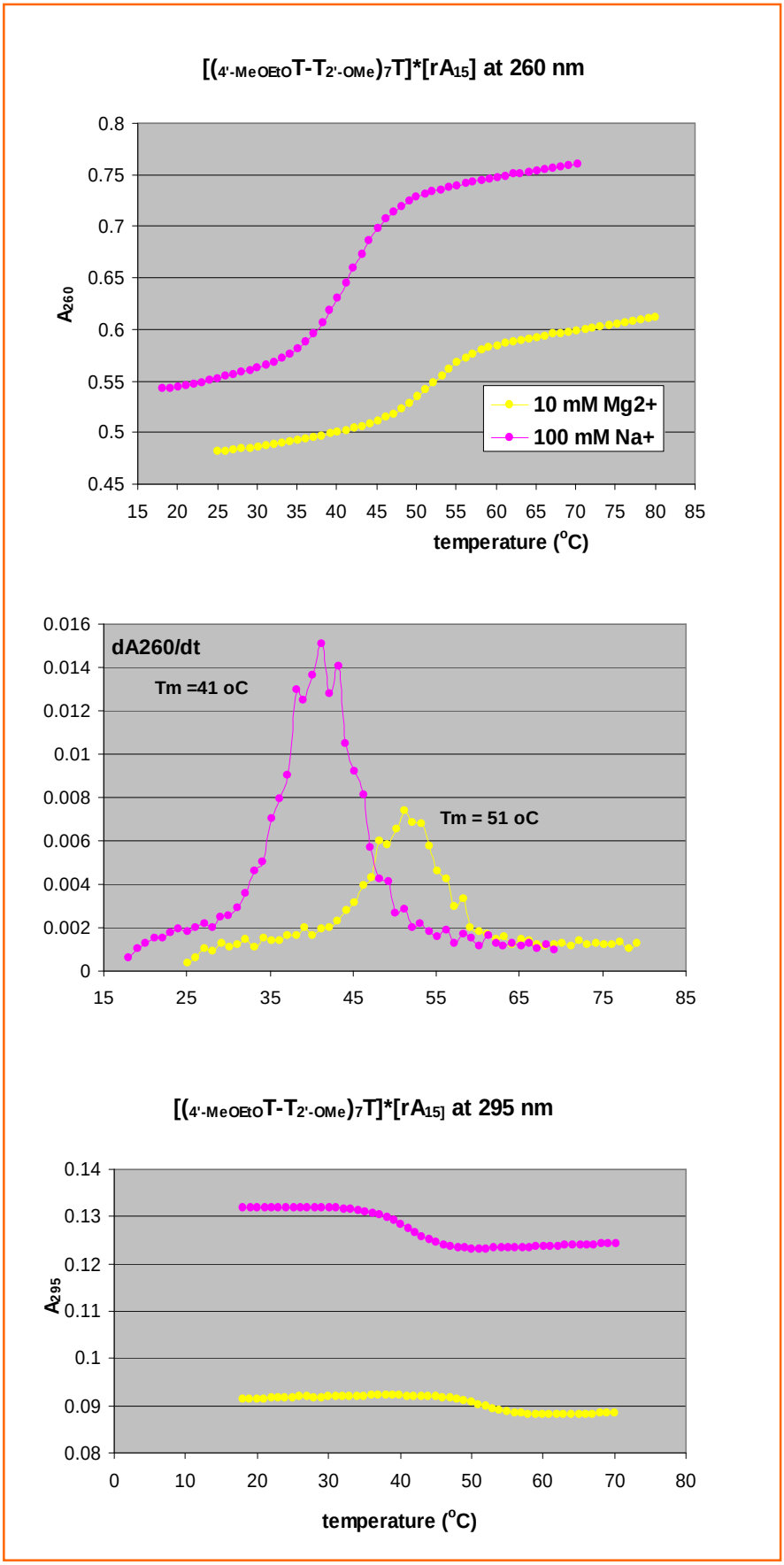

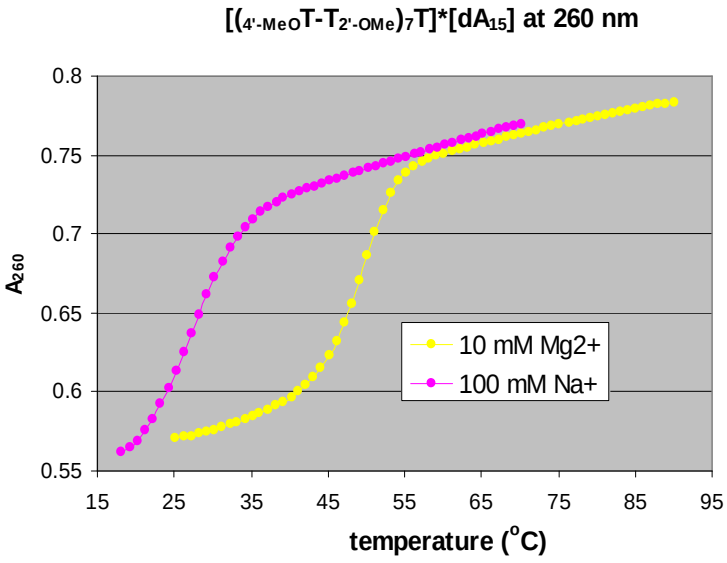

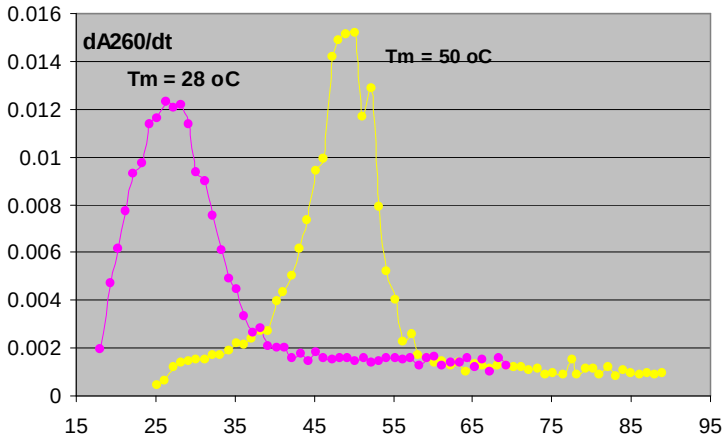

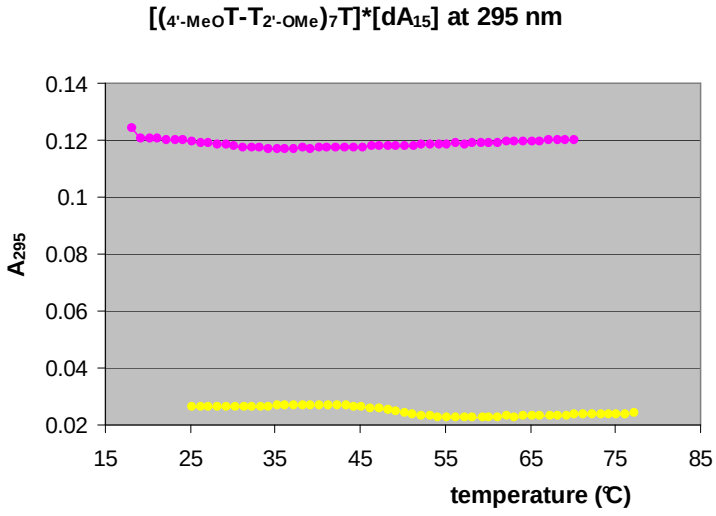

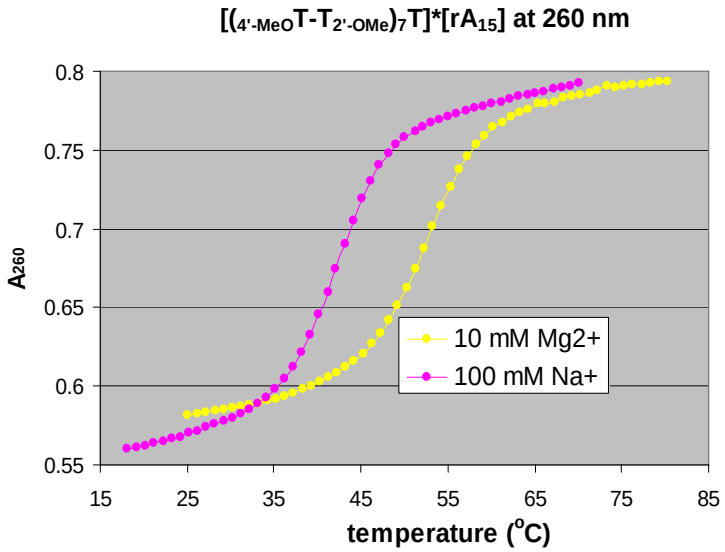

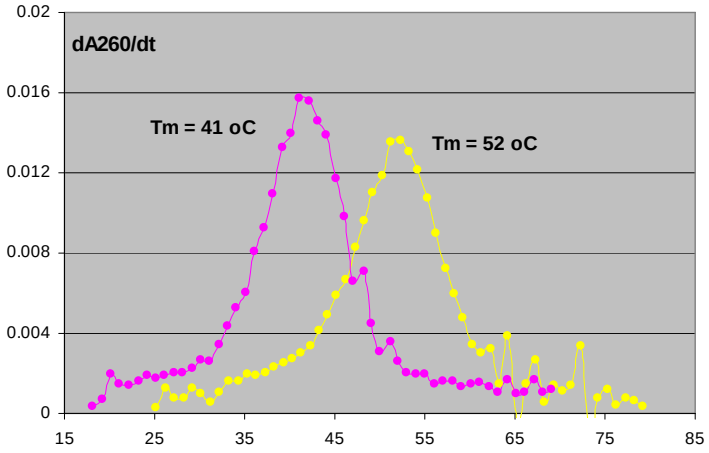

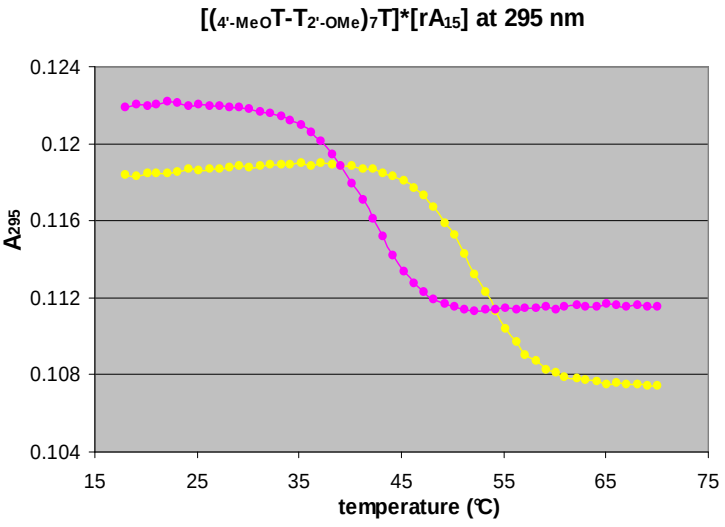

5. Normalized thermal difference spectra (TDS)

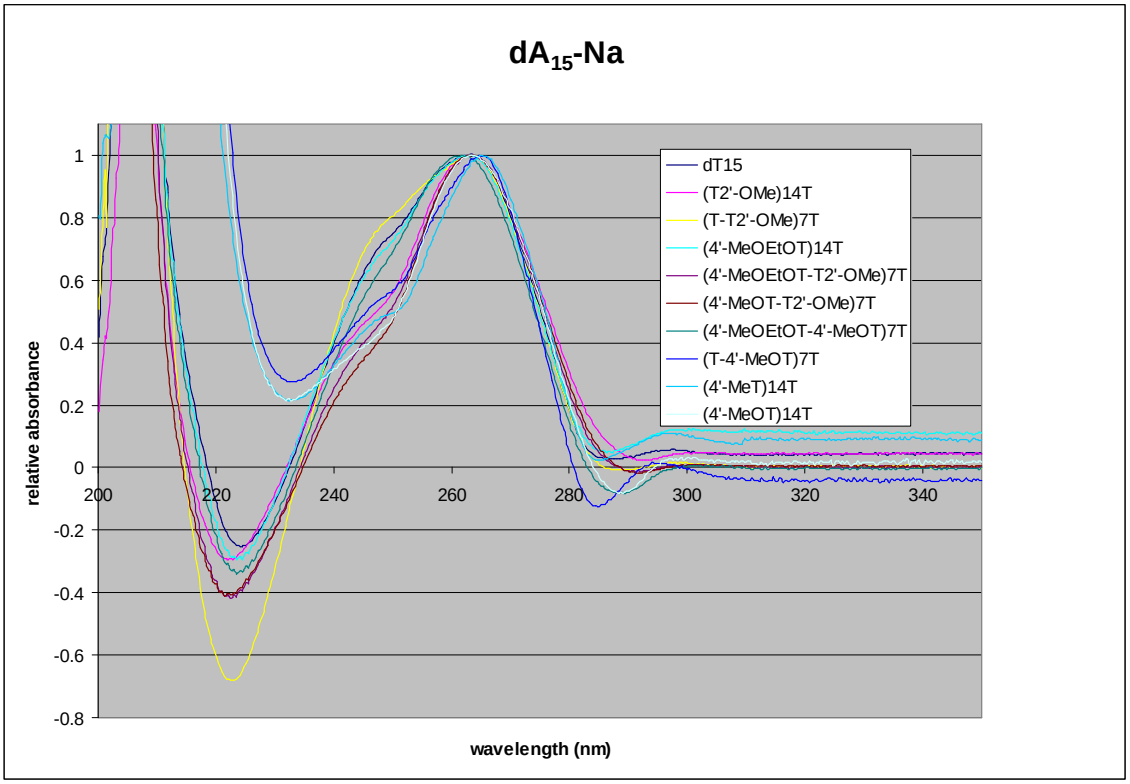

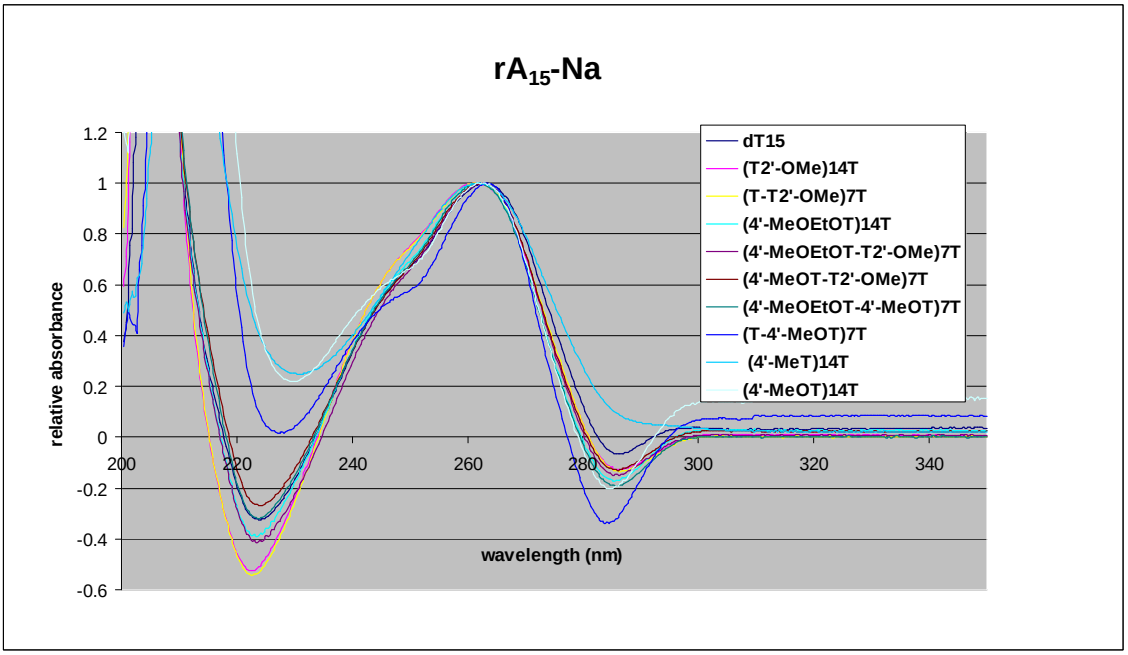

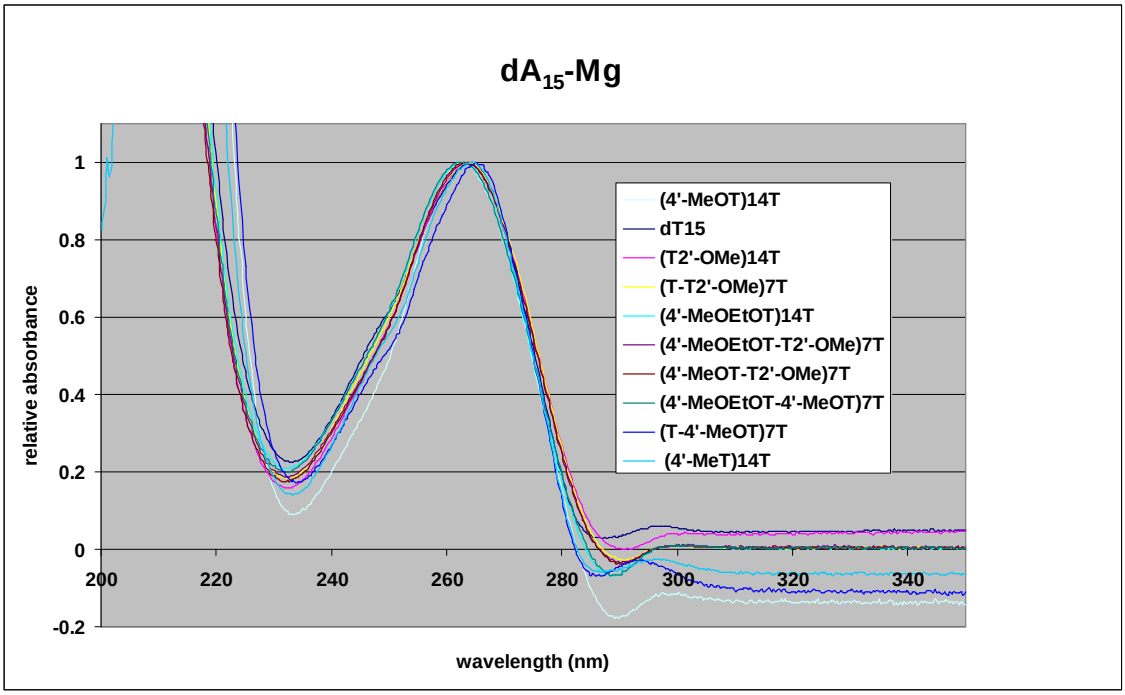

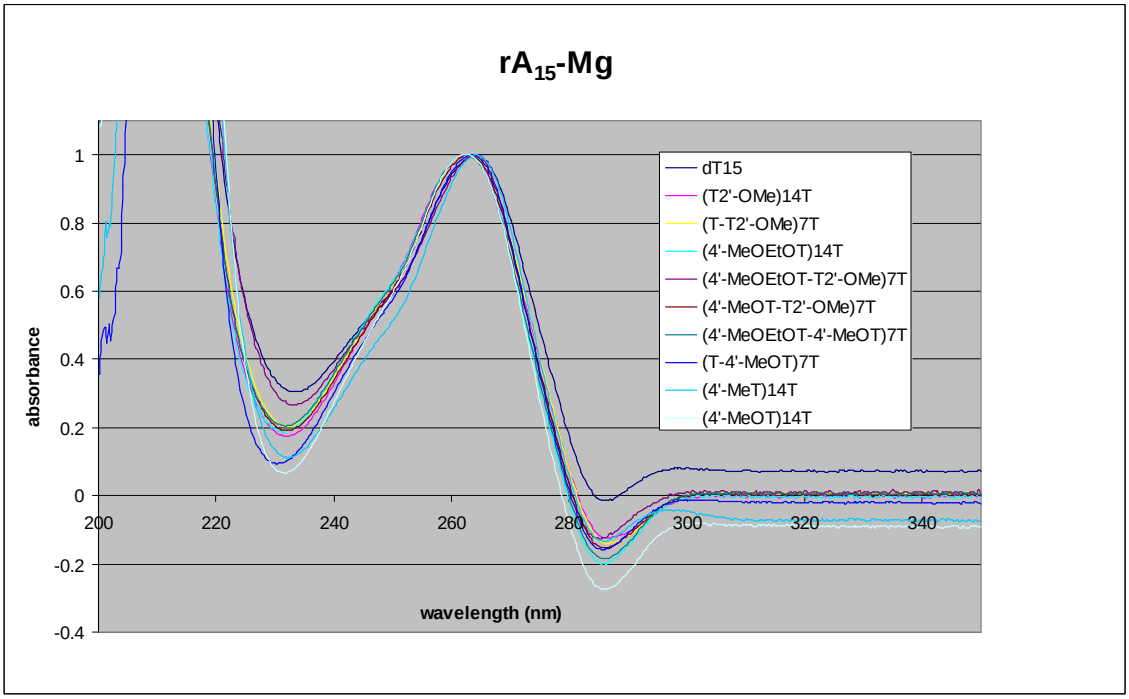

6. Determination of the type of complex by PAGE

Modified oligonucleotides (mT_{15}) were mixed with (^{32}P) 5´-end labelled dA_{15} or rA_{15} in 10 mM Tris, pH 7.4 and 150 mM NaCl (or 10 mM $MgCl_2$) at 1:1 molar ratios to obtain 100 nM final concentrations. Individual annealings were performed by heating the mixtures to 80 ^{o}C and slow cooling to room temperature. The samples were mixed with 10 mM Tris, pH 7.4 and 20% glycerol in 1:1 ratio and loaded onto 20% native polyacrylamide gels. The electrophoresis was run in 1xTBE (or 1x TB with 10 mM $MgCl_2$) at 12.5 V/cm for 10 hours at 15 ^{o}C. The gels were dried and visualized by autoradiography (Figure S4).

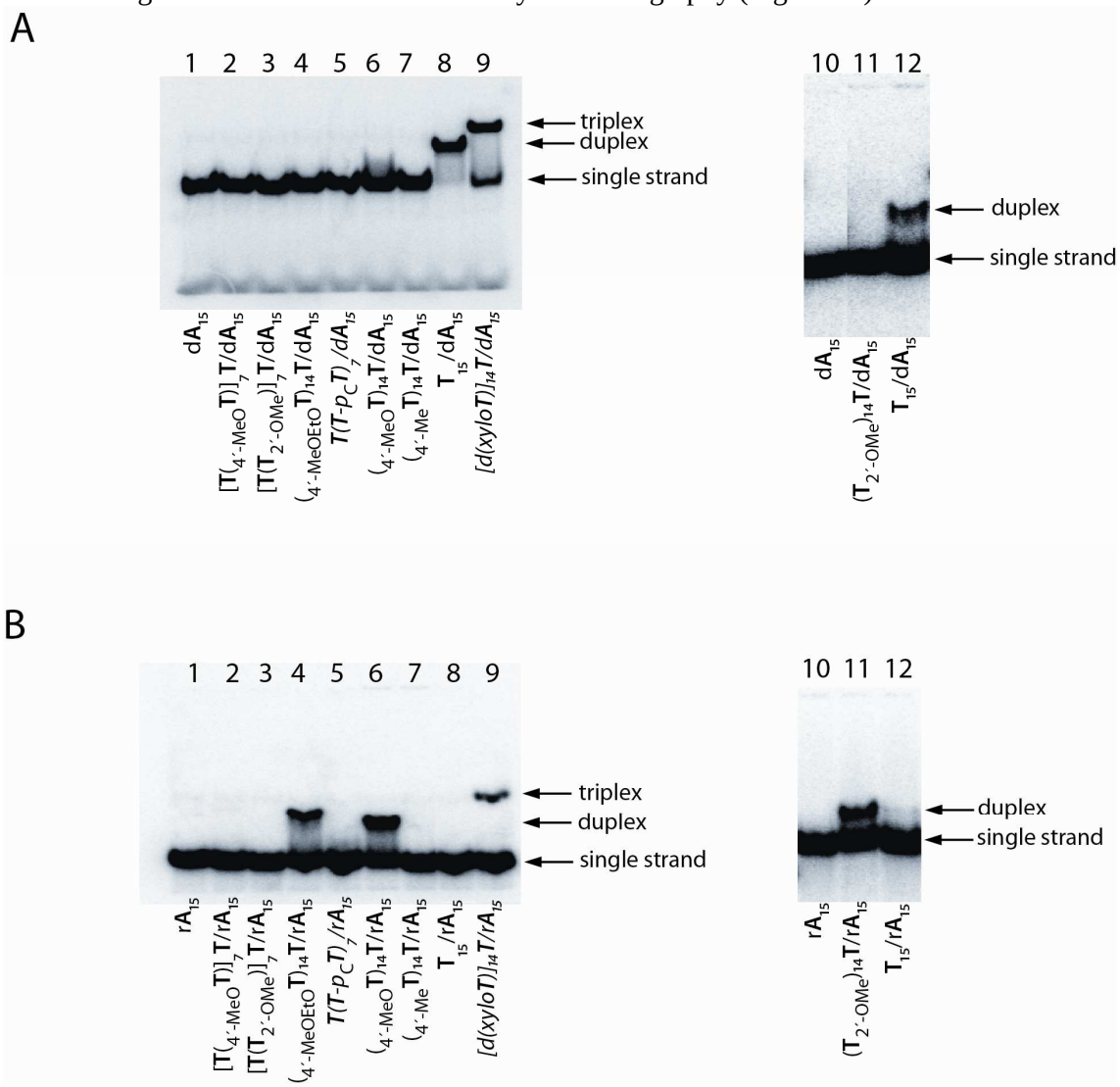

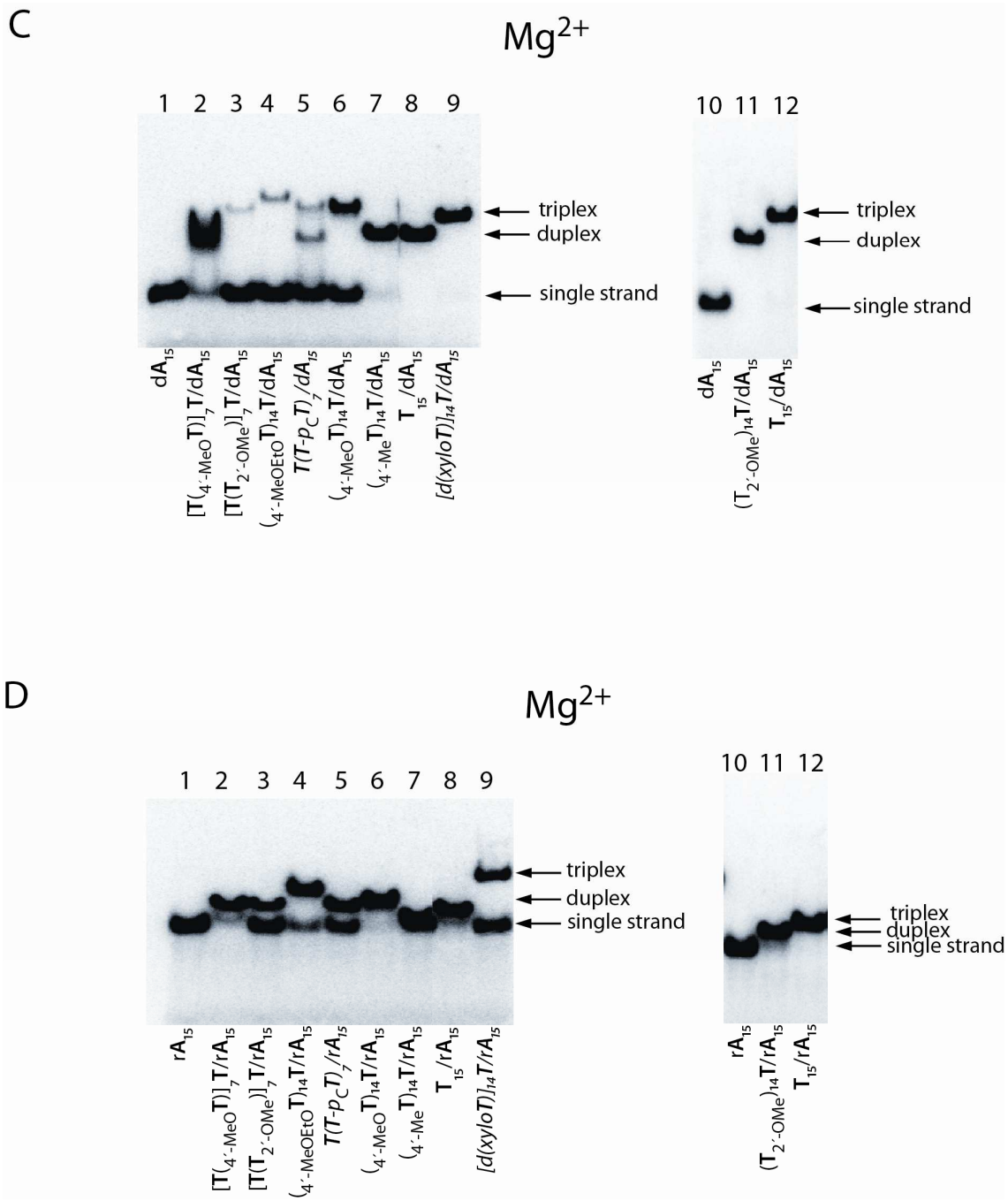

Figure S4. The native electrophoretic analysis of the **mT$_{15}$** multimeric states in complex mixtures with **dA$_{15}$** (Panels A and C) or **rA$_{15}$** (Panels B and D; the abbreviation **mT$_{15}$** stands for the "**m**odified"oligothymidylates.

Panel A: Individual annealings (**mT$_{15}$-dA$_{15}$**) proceeded in the absence of $MgCl_2$. Lane 1, **dA$_{15}$** alone; lane 2, **[T(4'-MeOT)]$_7$T** hybridized with **dA$_{15}$**; lane 3, **[T(T$_{2'-OMe}$)]$_7$T** with **dA$_{15}$**; lane 4, **(4'-MeOEtOT)$_{14}$T** with **dA$_{15}$**; lane 5, **T(T-p$_c$T)$_7$** with **dA$_{15}$**; lane 6, **(4'-MeOT)$_{14}$ T** with **dA$_{15}$**; lane

7, **$(_{4'\text{-Me}}T)_{14}T$** with **dA_{15}**; lane 8, **T_{15}** with **dA_{15}**; lane 9, **$[d(xyloT)]_{14}T$** with **dA_{15}**; lane 10, **dA_{15}** alone; lane 11, **$(T_{2'\text{-OMe}})_{14}T$** with **$dA_{15}$**; lane 12, **$T_{15}$** with **$dA_{15}$**.
Panel B: Individual annealings (**mT_{15}-rA_{15}**) proceeded in the absence of $MgCl_2$. Lane 1, **rA_{15}** alone; lane 2, **$[T(_{4'\text{-MeO}}T]_7T$** hybridized with **rA_{15}**; lane 3, **$[T(T_{2'\text{-OMe}})_7]T$** with **$rA_{15}$**; lane 4, **$(_{4'\text{-MeOEtO}}T)_{14}T$** with **$rA_{15}$**; lane 5, **$T(T\text{-}p_cT)_7$** with **$rA_{15}$**; lane 6, **$(_{4'\text{-MeO}}T)_{14}T$** with **$rA_{15}$**; lane 7, **$(_{4'\text{-Me}}T)_{14}T$** with **$rA_{15}$**; lane 8, **$T_{15}$** with **$rA_{15}$**; lane 9, **$[d(xyloT)]_{14}T$** with **$rA_{15}$**; lane 10, **$rA_{15}$** alone; lane 11, **$(T_{2'\text{-OMe}})_{14}T$** with **$rA_{15}$**; lane 12, **$T_{15}$** with **$rA_{15}$**.
Panel C: Individual annealings (**mT_{15}-dA_{15}**) proceeded in the presence of 10 mM $MgCl_2$. Lane 1, **dA_{15}**, alone; lane 2, **$(T_{4'\text{-MeO}}T)_7T$** hybridized with **dA_{15}**,; lane 3, **$[T(T_{2'\text{-OMe}})]_7T$** with **$dA_{15}$**; lane 4, **$(_{4'\text{-MeOEtO}}T)_{14}T$** with **$dA_{15}$**; lane 5, **$T(T\text{-}p_cT)_7$** with **$dA_{15}$**; lane 6, **$(_{4'\text{-MeO}}T)_{14}T$** with **$dA_{15}$**; lane 7, **$(_{4'\text{-Me}}T)_{14}T$** with **$dA_{15}$**; lane 8, **$T_{15}$** with **$dA_{15}$**; lane 9, **$[d(xyloT)]_{14}T$** with **$dA_{15}$**; lane 10, **$dA_{15}$** alone; lane 11, **$T_{15}$** with **$dA_{15}$**; lane 12, **$(T_{2'\text{-OMe}})_{14}T$** with **$dA_{15}$**.
Panel D: Individual annealings (**mT_{15}-rA_{15}**) proceeded in the presence of 10 mM $MgCl_2$. Lane 1, **rA_{15}** alone; lane 2, **$[T(_{4'\text{-MeO}}T)]_7T$** hybridized with **$rA_{15}$**; lane 3, **$[T(T_{2'\text{-OMe}})]_7T$** with **$rA_{15}$**; lane 4, **$(_{4'\text{-MeOEtO}}T)_{14}T$** with **$rA_{15}$**; lane 5, **$T(T\text{-}p_cT)_7$** with **$rA_{15}$**; lane 6, **$(_{4'\text{-MeO}}T)_{14}T$** with **$rA_{15}$**; lane 7, **$(_{4'\text{-Me}}T)_{14}T$** with **$rA_{15}$**; lane 8, **$T_{15}$** with **$rA_{15}$**; lane 9, **$[d(xyloT)]_{14}T$** with **$rA_{15}$**; lane 10, **$rA_{15}$** alone; lane 11, **$T_{15}$**with **$rA_{15}$**; lane 12, **$(T_{2'\text{-OMe}})_{14}T$** with **$rA_{15}$**.

Modified oligonucleotides **$[d(xyloT)]_{14}T$** and **$T(T\text{-}p_cT)_7$** (ref.[6]) in mixtures with **dA_{15}** or **rA_{15}** were used as reference entities to be run in native gels as markers indicating approximate migration positions of oligonucleotide duplexes and triplexes. The oligomer **$T(T\text{-}p_cT)_7$** formed a mixture of duplexes and triplexes with **dA_{15}**, and only duplexes with **rA_{15}** (all in the presence of Mg^{2+}), while **$[d(xyloT)]_{14}T$** formed triplexes with **dA_{15}** or **rA_{15}** in both the absence and presence of Mg^{2+}. The existence of the above mentioned indicative forms occurring under similar *in vitro* conditions was independently determined earlier using surface plasmon resonance experiments (data not shown).

7. Molecular dynamics simulation (MDS) – methodology and additional figures

Molecular dynamics simulations (MDS) lasting for 5ns with model oligonucleotide helical structures carrying chemical modifications on either C4' or C2' atoms ($[T(_{4'\text{-MeO}}T)_8T]^{W\text{-}C}\bullet rA_{10}*[T(_{4'\text{-MeO}}T)_8T]^{Hgstn}$, $[T(_{4'\text{-MeOEtO}}T)_8T]^{WC}\bullet rA_{10}*[T(_{4'\text{-MeOEtO}}T)_8T]^{Hgstn}$, $[T(T_{2'\text{-OMe}})_8T]^{W\text{-}C}\bullet rA_{10}*[T(T_{2'\text{-OMe}})_8T]^{Hgstn}$ - see Figures S5-S10) were produced at 310 K.

Additional groups of atoms (either $-O_A\text{-}CH_3$ or $-O_A\text{-}CH_2\text{-}CH_2\text{-}O_B\text{-}CH_3$) were anchored to the C2' and C4' atoms and manipulated manually (using VMD[7]) into reasonable starting configurations.

Simulated systems were surrounded by TIP3P water molecules,[8] which extended to a distance of 10A (in each direction) from solute atoms. This gives a periodic box size of 65A x 60A x 52A consisting of approximately 15,000 atoms.

We dealt with MD simulations of nucleic acids carrying chemical modifications on either C4' or C2' atoms. Therefore, necessary *.prep files describing topology of the modified residues were derived from those describing topology of natural nucleic acids in the AMBER force field.

Further, additional force constants were incorporated into the AMBER force field partially on the basis of analogy with force constants presented in literature.[9,10] Total energies of simple model systems were computed for either *2'-endo* or *3'-endo* conformers. It was found as

inevitable to introduce the CT-OS-CT-OS force constant to mimic the anomeric effect (*i. e.* preference for the *gauche* conformer consider the C1'-O4'-C4'-O_A torsion angle) and to impel the C4' modified sugars to prefer the *3'-endo* conformation within MD runs.

Large concentrations of ions, which are, however, obvious in the context of melting temperatures of the antisense oligonucleotides, were used in our experiments (10 mM Mg^{++} or 100 mM Na^{+}). Identity of ions (Na^{+}/Mg^{++}) was found to be influential, considering the stability of helical structures carrying various chemical modifications. We checked a hypothesis that the binding cavities for ions (consisting of O3', O_A and O_B atoms) are localised in the close proximity of the C4'-O_A-CH_3, C4'-O_A-CH_2-CH_2-O_B-CH_3 moieties. Binding of water molecules in similar binding sites was observed in the case of C2'-modified oligonucleotides.[10] The O3', O_A and O_B atoms compete in binding of ions with another potential ligands – oxygen atoms of water molecules (OW), as well as with the non-bridge oxygen atoms of the phosphate groups (O1P) situated in close proximity. Therefore, partial charges on all oxygen atoms must be carefully established to secure reliable relative binding frequencies within a MD run. Classical force fields were developed during the last three decades by a gradual accumulation of force constants from different sources (their detail consistency is not a matter, of course, up to now).

We took into account the partial charges determined in the previous studies of oligonucleotides bearing –OCH_3 and –$OCH_2CH_2OCH_3$ groups on C2' atoms.[9,10] Molecular mechanical (MM) partial charges (developed using the AMBER/RESP methodology - fitting of partial point charges to reproduce surrounding ab initio electrostatic potential) on O_A and O_B (-0.35), O3' (-.5232), O1P (-0.7761) and OW (-0.834) atoms are rather manifold. The so called Mulliken charges determined by ab initio calculations show lower dispersion (reaching from -0.59 to -0.85). Mulliken charges (comparing to AMBER/RESP charges) determined for O_A, O_B, O3' and O1P atoms show somewhat lower values. In contrast, the MM partial charge on the OW oxygen atom from the TIP3P water molecule is very close to its *ab initio* Mulliken value.

Therefore, we found necessary to unify a little bit partial charges of atoms considered here to compete in binding of ions. Total energies of several model systems were optimized using ab initio calculations: $Mg^{2+}.6H_2O$, $Mg^{2+}.5H_2O$, H_2O, $Mg^{2+}.5H_2O.CH_3OCH_3$ a CH_3OCH_3. Ab initio energy of 36 kcal/mol was found to stabilize H_2O as well as CH_3OCH_3 binding toward $Mg^{++}.5H_2O$. In contrast, molecular mechanical calculations using original partial charges (-0.35 for O_A/O_B atoms[9,10]) produced energy gap of 27 kcal/mol for CH_3OCH_3 and 42 kcal/mol for the TIP3P water molecule. Molecular mechanical calculations using refined partial charges (this means -0.5 for O_A/O_B atoms) pushed the stabilization energy toward the 42 kcal/mol too. Interestingly, the resulting gap between the old and new values of O_A, O_B charges is the same as the difference between AMBER/CHARMM partial charges for atom O4' of ribose moiety (-0.3691/-0.5). It should be noted, that CHARMM partial charges were derived to reproduce ab initio interaction energies between model compounds and water.

New *.inpcrd (initial coordinates) and *.prmtop (molecular topology, force field etc.) files for the whole simulated system were created by use of the TLEAP module (AMBER software package[11]). Fully solvated trajectories were computed with the aid of the NAMD software package.[12] Conventional computational procedures were used: periodic boundary conditions, cut off distances of 10A for the nonbonded interactions and the particle-mesh-Ewald method[13] for the summation of the coulombic interactions (PME grid size was chosen 64 in each direction), MD time step 0.002 ps. Initially, for 5 ps, the system was heated up to 310 K using

a Langevin temperature equilibration scheme while restraining the position of the solute. The MD was then continued for 5 ns at constant T and constant P (using Langevin Piston) with all restraints removed. Figures were produced with the aid of the VMD software package.[7]

Figures S5-S14:
Triple helical structures used as models in molecular dynamics simulations: $[T(T_{2'\text{-OMe}})_8T]^{W\text{-}C}\bullet rA_{10}*[T(T_{2'\text{-OMe}})_8T]^{Hgstn}$ (Figure S5, S6), $([T(_{4'\text{-MeO}}T)_8T]^{W\text{-}C}\bullet rA_{10}*[T(_{4'\text{-MeO}}T)_8T]^{Hgstn}$ (Figure S7, S8), $[T(_{4'\text{-MeOEtO}}T)_8T]^{WC}\bullet rA_{10}*[T(_{4'\text{-MeOEtO}}T)_8T]^{Hgstn}$ (Figure S9, S10). Binding of Mg^{2+} ions toward the $[T(_{4'\text{-MeOEtO}}T)_8T]^{WC}\bullet rA_{10}*[T(_{4'\text{-MeOEtO}}T)_8T]^{Hgstn}$ triple helical structure (Figure S11, S12). Two modes of contacts between Mg^{2+} ions and one and/or two oxygen atoms of C4'-$\underline{O}CH_2CH_2\underline{O}CH_3$ group in $[T(_{4'\text{-MeOEtO}}T)_8T]^{WC}\bullet rA_{10}*[T(_{4'\text{-MeOEtO}}T)_8T]^{Hgstn}$ (Figure S13). Na^+ binding to the C4'-OCH_3 moiety in $[T(_{4'\text{-MeO}}T)_8T]^{W\text{-}C}\bullet rA_{10}*[T(_{4'\text{-MeO}}T)_8T]^{Hgstn}$ triplex structure (Figure S14).

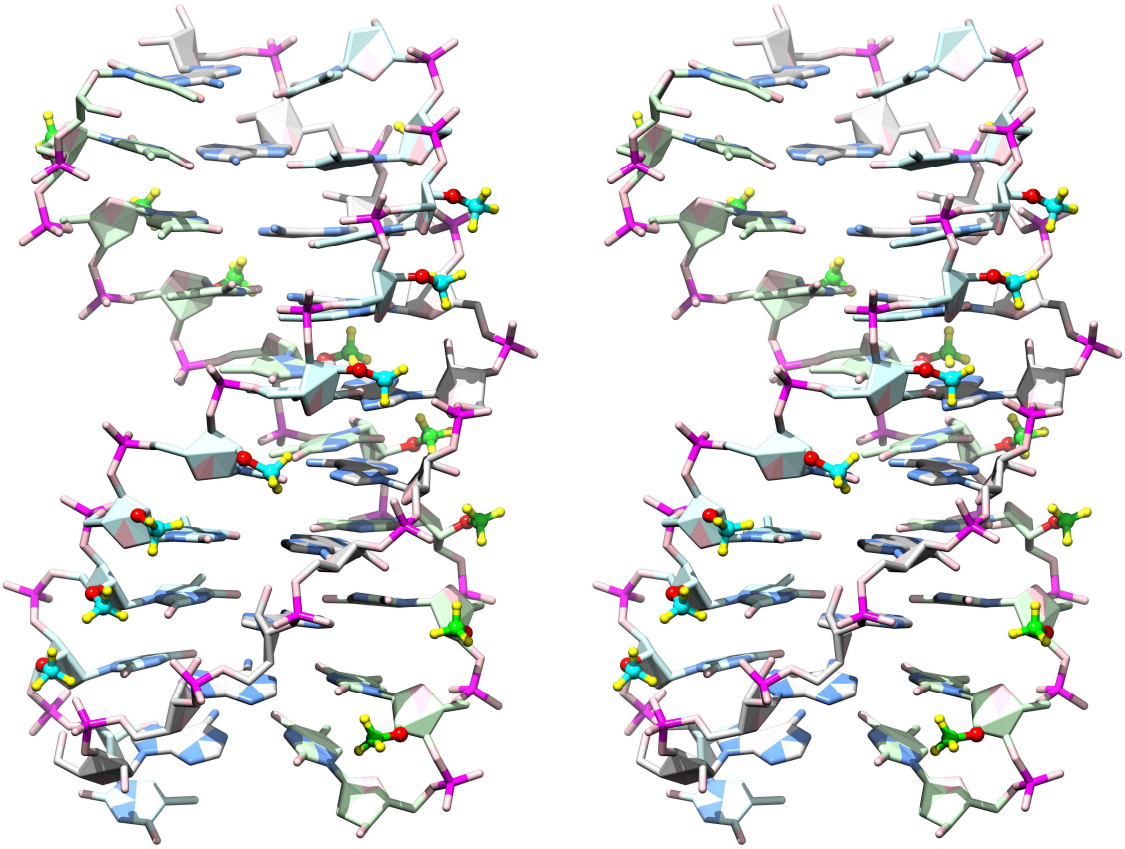

Figure S5: $[T(T_{2'\text{-OMe}})_8T]^{W\text{-}C}\bullet rA_{10}*[T(T_{2'\text{-OMe}})_8T]^{Hgstn}$ – hydrogen atoms omitted - stereo view

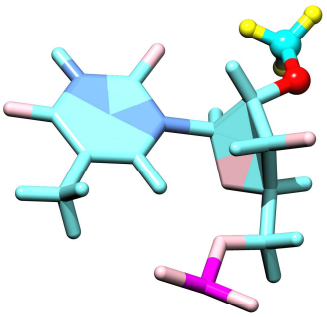

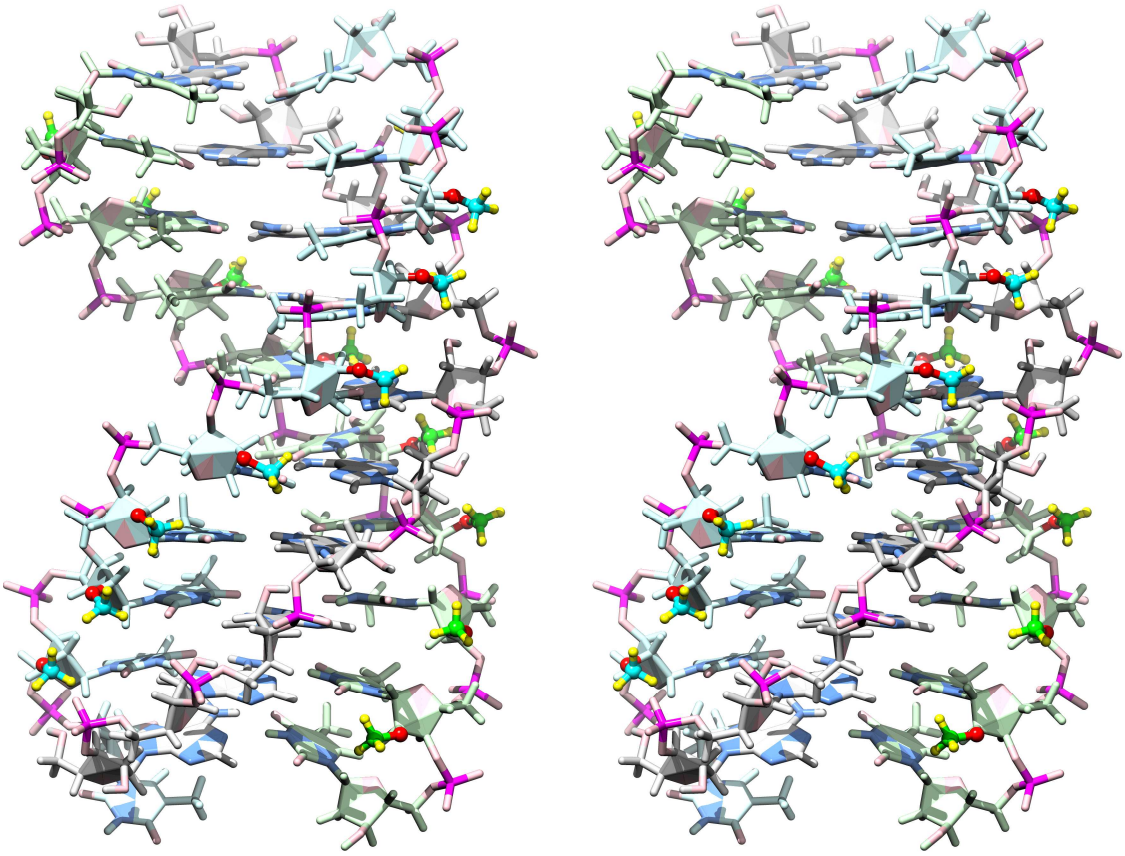

Figure S6: $[T(T_{2'\text{-OMe}})_8T]^{W\text{-}C}\bullet rA_{10}*[T(T_{2'\text{-OMe}})_8T]^{Hgstn}$ – all atoms depicted – stereo view

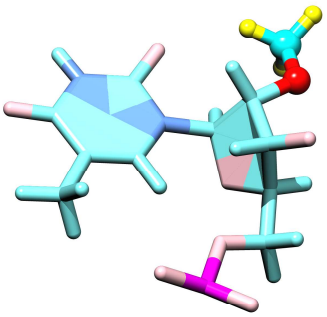

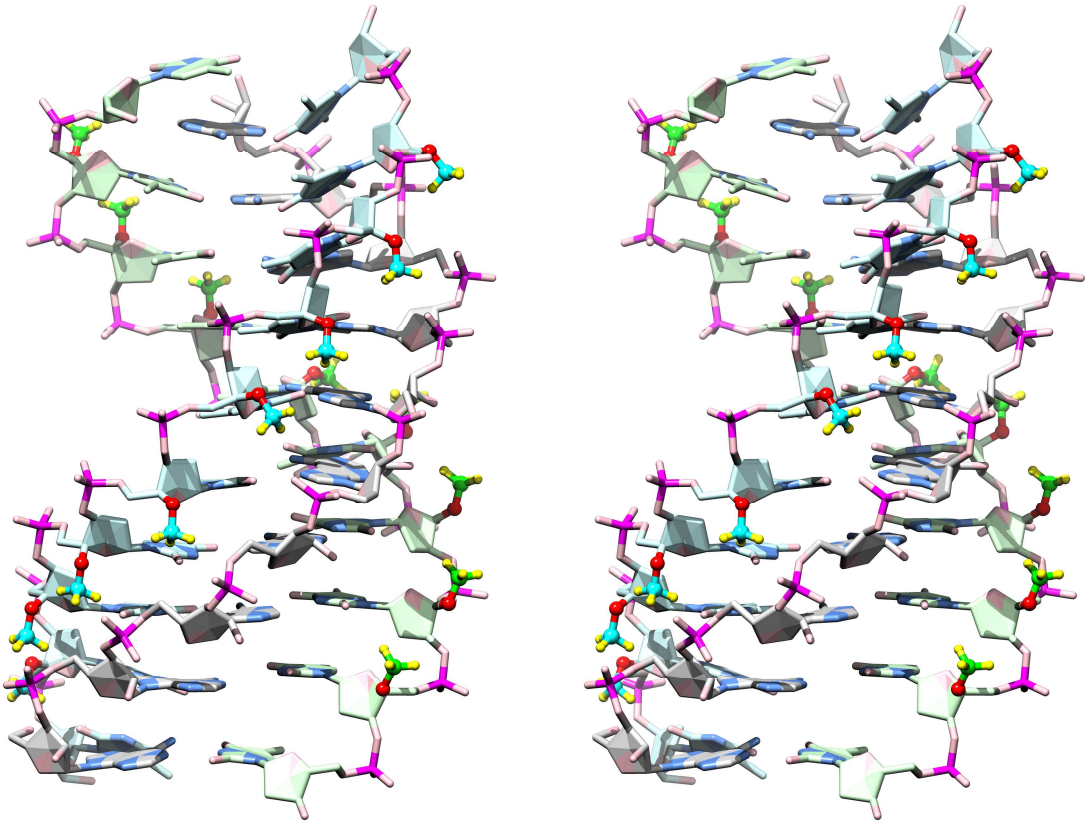

Figure S7: $[T(_{4'\text{-MeO}}T)_8T]^{W\text{-}C}\bullet rA_{10}*[T(_{4'\text{-MeO}}T)_8T]^{Hgstn}$ – hydrogen atoms omitted - stereo view

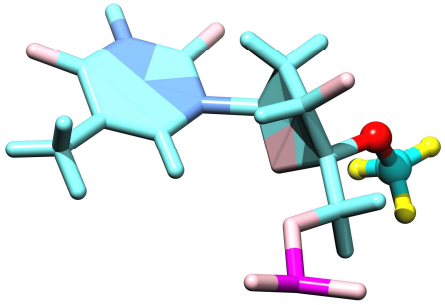

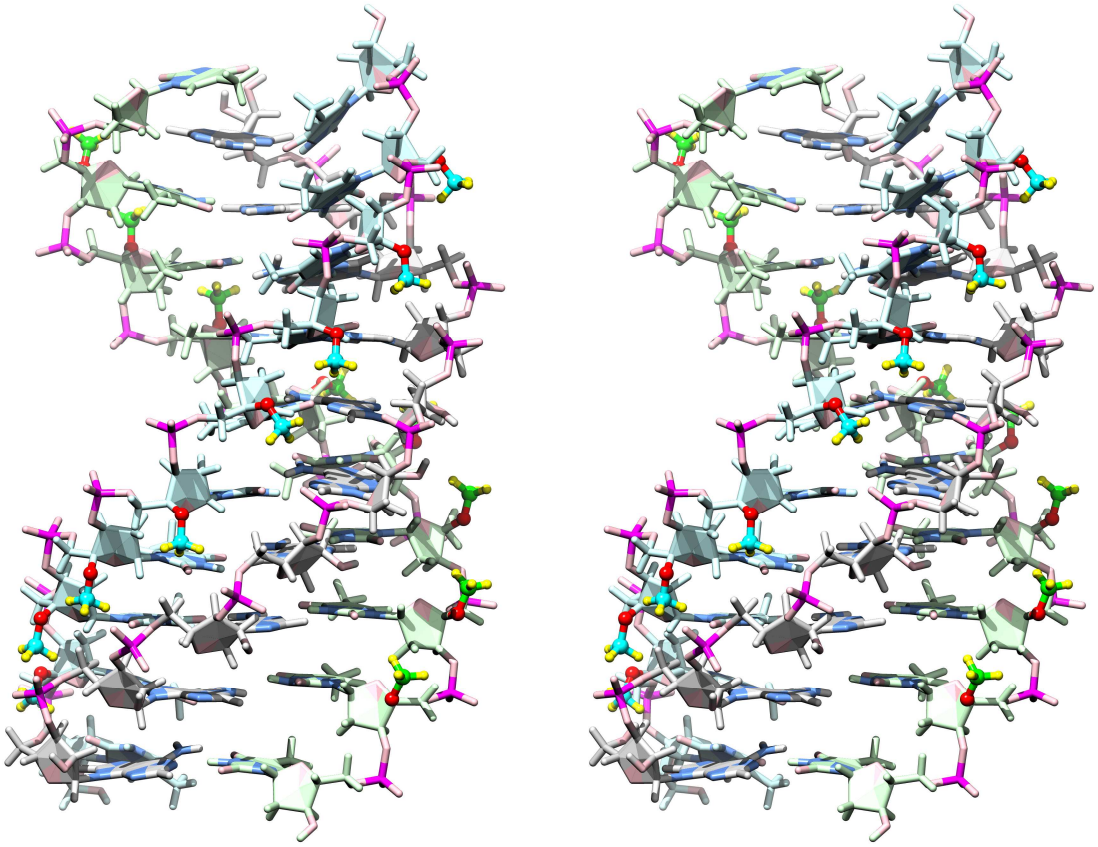

Figure S8: $[T(_{4'\text{-MeO}}T)_8T]^{W\text{-}C}\bullet rA_{10}*[T(_{4'\text{-MeO}}T)_8T]^{Hgstn}$ – all atoms depicted – stereo view

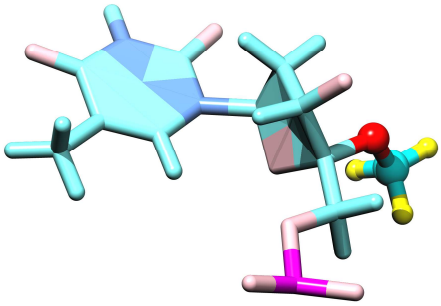

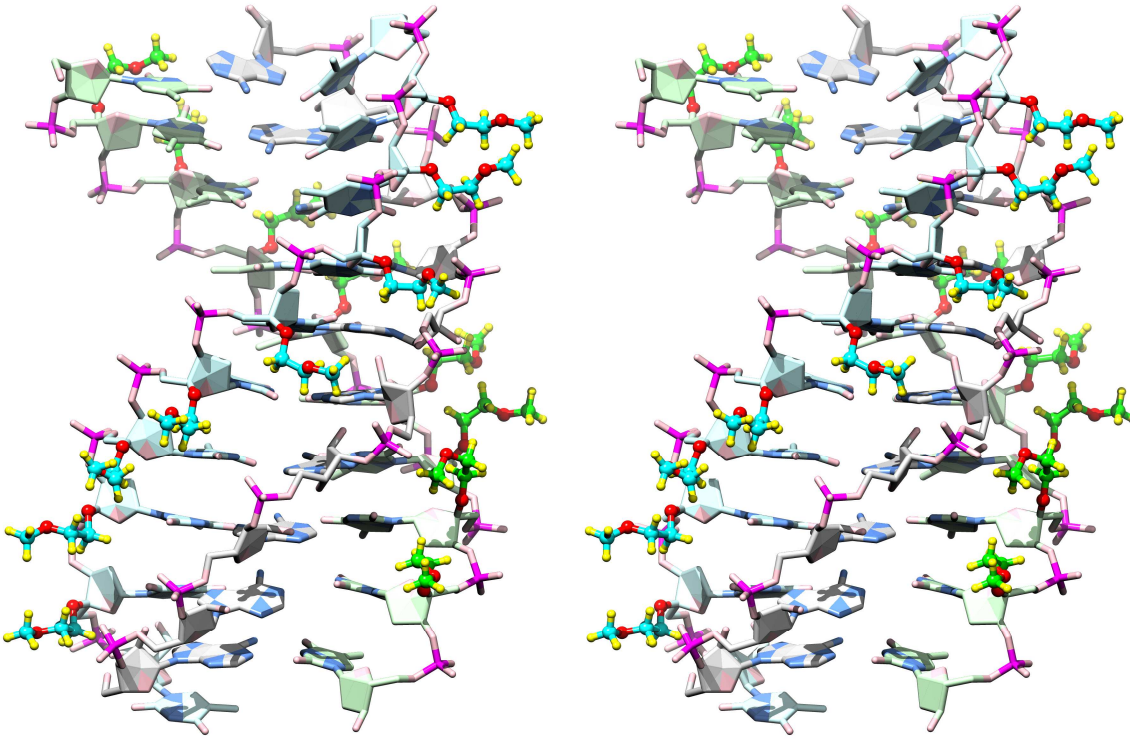

Figure S9: $[T(_{4'\text{-MeOEtO}}T)_8T]^{W\text{-}C}\bullet rA_{10}*[T(_{4'\text{-MeOEtO}}T)_8T]^{Hgstn}$ – hydrogen atoms omitted - stereo view

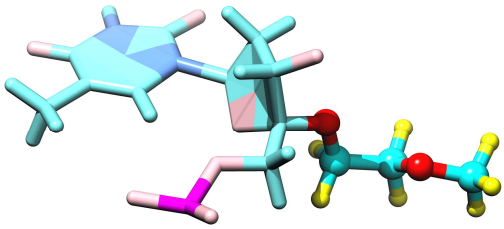

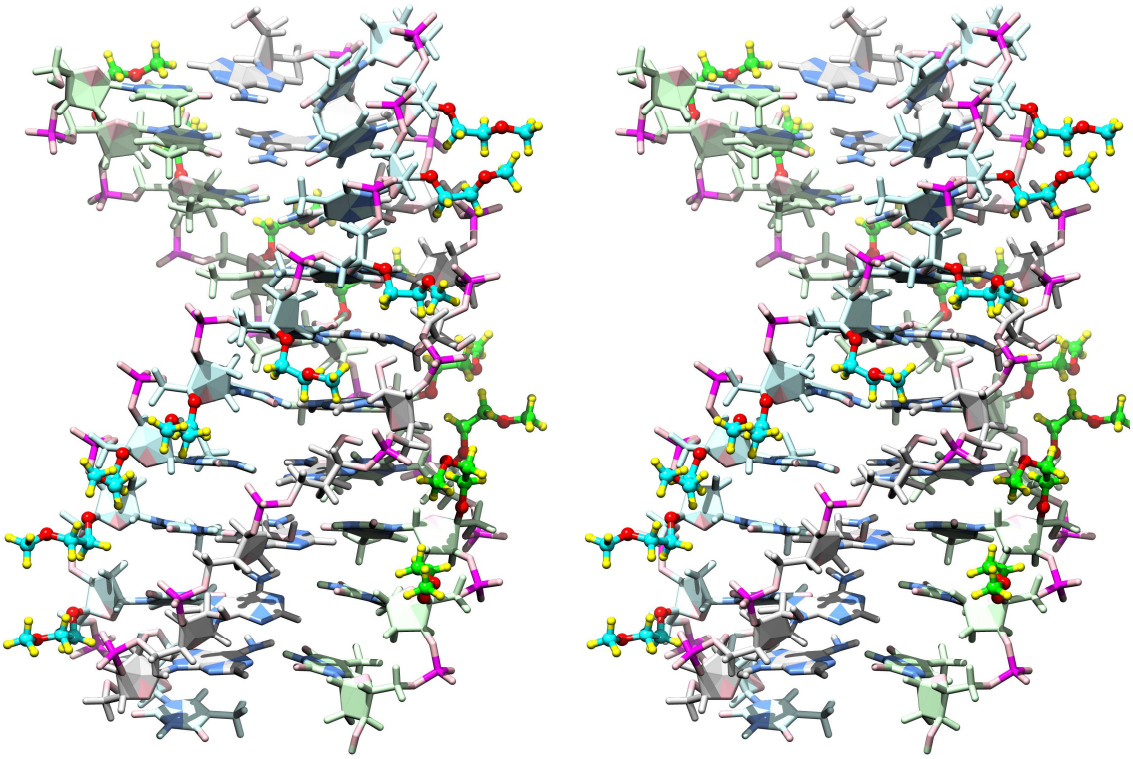

Figure S10: $[T(_{4'\text{-MeOEtO}}T)_8T]^{W\text{-}C}\bullet rA_{10}*[T(_{4'\text{-MeOEtO}}T)_8T]^{Hgstn}$ – all atoms depicted – stereo view

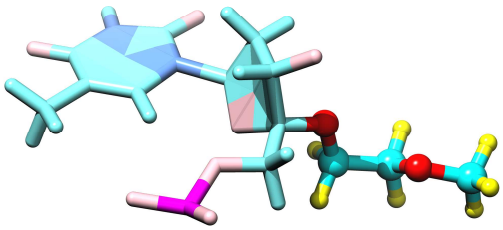

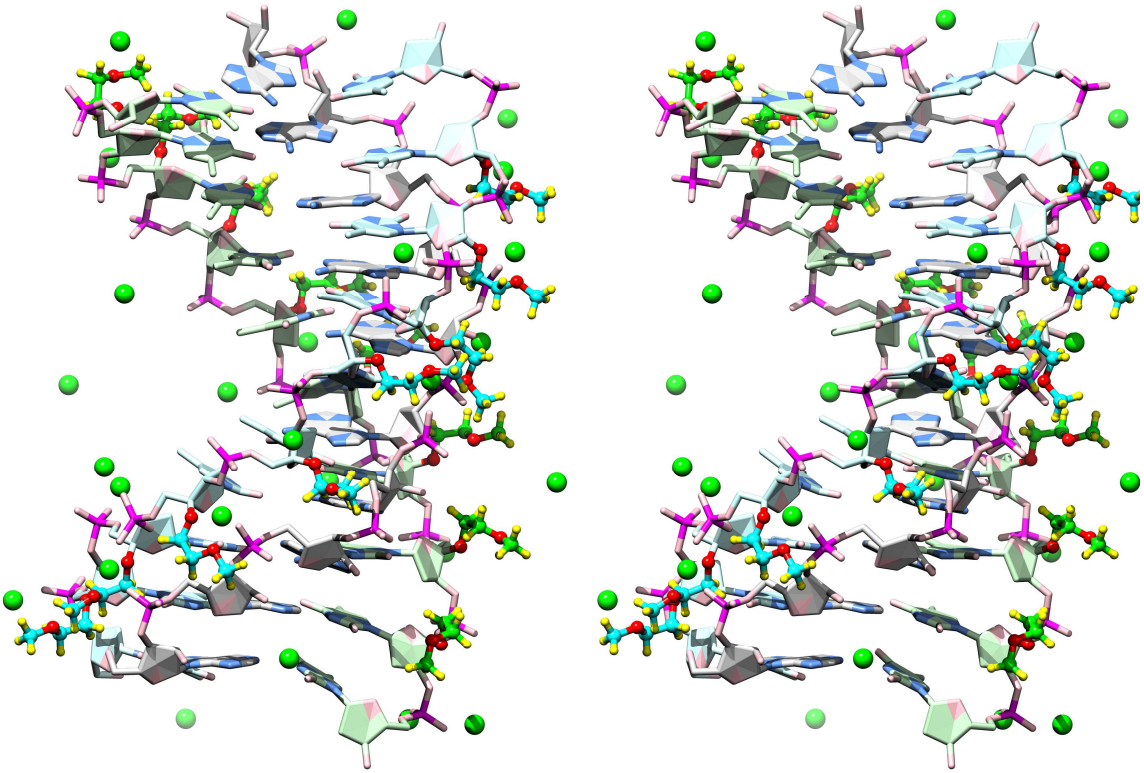

Figure S11: $[T(_{4'\text{-MeOEtO}}T)_8T]^{W\text{-}C}\bullet rA_{10}*[T(_{4'\text{-MeOEtO}}T)_8T]^{Hgstn}$ vs. Mg^{2+} ions– hydrogen atoms omitted - stereo view

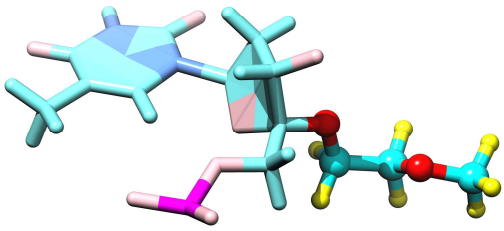

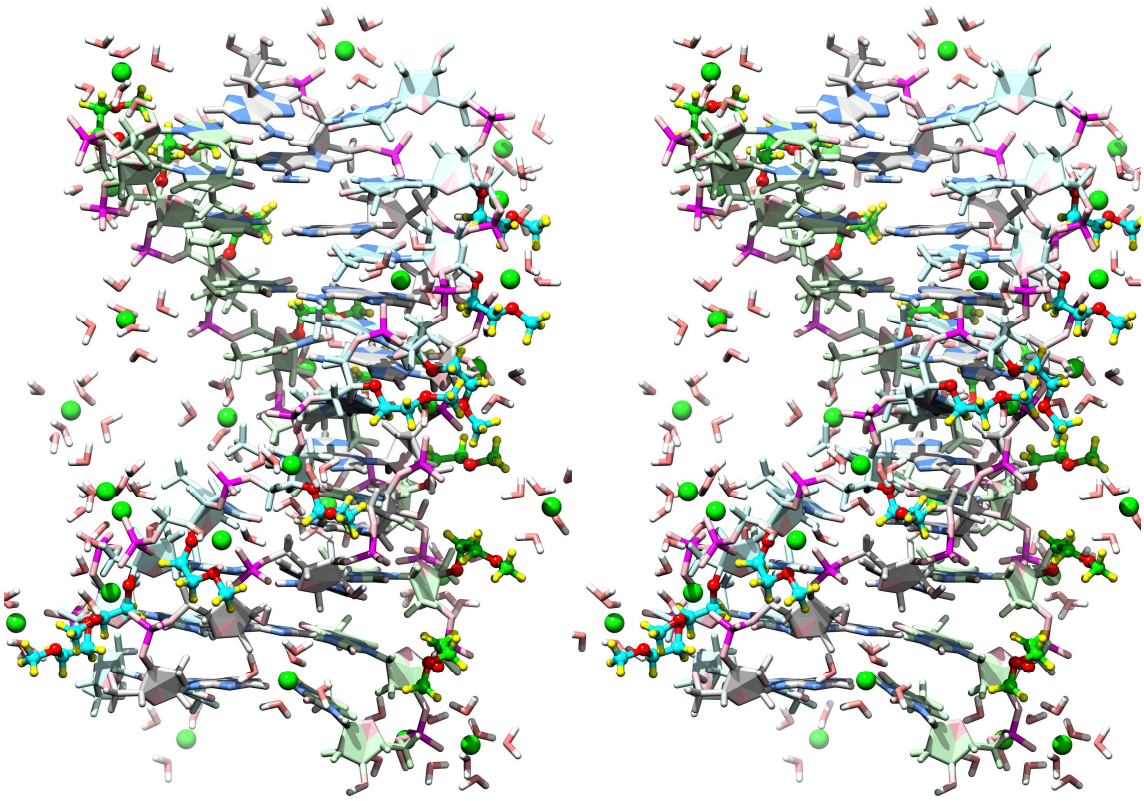

Figure S12: $[T(_{4'\text{-MeOEtO}}T)_8T]^{W\text{-}C}\bullet rA_{10}*[T(_{4'\text{-MeOEtO}}T)_8T]^{Hgstn}$ vs. Mg^{2+} ions – all atoms depicted – stereo view

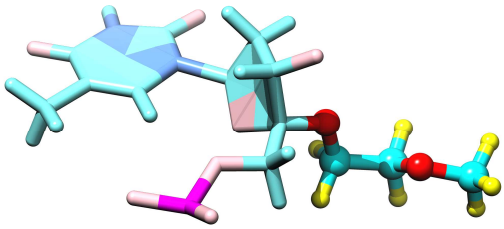

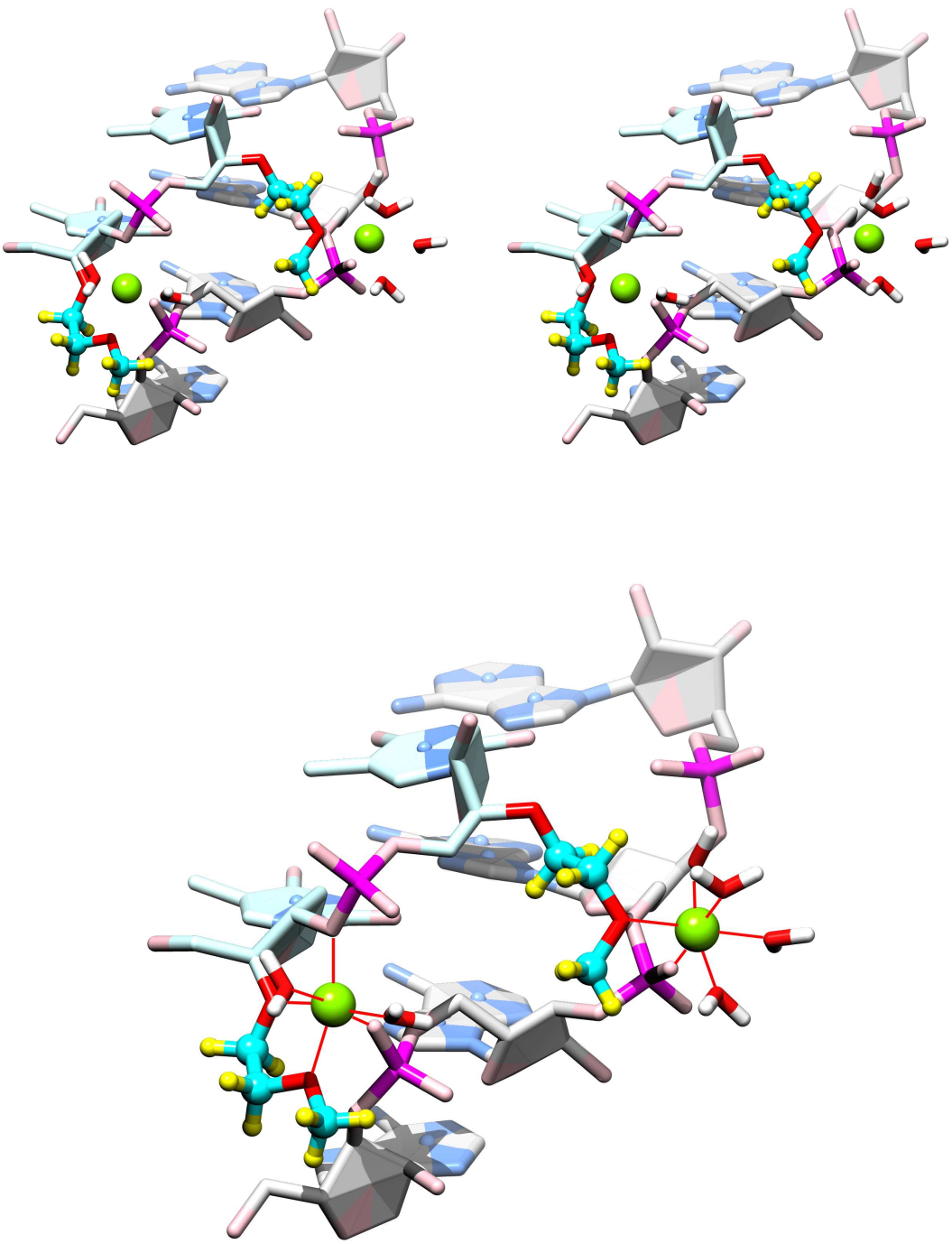

Figure S13: ($_{4'\text{-MeOEtO}}$T)26 and ($_{4'\text{-MeOEtO}}$T)27 and rA4-rA7 parts of [T-($_{4'\text{-MeOEtO}}$T)$_8$T]$_{W\text{-}C}$•A$_{10}$*[T($_{4'\text{-MeOEtO}}$T)$_8$T]$_{Hgstn}$ (where A$_{10}$ consists of residues 1-10, Watson-Crick strand – residues 11-20, Hoogsteen strand – residues 21-30) bridged by Mg^{2+} ions – (top) stereo view, (bottom) oxygen atoms serving as ligands for Mg^{++} are indicated by red lines

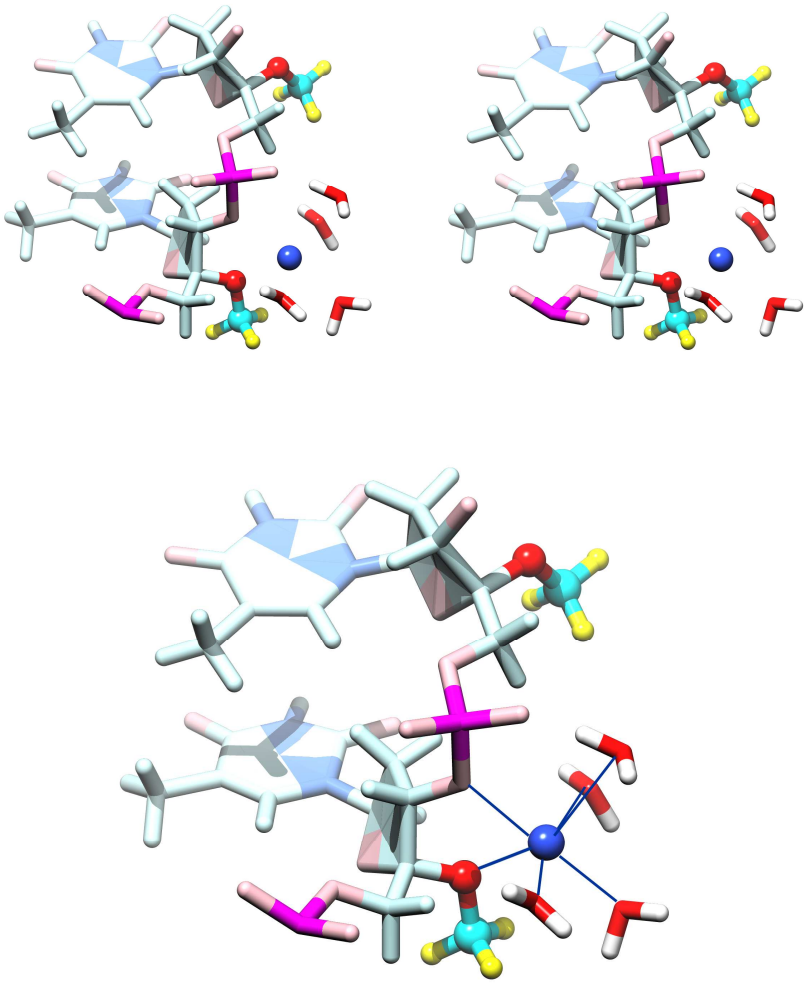

Figure S14: The ($_{4'\text{-MeO}}$T)26 and ($_{4'\text{-MeO}}$T)27 part of $[T(_{4'\text{-MeO}}T)_8T]^{W\text{-}C}\bullet rA_{10}*[T(_{4'\text{-MeO}}T)_8T]^{Hgstn}$ (where rA_{10} consists of residues 1-10, Watson-Crick strand – residues 11-20, Hoogsteen strand – residues 21-30) + $Na^+.4H_2O$ - (top) stereo view, (bottom) oxygen atoms serving as ligands for Na^+ are indicated by blue lines.

8. REFERENCES

[1] P.J. Garegg, B. Samuelson, *J. Chem. Soc., Perkin Trans.1*, 1980, 2866-2869.

[2] Z. Točík, I. Dvořáková, R. Liboska, M. Buděšínský, M. Masojídková, I. Rosenberg, *Tetrahedron*, 2007**, 63**, 4516-4534.

[3] (a) J. van Wijk, C. A. G. Haasnoot, F. A. A. M. de Leeuw, B. D. Huckriede, A. Westra Hoekzema, C. Altona, PSEUROT 6.2 1993, PSEUROT 6.3 1999; Leiden Institute of Chemistry, Leiden University. (b) de Leeuw, F. A. A. M. and Altona, C. Program PSEUROT. *J. Comput. Chem.* 1983, **4**, 428-437.

[4] L.J. Rinkel, C. Altona, *J. Biomed. Struct. Dynam.*, 1987, **4**, 621-649.

[5] C. Altona, M. Sundaralingam, *J. Am. Chem. Soc.* 1972, **94**, 8205-12.

[6] D. Rejman, J. Snášel, R. Liboska, Z. Točík, O. Pačes, Š. Králíková, M. Rinnová, P. Koiš and I. Rosenberg, *Nucleosides Nucleotides Nucl. Acids*, 2001, **20**, 819–823.

[7] W. Humphrey, A. Dalke and K. Schulten, *J. Mol. Graphics*, 1996, **14**, 33-38.

[8] W. L. Jorgensen, J. Chandrasekhar, J. D. Madura, R. W. Impey and M. L. Klein, *J. Chem. Phys.*, 1983, **79**, 926–935.

[9] D. Venkateswarlu, K. E. Lind, V. Mohan, M. Manoharan and D. M. Ferguson, *Nucleic Acids Res.*, 1999, **27**, 2189-2195.

[10] K. E. Lind, V. Mohan, M. Manoharan and D. M. Ferguson, *Nucleic Acids Res.*, 1998, **26**, 3694-3699.

[11] D. A. Pearlman, D. A. Case, J. W. Caldwell, W. S. Ross, T. E. Cheatham, S. Debolt, D. Ferguson, G. Seibel and P. Kollman, *Comput. Phys. Commun.*, 1995, **91**, 1-41.

[12] J. C. Phillips, R. Braun, W. Wang, J. Gumbart, E. Tajkhorshid, E. Villa, C. Chipot, R. D. Skeel, L. Kale and K. Schulten, *J. Comput. Chem.*, **26**, 2005, 1781–1802.

[13] T. E. Cheatham, J. L. Miller, T. Fox, T. A. Darden and P. A. Kollman, *J. Am. Chem. Soc.*, 1995, **117**, 4193–4194.